

JAERI - M  
89-214

NEANDC(J)-144/U  
INDC(JPN)-131/L

MEASUREMENT OF DOUBLE DIFFERENTIAL  
NEUTRON EMISSION CROSS SECTIONS AT  
14.1 MEV FOR Ca, Mn, Co and W

December 1989

Akito TAKAHASHI\*, Yasuhiro SASAKI\*  
Fujio MAEKAWA\* and Hisashi SUGIMOTO\*

「原子力研究機関」日本原子力研究所不定期に公刊している研究報告書です。  
入手の開拓方法は、日本原子力研究所技術情報部情報資料課（〒319-11茨城県那珂郡東海村一木原、若中）にて、料金、支拂い方、販賣方法を原子力販賣会資料欄、又  
〒319-11茨城県那珂郡東海村日本原子力研究所内「複写による実験結果分布」  
及び「E-mail」

JAFREM reports are issued irregularly.

Inquiries about availability of the reports should be addressed to Information Division  
Department of Technical Information, Japan Atomic Energy Research Institute, Tokai-  
mura, Naka-gun, Ibaraki-ken 319-11, Japan.

© Japan Atomic Energy Research Institute, 1989

編集兼発行　　日本原子力研究所  
刊　　刷　　V. G. N. 印刷所

Measurement of Double Differential Neutron Emission  
Cross Sections at 14.1 MeV for Ca, Mn, Co and W

Akito TAKAHASHI\*, Yasuhiro SASAKI\*, Fujio MAEKAWA\*  
and Hisashi SUGIMOTO\*

Department of Physics  
Tokai Research Establishment  
Japan Atomic Energy Research Institute  
Tokai-mura, Naka-gun, Ibaraki-ken

(Received November 28, 1989)

Using the neutron TOF spectrometer at OKTAVIAN, double differential neutron emission cross sections at 14.1 MeV were measured for Ca, Mn, Co and W which are of interest for shielding and structural material elements of fusion reactors. Data were obtained for 16 angle points from 15 to 160 deg in the LAB system for each element, covering the secondary neutron energy region from 0.5 MeV to 15 MeV. Statistics and energy resolution of obtained data are satisfactory.

The double differential cross sections in the LAB system were once converted to those in the center-of-mass system and integrated over scattering angle to obtain neutron emission spectra. Angle-differential cross sections were obtained for the elastic and discrete-inelastic scatterings whose peaks in DDX spectra could be resolved. The measured DDX data are so numerous that only their graphs are shown in this report. However, the graphs and numerical tables are given for the neutron emission spectra and the angle-differential cross sections.

In the graphs, preliminary comparisons are made with evaluated data (ENDF/B-IV and JENDL-3T). The ENDF/B-IV data for Ca are satisfactory in the high energy region, but overestimate the experimental values in the

---

This report is written by summarizing the study implemented under the Research-in-Trust in 1988 fiscal year from the Japan Atomic Energy Research Institute

\* Osaka University

low energy region. The JENDL-3T data for Mn reproduce well the angle-integrated neutron emission spectrum, though underestimation is seen in the 6-13 MeV region. It is noted that ENDF/B-IV underestimates the emission spectrum of Co in the 3-13 MeV region. The ENDF/B-IV data for W do not agree at all with the experimental spectral patterns.

Keywords: Double Differential Neutron Emission Cross Section, 14.1 MeV, TOF Experiment, Ca, Mn, Co, W, JENDL-3T, ENDF/B-IV

Ca, Mn, Co, Wの14.1 MeVにおける中性子放出二重微分断面積の測定

日本原子力研究所東海研究所物理部  
高橋 亮人<sup>\*</sup>・佐々木泰裕<sup>\*</sup>・前川 藤夫<sup>\*</sup>・杉本 久司<sup>\*</sup>

(1989年11月28日受理)

中性子遮蔽材及び構造材元素として重要なCa, Mn, Co, Wについて、14 MeV中性子入射に対する中性子放出二重微分断面積が阪大オクタビアンのTOF分析装置を用いて測定された。散乱角度は45°から160°にわたり16点である。一次中性子エネルギー範囲は0.5 MeVから15 MeVである。統計精度・エネルギー分解能ともに良好なデータを得られた。

得られた二重微分断面積を重心系に直し、角度積分して中性子放出スペクトルデータが導出された。

二重微分断面積のエネルギースペクトルで、ピークとして分離することができた弾性散乱と離散非弾性散乱については、角度微分断面積が導出された。二重微分断面積は大量のデータとなるので、本報ではグラフのみを与えていた。放出スペクトルと角度微分断面積については、グラフと数値表を与えている。

評価核データ(ENDF-B-IV, JENDL-3T)との予備的比較が行なわれた。その結果、Caについては、低エネルギーではENDF-B-IVの過大評価がみられるが、高エネルギー側では実験を良く再現している。Mnについては、JENDL-3Tは放出スペクトルをかなり良く再現しているが6~13 MeV領域で少し過小評価となっている。Coについては、ENDF-B-IVは3~13 MeVで放出スペクトルを大きく過小評価している。Wについては、ENDF-B-IVのデータは実験とスペクトルパターンが全く一致しない。

---

本報告書は日本原子力研究所から昭和63年度委託研究で行われた成果をまとめたものである。

東海研究所：〒319-11 茨城県那珂郡東海村白方字白根2-4

・ 大阪大学

## Contents

1. Introduction .....	1
2. Experiment .....	1
3. Results .....	2
3.1 DDX .....	2
3.2 Angle-integrated neutron emission spectra (EDX) .....	3
3.3 Angle-differential cross section (SDX) .....	3
4. Discussion .....	4
4.1 Calcium .....	4
4.2 Manganese .....	4
4.3 Cobalt .....	5
4.4 Tungsten .....	6
Acknowledgment .....	6
References .....	7

## 目 次

1. はじめに .....	1
2. 実験 .....	1
3. 結果 .....	2
3.1 DDX (二重微分断面積) .....	2
3.2 EDX (エネルギースペクトル) .....	3
3.3 SDX (角度微分断面積) .....	3
4. 考察 .....	4
4.1 カルシウム .....	4
4.2 マンガン .....	4
4.3 コバルト .....	5
4.4 タングステン .....	6
謝辞 .....	6
文献 .....	7

### i. Introduction

Double differential neutron emission cross sections (DDX) are of importance in fusion applications, namely not only for the neutronics calculations of blankets and shields but also for the calculational estimations of primary knock-on atom spectra and kerma factors. Neutron-induced nuclear reactions with incident energy around 14 MeV generally show the competing process between the direct, the precompound and the compound processes which reflected in the energy spectral shapes of DDX or emission spectrum. The DDX data have been therefore utilized also to the assessment of nuclear model codes for evaluation works.

In this report, measurements and results are described for Ca, Mn, Co and W. The DDX data of Ca are required as fundamental nuclear data for shielding designs using ordinary or low-activation (lime-stone) concrete, due to scarce experimental data. Tungsten is a candidate of the ITER inboard shield, whose available neutron data have large uncertainties and therefore new experimental data are strongly required. The DDX data of medium-heavy nuclei (Mn and Co) are of particular interest to assessing "standard" nuclear model codes. The data of angle-integrated neutron emission spectra and angle differential cross sections which can be obtained from the DDX data are also useful for the evaluation or code-assessing tasks. Therefore, measurements were carried out for a wide range of scattering angles (15-160 deg). Preliminary comparisons are made with a few evaluated nuclear data, e. g., ENDF/B-IV<sup>1</sup>) and JENDL-3T<sup>2</sup>).

### 2. Experiment

The details of our experimental method are described elsewhere<sup>3,4</sup>). A brief explanation is as follows: The pulsed D-T neutron source of OKTAVIAN<sup>3</sup>) is used with 2 ns pulse width and 1 MHz repetition frequency. A neutron TOF spectrometer has an 8.3 m long collimated flight path fixed in the 85 deg direction against the OKTAVIAN beam line. A 10 inch diam. × 10 cm thick NE213 detector is used as a main neutron detector with two (low- and high-gain) parallel pulse shape discrimination circuits. A scattering sample is set at 17 cm from the center of a TiT target (2 cm diam.) and moved along the 17 cm R arc when we change the

scattering angle. Incident neutron energy is 14.1 + 0.2 MeV, which was determined by observing the peak-energies of the elastic scatterings of many elements.

Cylindrical metallic rods are used for the scattering samples. Seven pellets of calcium metal (3 cm diam.  $\times$  1 cm thick) are packed with aluminum cooking foil to form the cylindrical sample (7 cm long). The effect of the aluminum foil has been proved to be ignored by background runs with and without the empty aluminum foil at sample position. The sizes of the Mn and W samples are 3 cm diam.  $\times$  7 cm long. For Co, a 2.5 cm diam.  $\times$  7 cm long metallic cylinder is used.

The calibration of the DDX values is made in usual way; the scattered neutron peaks of H(n, n) reaction are measured with a 1.5 cm diam.  $\times$  5 cm long polyethylene sample at the 7 angles (20-50 deg in LAB angle) and peak-area at each angle is normalized to be equal to the corresponding differential cross section of hydrogen.

Data processing procedure is described elsewhere<sup>4)</sup> in detail. For multiple scattering correction<sup>5)</sup>, the DDX data calculated from evaluated nuclear data were used; ENDF/B-IV for Ca, Co and W, and JENDL-3T for Mn. Since the correction is considerably dependent on the spectral shapes of the used nuclear data, we will have to reprocess the Co DDX data using improved data (JENDL-3 final version) when more accurate data are required. For W, the neutron emission spectra by ENDF/B-IV are so different from the measured ones that we can not make correction and have to show the uncorrected data in this report: we may estimate the correction for W to be within 10-15 %.

### 3. Results

#### 3.1 DDX

Results for Ca are shown in Fig. 1 through Fig. 15. In a spectrum at each angle, we can resolve six discrete inelastic scattering peaks (3.736-3.904 MeV sum peak, 4.492 MeV peak, 6.285 MeV peak, 6.510-7.536 MeV sum peak, 7.760-8.540 MeV sum peak and 9.6 MeV peak) and an elastic scattering peak (the most right-hand peak). Significant angular dependence is seen down to low emission energy where ENDF/B-IV overestimates the measured DDX. In the energy region higher than about 5 MeV, the

ENDF/B-IV data reproduce the measured spectral patterns though delicate differences are seen.

Results for Mn are shown in Fig. 16 through Fig. 31 compared with JENDL-3T. Three peaks of the discrete inelastic scatterings (0.984, 2.822, and 4.41 MeV levels) and the elastic scattering peak could be resolved.

Results for Co are shown in Fig. 32 through Fig. 47 compared with ENDF/B-IV. We can see the resolved peaks of the elastic scattering and of the two discrete inelastic scatterings (1.099 and 4.086 MeV levels).

Results for W are shown in Fig. 48 through Fig. 63 compared with ENDF/B-IV. Except for the elastic scattering peak, no distinct peaks of the inelastic scatterings are seen at any angle though delicate structures are observed in the 9-13 MeV region.

### 3.2 Angle-Integrated neutron emission spectra (EDX)

Results for Ca are shown in Fig. 64 and Fig. 65 for the LAB and the CM system, and numerical values for the CM system are given in Table 1(1).

Results for Mn are shown in Fig. 66 and Fig. 67. Numerical values are given in Table 1(2).

Results for Co are shown in Fig. 68 and Fig. 69. Numerical values are given in Table 1(3).

Results for W are shown in Fig. 70 and Fig. 71. Numerical values are given in Table 1(4).

### 3.3 Angle-differential cross sections (SDX)

Results for Ca are shown in Figs. 72, 73, 74 and 75, together with fitted curves using Legendre polynomials and evaluated curves of ENDF/B-IV. Numerical values are given in Table 2(1) and 2(2).

Results for Mn are shown in Figs. 76, 77 and 78. Fitting with the Legendre polynomials and the JENDL-3T curves are also shown. Numerical values are given in Table 2(3).

Results for Co are shown in Figs. 79 and 80. Numerical values are given in Table 2(4).

Results for W are shown in Figs. 81 and 82, for the elastic scattering, the inelastic continuum (integration of DDX within the 5.5-11

MeV region) and the ( $n$ ,  $2n$ ) neutron emissions. For the ( $n$ ,  $2n$ ) reaction, the DDX values are integrated within the 0-5.5 MeV region. Numerical values are given in Table 2(5).

#### 4. Discussion

##### 4.1 Calcium

As shown in Fig. 1 through Fig. 15, the calculated curves of ENDF/B-IV reproduce the measured DDX curves as a whole. Speaking the local agreements, ENDF/B-IV underestimates the measured values in the 4-11 MeV at forward angles (15-50 deg). Below 3 MeV the measured data show the forward enhancement of the neutron emission while the ENDF/B-IV data give isotropic angular distribution and therefore overestimate the experimental values at the angles greater than 60 deg.

Looking at the angle-integrated neutron emission spectrum in the CM system shown in Fig. 65, the ENDF/B-IV data reproduce very well the measured values in the energy region above 4 MeV while significant (by 30-50 %) overestimation is seen below 4 MeV.

As for the single differential cross sections of the elastic scattering shown in Fig. 72, ENDF/B-IV overestimates 2 times the experimental values at the backward angles (110-150 deg), though the angular distribution resembles one another. For the resolved discrete inelastic scatterings shown in Figs. 73 through 75, the underestimation of ENDF/B-IV is pointed out at the forward angles for the 3.736-3.904 and 4.492 MeV levels.

##### 4.2 Manganese

DDX: As shown in Fig. 16 through 31, the calculated DDXs by JENDL-3T reproduce the overall spectral shapes of the experimental ones but the significant underestimations at the forward angles (15-80 deg) should be pointed out. At the backward angles (90-160 deg), very good agreement is seen except for the elastic scattering peaks at the backward angles (100-160 deg). The angular distribution of the pre-equilibrium neutron emission shall be taken into account to fill the large differences at the forward angles.

Seeing the angle-integrated neutron emission spectrum shown in Fig. 67, we can say that the underestimation of JENDL-3T is obvious in the 6-13 MeV region. We see a distinct peak around 9.5 MeV of the measured spectrum, which is attributed to the excitation of one phonon state of octapole vibration (excitation energy 4.41 MeV). A hump at 6-7 MeV may be due to the excitation of the low energy octapole vibration (two phonon state). A shoulder at 11.5 MeV can correspond to the 1.884 MeV level excitation.

For the differential elastic scattering cross sections shown in Fig. 76, the considerable underestimation of JENDL-3T is seen at the forward angles (15-30 deg) while overestimating about twice at the backward angles (100-160 deg). For the 0.984 MeV level excitation, fairly good agreement is seen as shown in Fig. 77 as far as the angle-dependence is concerned. As shown in Fig. 78, the JENDL-3T cross sections for the 2.822 MeV level should be doubled though their shapes of angular distribution curve agree with the measured one. Since the cross section of 4.41 MeV level seems to be large, it is recommended to include this level into the evaluations.

#### 4.3 Cobalt

As shown in Fig. 32 through Fig. 47, the measured spectral shapes and the angular distribution of DDX are very different from those of ENDF/B-IV; especially in the 3-13 MeV region and at the forward angles, the used nuclear models seem to have problems, i. e., the direct collective excitation of the inelastic scattering and the preequilibrium neutron emission are not taken into account or are treated incorrectly.

The results of the angle-integrated emission spectrum shown in Fig. 69 lead us to a similar conclusion.

The differential cross sections of the elastic scattering are shown in Fig. 79. At the backward angles (70-160 deg), ENDF/B-IV is 2-3 times larger than the experimental values. Overestimation over the whole angle and the difference of the distribution shape may suggest us the necessity of the reestimation of optical parameters. No comparisons with the evaluated curves are made for the 1.099 and 4.086 MeV levels, and the analyses with DWUCK4 are desirable.

#### 4.4 Tungsten

Obviously the drastic underestimation of ENDF/B-IV in the 5-13 MeV region shows the ignorance of the direct and preequilibrium neutron emissions. Basically we can apply the EGNASH<sup>6)</sup> + DWUCK4<sup>7)</sup> analysis for the evaluation tasks. However, the measured DDX spectra in the 5-13 MeV region show us the existence of so many discrete levels of the direct excitations. Natural tungsten contains 5 isotopes, so that the energy spectrum may be monotonous in this region. In the case of Ta<sup>8)</sup> which is mono-isotopic, we have observed the quite similar monotonous spectra of DDX in the corresponding energy region. Therefore we can speculate that the many direct excitations with similar magnitudes are possible for these heavy mass elements (from Ta to W). This situation requires us laborious calculations of the direct process neutron emissions.

The differential cross sections of the elastic scattering are shown in Fig. 81 compared with ENDF/B-IV. The measured data are larger on an average than those of ENDF/B-IV at the backward angles (90-160 deg). As shown in Fig. 82, a slight forward-enhancement of ( $n, 2n$ ) neutrons is seen and the integrated ( $n, 2n$ ) cross section of the experiment is about 15 % smaller than that of ENDF/B-IV.

#### Acknowledgment

The authors appreciate the operation crew of OKTAVIAN. The appreciation is also due to the continuous support of this work by Dr. S. Igarasi, Dr. T. Asami and Dr. Y. Kikuchi of JAERI Nuclear Data Center.

References

- 1) ENDF/B Summary Documentation, BNL-NCS-17541 (1975)
- 2) JENDL compilation Group (Nuclear Data Center, JAERI): JENDL-3T,  
private communication (1987)
- 3) Takahashi, A., et al.: J. Nucl. Sci. Technol., 25, 215 (1988)
- 4) Takahashi, A., et al.: JAERI-M 88-102 (1988)
- 5) Ichimura, E., Takahashi, A.: OKTAVIAN Rep. A-87-02, Osaka Univ.,  
(1987)
- 6) Yamamuro, N.,: Proc. Nucl. Data Sci. Tech., 1988, Mito, pp.489 SAIKON  
Publ., (1988)
- 7) Kunz, P.O.: "Distorted Wave Code DWUCK4", Univ. Colorado (1974)
- 8) Takahashi, A., et al.: INDC(JPN) 118L (1989)

Table 1(1) Angle-integrated neutron emission spectrum in the CM system with En = 14.1 MeV, for Ca

SUBENTRY	00021003	880201	00021003	1		
BIB	2	8	00021003	2		
COMMENT	TWO DATA SETS ARE GIVEN			3		
	DATA OBTAINED FROM RAW DDX DATA , IN LEFT HAND SIDE			4		
	DATA OBTAINED FROM CORRECTED DDX DATA WITH MUSC3 CODE			5		
REACTION	(20-CA-0(N,SCT)...,DE') SECONDARY NEUTRON SPECTRUM			6		
	IN THE CENTER-OF-MASS SYSTEM			7		
ENDBIB	8		00021003	8		
COMMON	1	5	00021003	9		
EN			00021003	10		
MEV			00021003	11		
14 10000			00021003	12		
ENDCOMMON	5		00021003	13		
DATA	6	66	00021003	14		
E-MAX	E-MIN	DATA	DATA-ERR	DATA		
MEV	MEV	B/MEV	B/MEV	B/MEV		
14 20000	14.00000	9.95E-02	2.98E-03	9.27E-02	2.95E-0300021003	18
14 00000	13.80000	3.11E-01	3.84E-03	3.01E-01	3.82E-0300021003	19
13 80000	13.60000	7.14E-01	4.66E-03	7.23E-01	4.71E-0300021003	20
13 60000	13.40000	1.27E+00	5.27E-03	1.29E+00	5.30E-0300021003	21
13 40000	13.20000	1.15E+00	4.66E-03	1.16E+00	4.67E-0300021003	22
13 20000	13.00000	6.07E-01	3.58E-03	6.16E-01	3.56E-0300021003	23
13 00000	12.80000	2.72E-01	2.70E-03	2.72E-01	2.65E-0300021003	24
12 80000	12.60000	1.22E-01	2.20E-03	1.22E-01	2.15E-0300021003	25
12 60000	12.40000	6.19E-02	2.05E-03	6.22E-02	2.00E-0300021003	26
12 40000	12.20000	3.62E-02	1.93E-03	3.66E-02	1.88E-0300021003	27
12 20000	12.00000	2.37E-02	1.88E-03	2.40E-02	1.83E-0300021003	28
12 00000	11.80000	1.57E-02	1.85E-03	1.60E-02	1.79E-0300021003	29
11 80000	11.60000	1.24E-02	1.78E-03	1.27E-02	1.72E-0300021003	30
11 60000	11.40000	5.30E-03	1.71E-03	5.46E-03	1.67E-0300021003	31
11 40000	11.20000	1.96E-03	1.66E-03	2.02E-03	1.62E-0300021003	32
11 20000	11.00000	1.28E-03	1.61E-03	1.31E-03	1.59E-0300021003	33
11 00000	10.80000	2.22E-03	1.52E-03	2.24E-03	1.52E-0300021003	34
10 80000	10.60000	4.43E-03	1.46E-03	4.47E-03	1.46E-0300021003	35
10 60000	10.40000	9.96E-03	1.42E-03	1.01E-02	1.42E-0300021003	36
10 40000	10.20000	1.80E-02	1.42E-03	1.82E-02	1.43E-0300021003	37
10 20000	10.00000	4.09E-02	1.49E-03	4.12E-02	1.50E-0300021003	38
10 00000	9.80000	8.27E-02	1.65E-03	8.34E-02	1.66E-0300021003	39
9 80000	9.60000	9.75E-03	1.68E-03	9.80E-02	1.69E-0300021003	40
9 60000	9.40000	5.65E-02	1.54E-03	5.63E-02	1.53E-0300021003	41
9 40000	9.20000	3.55E-02	1.45E-03	3.50E-02	1.43E-0300021003	42
9 20000	9.00000	4.42E-02	1.51E-03	4.01E-02	1.42E-0300021003	43
9 00000	8.80000	3.94E-02	1.57E-03	2.94E-02	1.27E-0300021003	44
8 80000	8.60000	2.41E-02	1.55E-03	1.63E-02	1.19E-0300021003	45
8 60000	8.40000	1.49E-02	1.53E-03	9.96E-03	1.19E-0300021003	46
8 40000	8.20000	1.60E-02	1.48E-03	1.12E-02	1.23E-0300021003	47
8 20000	8.00000	2.36E-02	1.51E-03	1.86E-02	1.30E-0300021003	48
8 00000	7.80000	2.38E-02	1.52E-03	1.84E-02	1.32E-0300021003	49
7 80000	7.60000	2.12E-02	1.52E-03	1.74E-02	1.37E-0300021003	50
7 60000	7.40000	2.68E-02	1.54E-03	2.37E-02	1.44E-0300021003	51
7 40000	7.20000	3.30E-02	1.57E-03	3.01E-02	1.48E-0300021003	52
7 20000	7.00000	3.21E-02	1.59E-03	2.97E-02	1.49E-0300021003	53
7 00000	6.80000	4.01E-02	1.64E-03	3.62E-02	1.48E-0300021003	54
6 80000	6.60000	5.38E-02	1.69E-03	4.74E-02	1.50E-0300021003	55
6 60000	6.40000	5.00E-02	1.69E-03	4.27E-02	1.45E-0300021003	56
6 40000	6.20000	3.65E-02	1.66E-03	3.06E-02	1.44E-0300021003	57
6 20000	6.00000	3.83E-02	1.68E-03	3.37E-02	1.47E-0300021003	58
6 00000	5.80000	3.97E-02	1.70E-03	3.54E-02	1.51E-0300021003	59
5 80000	5.60000	3.85E-02	1.70E-03	3.29E-02	1.49E-0300021003	60
5 60000	5.40000	3.71E-02	1.73E-03	3.29E-02	1.50E-0300021003	61
5 40000	5.20000	3.96E-02	1.74E-03	3.43E-02	1.47E-0300021003	62
5 20000	5.00000	3.82E-02	1.74E-03	3.03E-02	1.42E-0300021003	63
5 00000	4.80000	3.51E-02	1.75E-03	2.59E-02	1.38E-0300021003	64
4 80000	4.60000	4.08E-02	1.77E-03	3.08E-02	1.39E-0300021003	65
4 60000	4.40000	4.47E-02	1.76E-03	3.40E-02	1.40E-0300021003	66
4 40000	4.20000	4.76E-02	1.77E-03	3.73E-02	1.43E-0300021003	67
4 20000	4.00000	5.09E-02	1.78E-03	3.97E-02	1.44E-0300021003	68
4 00000	3.80000	5.24E-02	1.77E-03	3.89E-02	1.42E-0300021003	69
3 80000	3.60000	5.82E-02	1.80E-03	4.36E-02	1.44E-0300021003	70
3 60000	3.40000	6.10E-02	1.81E-03	4.70E-02	1.47E-0300021003	71
3 40000	3.20000	6.87E-02	1.85E-03	5.37E-02	1.52E-0300021003	72
3 20000	3.00000	7.80E-02	1.94E-03	6.29E-02	1.62E-0300021003	73
3 00000	2.80000	9.41E-02	2.06E-03	7.80E-02	1.73E-0300021003	74
2 80000	2.60000	1.06E-01	2.20E-03	8.72E-02	1.86E-0300021003	75
2 60000	2.40000	1.20E-01	2.37E-03	9.43E-02	1.91E-0300021003	76
2 40000	2.20000	1.52E-01	2.52E-03	1.17E-01	1.97E-0300021003	77
2 20000	2.00000	1.58E-01	2.71E-03	1.26E-01	2.19E-0300021003	78
2 00000	1.80000	1.71E-01	2.92E-03	1.43E-01	2.43E-0300021003	79
1 80000	1.60000	1.79E-01	3.28E-03	1.47E-01	2.70E-0300021003	80
1 60000	1.40000	1.91E-01	3.92E-03	1.57E-01	3.25E-0300021003	81
1 40000	1.20000	1.94E-01	5.20E-03	1.61E-01	4.37E-0300021003	82
1 20000	1.00000	2.43E-01	1.14E-02	1.97E-01	9.39E-0300021003	83
ENDDATA	70			00021003	84	
ENDSUBENTRY	85			00021003999999		
ENDENTRY	3			00021999999999		

Table 1(2) Angle-integrated neutron emission spectrum in the CM system with En = 14.1 MeV, for Mn

SUBENTRY	00020003	881201		00020003	1
BIB	2	8		00020003	2
COMMENT	TWO DATA SETS ARE GIVEN.			00020003	3
	DATA OBTAINED FROM RAW DDX DATA , IN LEFT HAND SIDE.			00020003	4
	DATA OBTAINED FROM CORRECTED DDX DATA WITH MUSCC3 CODE			00020003	5
REACTION	(25-MN-55(N,SCT),,DE)	SECONDARY NEUTRON SPECTRUM		00020003	6
	IN THE CENTER-OF-MASS SYSTEM			00020003	7
ENDBJB	8			00020003	8
COMMON	1	5		00020003	10
EN				00020003	11
MEV				00020003	12
14.10000				00020003	13
ENDCOMMON	5			00020003	14
DATA	6	68		00020003	15
E-MAX	E-MIN	DATA	DATA-ERR	DATA	DATA-ERR
MEV	MEV	B/MEV	B/MEV	B/MEV	B/MEV
14.60000	14.40000	1.02E-02	6.39E-04	1.23E-02	7.82E-0400020003
14.40000	14.20000	4.75E-02	1.19E-03	0.00E+00	1.36E-0300020003
14.20000	14.00000	2.22E-01	1.98E-03	2.69E-01	2.20E-0300020003
14.00000	13.80000	8.08E-01	2.63E-03	9.91E-01	3.08E-0300020003
13.80000	13.60000	1.59E+00	3.25E-03	1.96E+00	3.91E-0300020003
13.60000	13.40000	1.64E+00	3.18E-03	2.02E+00	3.84E-0300020003
13.40000	13.20000	9.59E-01	2.47E-03	1.17E+00	2.94E-0300020003
13.20E00	13.00000	4.12E-01	1.80E-03	4.93E-01	2.08E-0300020003
13.00000	12.80000	2.01E-01	1.44E-03	2.36E-01	1.63E-0300020003
12.80000	12.60000	1.28E-01	1.27E-03	1.52E-01	1.46E-0300020003
12.60000	12.40000	9.07E-02	1.16E-03	1.09E-01	1.35E-0300020003
12.40000	12.20000	6.14E-02	1.07E-03	7.44E-02	1.25E-0300020003
12.20000	12.00000	4.32E-02	1.01E-03	5.24E-02	1.18E-0300020003
12.00000	11.80000	3.81E-02	9.85E-04	4.62E-02	1.16E-0300020003
11.80000	11.60000	3.47E-02	9.51E-04	4.21E-02	1.12E-0300020003
11.60000	11.40000	3.25E-02	9.33E-04	3.94E-02	1.11E-0300020003
11.40000	11.20000	2.81E-02	9.08E-04	3.41E-02	1.08E-0300020003
11.20000	11.00000	2.34E-02	8.87E-04	2.81E-02	1.06E-0300020003
11.00000	10.80000	2.38E-02	8.69F-04	2.81E-02	1.04E-0300020003
10.80000	10.60000	2.53E-02	8.70E-04	3.03E-02	1.04E-0300020003
10.60000	10.40000	2.42E-02	8.54E-04	2.88E-02	1.02E-0300020003
10.40000	10.20000	2.27E-02	8.42E-04	2.71E-02	1.00E-0300020003
10.20000	10.00000	2.41E-02	8.50E-04	2.86E-02	1.01E-0300020003
10.00000	9.80000	2.73E-02	8.67E-04	3.24E-02	1.03E-0300020003
9.80000	9.60000	3.0GE-02	8.91E-04	3.63E-02	1.06E-0300020003
9.60000	9.40000	4.36E-02	9.27E-04	5.16E-02	1.11E-0300020003
9.40000	9.20000	4.72E-02	9.51E-04	5.47E-02	1.12E-0300020003
9.20000	9.00000	4.21E-02	9.28E-04	4.28E-02	9.56E-0400020003
9.00000	8.80000	3.75E-02	9.14E-04	3.68E-02	9.38E-0400020003
8.80000	8.60000	3.79E-02	9.21E-04	3.74E-02	9.53E-0400020003
8.60000	8.40000	3.82E-02	9.21E-04	3.92E-02	9.67E-0400020003
8.40000	8.20000	3.76E-02	9.25E-04	3.94E-02	9.82E-0400020003
8.20000	8.00000	4.09E-02	9.29E-04	4.32E-02	9.97E-0400020003
8.00000	7.80000	4.37E-02	9.41E-04	4.66E-02	1.01E-0300020003
7.80000	7.60000	4.83E-02	9.51E-04	5.16E-02	1.03E-0300020003
7.60000	7.40000	5.20E-02	9.53E-04	5.60E-02	1.04E-0300020003
7.40000	7.20000	5.22E-02	9.64E-04	6.16E-02	1.05E-0300020003
7.20000	7.00000	6.03E-02	9.66E-04	6.62E-02	1.06E-0300020003
7.00000	6.80000	6.26E-02	9.66E-04	6.90E-02	1.07E-0300020003
6.80000	6.60000	6.38E-02	9.62E-04	6.99E-02	1.06E-0300020003
6.60000	6.40000	6.72E-02	9.69E-04	7.34E-02	1.07E-0300020003
6.40000	6.20000	6.86E-02	9.62E-04	7.52E-02	1.06E-0300020003
6.20000	6.00000	7.33E-02	9.74E-04	8.06E-02	1.08E-0300020003
6.00000	5.80000	7.59E-02	9.77E-04	8.38E-02	1.09E-0300020003
5.80000	5.60000	7.76E-02	9.84E-04	8.60E-02	1.10E-0300020003
5.60000	5.40000	8.20E-02	9.92E-04	9.12E-02	1.11E-0300020003
5.40000	5.20000	8.78E-02	1.01E-03	9.75E-02	1.13E-0300020003
5.20000	5.00000	9.39E-02	1.02E-03	1.04E-01	1.14E-0300020003
5.00000	4.80000	1.02E-01	1.04E-03	1.13E-01	1.16E-0300020003
4.80000	4.60000	1.09E-01	1.05E-03	1.20E-01	1.17E-0300020003
4.60000	4.40000	1.17E-01	1.07E-03	1.29E-01	1.18E-0300020003
4.40000	4.20000	1.25E-01	1.09E-03	1.39E-01	1.21E-0300020003
4.20000	4.00000	1.36E-01	1.11E-03	1.51E-01	1.23E-0300020003
4.00000	3.80000	1.45E-01	1.15E-03	1.60E-01	1.26E-0300020003
3.80000	3.60000	1.55E-01	1.17E-03	1.70E-01	1.29E-0300020003
3.60000	3.40000	1.67E-01	1.20E-03	1.82E-01	1.31E-0300020003
3.40000	3.20000	1.87E-01	1.25E-03	2.04E-01	1.35E-0300020003
3.20000	3.00000	2.11E-01	1.32E-03	2.28E-01	1.42E-0300020003
3.00000	2.80000	2.45E-01	1.40E-03	2.64E-01	1.50E-0300020003
2.80000	2.60000	2.79E-01	1.49E-03	2.97E-01	1.58E-0300020003
2.60000	2.40000	3.32E-01	1.59E-03	3.39E-01	1.61E-0300020003
2.40000	2.20000	4.01E-01	1.68E-03	4.07E-01	1.68E-0300020003
2.20000	2.00000	4.56E-01	1.78E-03	4.73E-01	1.82E-0300020003
2.00000	1.80000	5.10E-01	1.88E-03	5.34E-01	1.97E-0300020003
1.80000	1.60000	5.92E-01	2.08E-03	6.14E-01	2.16E-0300020003
1.60000	1.40000	6.76E-01	2.38E-03	6.90E-01	2.43E-0300020003
1.40000	1.20000	7.55E-01	2.87E-03	7.58E-01	2.88E-0300020003
1.20000	1.00000	7.93E-01	4.04E-03	7.82E-01	3.99E-0300020003
ENDDATA	72			00020003	86
ENDSUBENTRY	87			0002000399999999	
ENDENTRY	3			00020999999999	

Table 1(3) Angle-integrated neutron emission spectrum in the CM system with En = 14.1 MeV, for Co

SUBENTRY	00019003	881201	00019003	1
BIB	2	8	00019003	2
COMMENT	TWO DATA SETS ARE GIVEN.			3
	DATA OBTAINED FROM RAW DDX DATA , IN LEFT HAND SIDE .			4
	DATA OBTAINED FROM CORRECTED DDX DATA WITH MUSCC3 CODE			5
REACTION	(27-CO-59(N,SCT)...DE) SECONDARY NEUTRON SPECTRUM			6
	IN THE CENTER-OF-MASS SYSTEM			7
ENDBIB	8		00019003	8
COMMON	1	5	00019003	10
EN			00019003	11
MEV			00019003	12
14.10000			00019003	13
ENDCOMMON	5		00019003	14
DATA	6	69	00019003	15
E-MAX	E-MIN	DATA	DATA-ERR	DATA
MEV	MEV	B/MEV	B/MEV	B/MEV
14.60000	14.40000	3.90E-02	5.30E-04	3.85E-02
14.40000	14.20000	4.33E-02	1.20E-03	5.29E-02
14.20000	14.00000	2.66E-01	1.79E-03	3.37E-01
14.00000	13.80000	7.81E-01	2.46E-03	1.04E+00
13.80000	13.60000	1.41E+00	3.07E-03	1.88E+00
13.60000	13.40000	1.22E+00	2.80E-03	1.60E+00
13.40000	13.20000	5.66E-01	1.98E-03	3.31E-01
13.20000	13.00000	2.28E-01	1.41E-03	2.92E-01
13.00000	12.80000	1.14E-01	1.14E-03	1.45E-01
12.80000	12.60000	8.63E-02	1.07E-03	1.08E-01
12.60000	12.40000	8.15E-02	1.06E-03	1.01E-01
12.40000	12.20000	6.67E-02	1.01E-03	8.38E-02
12.20000	12.00000	4.64E-02	9.40E-04	5.92E-02
12.00000	11.80000	3.09E-02	8.77E-04	4.01E-02
11.80000	11.60000	2.15E-02	8.38E-04	2.82E-02
11.60000	11.40000	1.69E-02	8.16E-04	2.22E-02
11.40000	11.20000	1.21E-02	7.86E-04	1.57E-02
11.20000	11.00000	8.89E-03	7.61E-04	1.15E-02
11.00000	10.80000	8.15E-03	7.43E-04	1.04E-02
10.80000	10.60000	1.17E-02	7.34E-04	1.46E-02
10.60000	10.40000	1.10E-02	7.29E-04	1.35E-02
10.40000	10.20000	1.41E-02	7.09E-04	1.73E-02
10.20000	10.00000	2.15E-02	7.27E-04	2.65E-02
10.00000	9.80000	2.99E-02	7.48E-04	3.69E-02
9.80000	9.60000	6.69E-02	7.29E-04	3.32E-02
9.60000	9.40000	2.45E-02	7.10E-04	3.04E-02
9.40000	9.20000	6.68E-02	7.04E-04	3.19E-02
9.20000	9.00000	2.83E-02	7.19E-04	2.98E-02
9.00000	8.80000	2.80E-02	7.04E-04	2.88E-02
8.80000	8.60000	2.65E-02	7.09E-04	2.73E-02
8.60000	8.40000	2.87E-02	7.11E-04	3.01E-02
8.40000	8.20000	2.94E-02	7.24E-04	3.15E-02
8.20000	8.00000	3.06E-02	7.18E-04	3.29E-02
8.00000	7.80000	3.02E-02	7.31E-04	3.26E-02
7.80000	7.60000	3.03E-02	7.33E-04	3.34E-02
7.60000	7.40000	3.16E-02	7.47E-04	3.47E-02
7.40000	7.20000	3.43E-02	7.47E-04	3.76E-02
7.20000	7.00000	3.67E-02	7.57E-04	4.08E-02
7.00000	6.80000	3.88E-02	7.58E-04	4.34E-02
6.80000	6.60000	4.25E-02	7.64E-04	4.75E-02
6.60000	6.40000	4.41E-02	7.71E-04	4.86E-02
6.40000	6.20000	4.67E-02	7.77E-04	5.14E-02
6.20000	6.00000	5.15E-02	7.95E-04	5.66E-02
6.00000	5.80000	5.41E-02	8.10E-04	5.95E-02
5.80000	5.60000	5.80E-02	8.26E-04	6.41E-02
5.60000	5.40000	6.32E-02	8.49E-04	6.93E-02
5.40000	5.20000	6.90E-02	8.65E-04	7.54E-02
5.20000	5.00000	7.52E-02	8.92E-04	8.22E-02
5.00000	4.80000	8.17E-02	9.18E-04	8.82E-02
4.80000	4.60000	9.10E-02	9.44E-04	9.68E-02
4.60000	4.40000	9.74E-02	9.67E-04	1.03E-01
4.40000	4.20000	1.05E-01	9.92E-04	1.13E-01
4.20000	4.00000	1.13E-01	1.01E-03	1.23E-01
4.00000	3.80000	1.18E-01	1.03E-03	1.29E-01
3.80000	3.60000	1.27E-01	1.05E-03	1.40E-01
3.60000	3.40000	1.37E-01	1.09E-03	1.52E-01
3.40000	3.20000	1.51E-01	1.13E-03	1.71E-01
3.20000	3.00000	1.68E-01	1.17E-03	1.95E-01
3.00000	2.80000	1.91E-01	1.24E-03	2.22E-01
2.80000	2.60000	2.17E-01	1.27E-03	2.52E-01
2.60000	2.40000	2.49E-01	1.36E-03	2.83E-01
2.40000	2.20000	2.96E-01	1.41E-03	3.34E-01
2.20000	2.00000	3.34E-01	1.52E-03	3.79E-01
2.00000	1.80000	3.93E-01	1.64E-03	4.46E-01
1.80000	1.60000	4.64E-01	1.85E-03	5.20E-01
1.60000	1.40000	5.38E-01	2.14E-03	5.88E-01
1.40000	1.20000	6.19E-01	2.73E-03	6.64E-01
1.20000	1.00000	7.41E-01	4.59E-03	7.76E-01
1.00000	0.80000	8.85E-01	1.40E-02	1.45E-02
ENDDATA	73		00019003	87
ENDSUBENTRY	88		00019003999999	
ENDENTRY	3		00019999999999	

Table 1(4) Angle-integrated neutron emission spectrum in the CM system with En = 14.1 MeV, for W

SUBENTRY	00023003	890601	00023003	1
BIB	2	8	00023003	2
COMMENT	TWO DATA SETS ARE GIVEN.			00023003
	DATA OBTAINED FROM RAW DDX DATA , IN LEFT HAND SIDE.			00023003
	DATA OBTAINED FROM CORRECTED DDX DATA WITH MUSCC3 CODE			00023003
REACTION	(74-W-0(N,SCT)...,DE} SECONDARY NEUTRON SPECTRUM			00023003
	IN THE CENTER-OF-MASS SYSTEM			00023003
ENDBIB	8		00023003	9
COMMON	1	5	00023003	10
EN			00023003	11
MEV			00023003	12
14 10000			00023003	13
ENDCOMMON	5		00023003	14
DATA	6	72	00023003	15
E-MAX	E-MIN	DATA	DATA-ERR	
MEV	MEV	B/MEV	B/MEV	
15 00000	14 80000	1.83E-10	1.45E-03	6.40E-10 1.99E-0300023003
14 80000	14 60000	3.24E-02	1.06E-03	4.36E-02 1.31E-0300023003
14 60000	14 40000	2.19E-01	1.55E-03	2.95E-01 1.86E-0300023003
14 40000	14 20000	9.09E-01	1.91E-03	1.22E+00 2.38E-0300023003
14 20000	14 00000	2.02E+00	2.42E-03	2.71E+00 3.10E-0300023003
14 00000	13 80000	2.38E+00	2.57E-03	3.12E+00 3.25E-0300023003
13 80000	13 60000	1.50E+00	2.08E-03	1.88E+00 2.50E-0300023003
13 60000	13 40000	6.20E-01	1.45E-03	7.44E-01 1.65E-0300023003
13 40000	13 20000	2.54E-01	1.07E-03	3.02E-01 1.19E-0300023003
13 20000	13 00000	1.45E-01	8.99E-04	1.78E-01 1.04E-0300023003
13 00000	12 80000	9.80E-02	8.17E-04	1.24E-01 9.66E-0400023003
12 80000	12 60000	7.50E-02	7.72E-04	9.53E-02 9.20E-0400023003
12 60000	12 40000	6.01E-02	7.37E-04	7.71E-02 8.92E-0400023003
12 40000	12 20000	5.00E-02	7.01E-04	6.46E-02 8.60E-0400023003
12 20000	12 00000	4.32E-02	6.81E-04	5.49E-02 8.22E-0400023003
12 00000	11 80000	3.94E-02	6.56E-04	4.93E-02 7.87E-0400023003
11 80000	11 60000	3.62E-02	6.30E-04	4.48E-02 7.57E-0400023003
11 60000	11 40000	3.62E-02	6.17E-04	4.45E-02 7.41E-0400023003
11 40000	11 20000	3.70E-02	6.04E-04	4.57E-02 7.32E-0400023003
11 20000	11 00000	3.65E-02	5.95E-04	4.53E-02 7.29E-0400023003
11 00000	10 80000	3.64E-02	5.94E-04	4.52E-02 7.28E-0400023003
10 80000	10 60000	3.66E-02	5.94E-04	4.56E-02 7.34E-0400023003
10 60000	10 40000	3.76E-02	5.99E-04	4.68E-02 7.41E-0400023003
10 40000	10 20000	3.88E-02	6.01E-04	4.86E-02 7.53E-0400023003
10 20000	10 00000	3.85E-02	5.98E-04	4.86E-02 7.52E-0400023003
10 00000	9 80000	3.75E-02	5.96E-04	4.72E-02 7.50E-0400023003
9 80000	9 60000	3.70E-02	5.96E-04	4.60E-02 7.37E-0400023003
9 60000	9 40000	3.61E-02	6.00E-04	2.56E-02 4.49E-0400023003
9 40000	9 20000	3.63E-02	6.09E-04	6.50E-03 1.32E-0400023003
9 20000	9 00000	3.55E-02	6.09E-04	4.46E-03 1.29E-0400023003
9 00000	8 80000	3.55E-02	6.14E-04	5.46E-03 1.59E-0400023003
8 80000	8 60000	3.47E-02	6.16E-04	5.98E-03 1.73E-0400023003
8 60000	8 40000	3.44E-02	6.23E-04	7.10E-03 2.18E-0400023003
8 40000	8 20000	3.50E-02	6.30E-04	8.36E-03 2.39E-0400023003
8 20000	8 00000	3.42E-02	6.36E-04	1.15E-02 3.29E-0400023003
8 00000	7 80000	3.30E-02	6.39E-04	1.49E-02 4.12E-0400023003
7 80000	7 60000	3.31E-02	6.49E-04	1.57E-02 4.27E-0400023003
7 60000	7 40000	3.42E-02	6.54E-04	1.86E-02 4.85E-0400023003
7 40000	7 20000	3.44E-02	6.57E-04	2.18E-02 5.27E-0400023003
7 20000	7 00000	3.43E-02	6.54E-04	2.27E-02 5.30E-0400023003
7 00000	6 80000	3.57E-02	6.55E-04	2.64E-02 5.95E-0400023003
6 80000	6 60000	3.68E-02	6.54E-04	3.07E-02 6.50E-0400023003
6 60000	6 40000	3.68E-02	6.54E-04	3.20E-02 6.56E-0400023003
6 40000	6 20000	3.63E-02	6.63E-04	3.32E-02 7.02E-0400023003
6 20000	6 00000	3.82E-02	6.78E-04	3.65E-02 7.50E-0400023003
6 00000	5 80000	3.87E-02	6.89E-04	3.90E-02 7.88E-0400023003
5 80000	5 60000	3.91E-02	6.99E-04	4.15E-02 8.11E-0400023003
5 60000	5 40000	4.17E-02	7.12E-04	4.56E-02 8.37E-0400023003
5 40000	5 20000	4.47E-02	7.25E-04	4.96E-02 8.63E-0400023003
5 20000	5 00000	4.70E-02	7.37E-04	5.28E-02 8.78E-0400023003
5 00000	4 80000	5.07E-02	7.55E-04	5.80E-02 9.08E-0400023003
4 80000	4 60000	5.62E-02	7.72E-04	6.57E-02 9.45E-0400023003
4 60000	4 40000	6.18E-02	7.87E-04	7.36E-02 9.72E-0400023003
4 40000	4 20000	7.13E-02	8.14E-04	8.61E-02 1.01E-0300023003
4 20000	4 00000	8.10E-02	8.32E-04	9.88E-02 1.04E-0300023003
4 00000	3 80000	9.32E-02	8.56E-04	1.16E-01 1.10E-0300023003
3 80000	3 60000	1.08E-01	8.74E-04	1.36E-01 1.12E-0300023003
3 60000	3 40000	1.28E-01	9.14E-04	1.62E-01 1.18E-0300023003
3 40000	3.20000	1.51E-01	9.57E-04	1.93E-01 1.24E-0300023003
3 20000	3.00000	1.85E-01	1.02E-03	2.40E-01 1.34E-0300023003
3 00000	2.80000	2.23E-01	1.09E-03	2.91E-01 1.45E-0300023003
2 80000	2.60000	2.79E-01	1.20E-03	3.57E-01 1.55E-0300023003
2 60000	2.40000	3.56E-01	1.34E-03	4.52E-01 1.74E-0300023003
2 10000	2.20000	4.52E-01	1.43E-03	5.83E-01 1.87E-0300023003
2 20000	2.00000	5.60E-01	1.57E-03	7.36E-01 2.08E-0300023003
1 80000	1.60000	8.82E-01	2.00E-03	1.16E+00 2.65E-0300023003
1 60000	1.40000	1.11E+00	2.36E-03	1.44E+00 3.08E-0300023003
1 40000	1.20000	1.42E+00	3.01E-03	1.81E+00 3.88E-0300023003
1 30000	1.00000	1.84E+00	4.42E-03	2.29E+00 5.54E-0300023003
1 00000	0.80000	2.54E+00	1.05E-02	3.09E+00 1.28E-0200023003
0 80000	0.60000	2.40E+00	4.39E-02	2.79E+00 5.12E-0200023003
ENDDATA	76		00023003	90
ENDSUBENTRY	91		00023003999999	
ENDENTRY	3		00023999999999	

Table 2(1) Partial differential cross sections for Ca at En = 14.1 MeV

$\theta_{\text{LAB}}$ (deg)	e l a s t i c		Q = -3.736~3.904 MeV		Q = -4.492 MeV		Q = -6.285 MeV	
	dσ/dΩ(b/sr)	error	dσ/dΩ(b/sr)	error	dσ/dΩ(b/sr)	error	dσ/dΩ(b/sr)	error
1 5	1.06E+0	3.2E-2	7.73E-3	1.2E-3	3.57E-3	7.1E-4	1.81E-3	5.4E-4
2 0	6.63E-1	2.0E-2	7.53E-3	7.5E-4	3.85E-3	5.8E-4	2.99E-3	4.5E-4
3 0	1.56E-1	4.7E-3	7.37E-3	5.2E-4	3.67E-3	3.7E-4	3.39E-3	3.4E-4
4 2 . 5	3.61E-2	1.1E-3	6.90E-3	3.4E-4	2.90E-3	2.9E-4	3.47E-3	3.5E-4
5 0	5.94E-2	1.8E-3	7.02E-3	3.5E-4	2.39E-3	2.4E-4	2.74E-3	2.7E-4
6 0	5.26E-2	1.6E-3	6.88E-3	3.4E-4	2.48E-3	2.5E-4	1.75E-3	2.6E-4
7 0	2.39E-2	7.2E-4	6.19E-3	3.1E-4	1.74E-3	2.6E-4	9.37E-4	1.9E-4
8 0	1.49E-2	5.6E-4	4.77E-3	2.9E-4	1.69E-3	2.5E-4	6.46E-4	1.9E-4
9 0	2.07E-2	6.2E-4	3.79E-3	2.6E-4	1.85E-3	2.8E-4	5.77E-4	2.0E-4
1 0 0	2.27E-2	6.8E-4	3.25E-3	2.6E-4	1.42E-3	2.1E-4	7.84E-4	2.0E-4
1 1 0	1.49E-2	4.5E-4	2.53E-3	2.3E-4	1.07E-3	2.1E-4	6.73E-4	2.0E-4
1 2 0	5.37E-3	3.4E-4	2.60E-3	2.3E-4	7.49E-4	1.9E-4	7.75E-4	1.9E-4
1 3 0	3.89E-3	3.3E-4	2.92E-3	2.6E-4	9.46E-4	1.9E-4	1.08E-3	2.2E-4
1 4 0	3.85E-3	3.2E-4	2.95E-3	2.7E-4	1.08E-3	2.2E-4	7.65E-4	1.9E-4
1 5 0	3.44E-3	4.1E-4	2.92E-3	3.5E-4	8.02E-4	2.8E-4	7.69E-4	2.7E-4
$\sigma_{\text{total}}$ (barn)	8.96E-1	3.6E-2	5.78E-2	2.9E-3	2.21E-2	3.3E-3	1.71E-2	2.6E-3

Table 2(2) Partial differential cross sections for Ca at En = 14.1 MeV (continued)

$\theta_{\text{LAB}}$ (deg)	Q = -6.510~7.536 MeV		Q = -7.760~8.540 MeV		Q = -9.6 MeV	
	d $\sigma$ /d $\Omega$ (b/sr)	error	d $\sigma$ /d $\Omega$ (b/sr)	error	d $\sigma$ /d $\Omega$ (b/sr)	error
15	1.76E-3	4.4E-4	1.43E-3	5.7E-4	2.27E-3	6.8E-4
20	2.28E-3	3.4E-4	3.34E-3	6.7E-4	2.59E-3	5.2E-4
30	3.67E-3	3.7E-4	4.20E-3	8.5E-4	2.97E-3	5.9E-4
42.5	3.78E-3	3.8E-4	4.08E-3	9.4E-4	3.31E-3	6.6E-4
50	3.47E-3	3.5E-4	4.35E-3	8.7E-4	3.56E-3	7.1E-4
60	2.77E-3	2.8E-4	2.63E-3	5.3E-4	2.30E-3	4.6E-4
70	2.63E-3	2.6E-4	2.53E-3	5.1E-4	2.56E-3	5.1E-4
80	1.85E-3	2.8E-4	2.89E-3	5.8E-4	2.02E-3	4.0E-4
90	1.82E-3	2.7E-4	2.69E-3	5.4E-4	1.95E-3	3.9E-4
100	1.75E-3	2.6E-4	2.68E-3	5.4E-4	1.74E-3	3.5E-4
110	1.35E-3	2.0E-4	1.97E-3	3.9E-4	1.70E-3	3.4E-4
120	1.57E-3	2.4E-4	2.46E-3	4.9E-4	1.73E-3	3.5E-4
130	1.56E-3	2.3E-4	2.18E-3	4.4E-4	1.67E-3	3.3E-4
140	1.71E-3	2.6E-4	2.28E-3	4.6E-4	1.47E-3	2.9E-4
150	1.95E-3	3.7E-4	2.61E-3	5.2E-4	1.55E-3	4.6E-4
$\sigma_{\text{Total}}$ (barn)	2.73E-2	3.3E-3	3.74E-2	7.5E-3	2.69E-2	5.4E-3

Table 2(3) Partial differential cross sections for Mn at En = 14.1 MeV

$\theta_{LAB}$ (deg)	e l a s t i c		Q = -0.984 MeV		Q = -2.822 MeV		Q = -4.11 MeV	
	$d\sigma/d\Omega(b/sr)$	error	$d\sigma/d\Omega(b/sr)$	error	$d\sigma/d\Omega(b/sr)$	error	$d\sigma/d\Omega(b/sr)$	error
1 5	1.89E+0	5.7E-2	-----	-----	-----	-----	-----	-----
2 0	1.17E+0	3.5E-2	-----	-----	-----	-----	-----	-----
3 0	3.14E-1	9.4E-3	-----	-----	-----	-----	-----	-----
4 0	7.39E-2	2.2E-3	5.62E-3	1.7E-3	2.08E-3	2.1E-4	5.07E-3	3.0E-4
5 0	5.85E-2	1.8E-3	3.94E-3	7.9E-4	1.95E-3	1.9E-4	4.15E-3	2.5E-4
6 0	2.56E-2	7.7E-4	4.01E-3	8.0E-4	1.50E-3	1.5E-4	5.13E-3	3.1E-4
7 0	1.40E-2	4.2E-4	2.59E-3	3.9E-4	1.79E-3	1.8E-4	3.29E-3	2.3E-4
8 0	2.63E-2	7.9E-4	3.86E-3	5.8E-4	1.12E-3	1.3E-4	2.99E-3	2.1E-4
9 0	3.04E-2	9.1E-4	3.74E-3	5.6E-4	6.77E-4	1.1E-4	2.98E-3	2.1E-4
1 0 0	1.94E-2	5.8E-4	2.48E-3	3.7E-4	6.73E-4	9.4E-5	2.94E-3	2.1E-4
1 1 0	1.07E-2	3.2E-4	1.27E-3	1.9E-4	6.95E-4	1.0E-4	2.90E-3	2.0E-4
1 2 0	1.04E-2	3.1E-4	1.34E-3	2.7E-4	8.61E-4	1.1E-4	2.21E-3	1.5E-4
1 3 0	1.16E-2	3.5E-4	9.29E-4	1.9E-4	-----	-----	1.67E-3	1.3E-4
1 4 0	1.37E-2	4.1E-4	7.10E-4	1.4E-4	-----	-----	2.68E-3	1.9E-4
1 5 0	1.52E-2	4.6E-4	9.51E-4	1.9E-4	-----	-----	2.21E-3	2.2E-4
1 6 0	1.38E-2	5.4E-4	5.49E-4	2.5E-4	-----	-----	-----	-----
$\sigma_{total}$ (barn)	1.38E+0	2.1E-1	3.42E-2	6.8E-3	1.60E-2	1.9E-3	4.12E-2	2.9E-3

Table 2(4) Partial differential cross sections for Co at En = 14.1 MeV

$\theta_{LAB}$ (deg)	e l a s t i c		Q= -1.099 MeV		Q= -4.086 MeV	
	d $\sigma$ /d $\Omega$ (b/sr)	error	d $\sigma$ /d $\Omega$ (b/sr)	error	d $\sigma$ /d $\Omega$ (b/sr)	error
1 5	1.61E+0	4.8E-2	—	—	—	—
2 0	1.01E+0	3.0E-2	—	—	—	—
3 0	2.53E-1	7.6E-3	1.95E-2	2.3E-3	2.96E-3	2.4E-4
4 0	5.52E-2	1.7E-3	1.20E-2	8.4E-4	3.02E-3	2.4E-4
5 0	3.30E-2	9.9E-4	7.33E-3	2.9E-4	3.50E-3	2.8E-4
6 0	1.32E-2	3.9E-4	4.05E-3	1.6E-4	2.09E-3	1.9E-4
7 0	1.21E-2	3.6E-4	4.12E-3	2.1E-4	1.54E-3	1.5E-4
8 0	2.36E-2	7.1E-4	4.22E-3	2.1E-4	1.11E-3	1.2E-4
9 0	2.49E-2	7.5E-4	3.32E-3	2.0E-4	1.68E-3	1.8E-4
1 0 0	1.11E-2	3.3E-4	2.03E-3	1.6E-4	1.32E-3	1.5E-4
1 1 0	6.66E-3	2.0E-4	1.18E-3	1.3E-4	1.25E-3	1.4E-4
1 2 0	8.52E-3	2.6E-4	6.66E-4	1.1E-4	1.41E-3	1.6E-4
1 3 0	9.19E-3	2.8E-4	7.13E-4	1.1E-4	1.14E-3	1.4E-4
1 4 0	8.30E-3	2.5E-4	1.01E-3	1.3E-4	1.40E-3	1.7E-4
1 5 0	8.19E-3	2.6E-4	1.05E-3	1.9E-4	1.53E-3	2.3E-4
1 6 0	6.80E-3	3.3E-4	1.43E-3	2.4E-4	—	—
$\sigma_{total}$ (barn)	1.17E+0	1.8E-1	6.61E-2	5.3E-3	2.23E-2	2.2E-3

Table 2(5) Partial differential cross sections for W at En = 14.1 MeV

$\theta_{LAB}$ (deg)	e l a s t i c		c o n t i n u u m		(n, 2n)	
	$d\sigma/d\Omega(b/sr)$	error	$d\sigma/d\Omega(b/sr)$	error	$d\sigma/d\Omega(b/sr)$	error
1 5	2.29E+0	2.3E-1	5.67E-2	4.0E-3	3.68E-1	2.6E-2
2 0	9.81E-1	9.8E-2	4.44E-2	3.1E-3	3.31E-1	2.3E-2
3 0	1.54E-1	1.5E-2	3.05E-2	2.1E-3	3.35E-1	2.3E-2
4 0	2.05E-1	2.1E-2	2.67E-2	1.9E-3	3.13E-1	2.2E-2
5 0	9.60E-2	9.6E-3	2.45E-2	1.7E-3	3.11E-1	2.2E-2
6 0	3.07E-2	3.1E-3	1.94E-2	1.4E-3	2.91E-1	2.0E-2
7 0	3.26E-2	3.3E-3	1.63E-2	1.1E-3	2.94E-1	2.1E-2
8 0	2.29E-2	2.3E-3	1.43E-2	1.0E-3	2.58E-1	1.8E-2
9 0	1.15E-2	1.2E-3	1.25E-2	8.8E-4	2.74E-1	1.9E-2
1 0 0	9.93E-3	9.9E-4	1.12E-2	7.8E-4	2.54E-1	1.8E-2
1 1 0	9.06E-3	9.1E-4	9.48E-3	6.6E-4	2.65E-1	1.9E-2
1 2 0	7.36E-3	7.4E-4	7.70E-3	5.4E-4	2.42E-1	1.7E-2
1 3 0	4.87E-3	4.9E-4	8.45E-3	5.9E-4	2.51E-1	1.8E-2
1 4 0	5.82E-3	5.8E-4	8.06E-3	5.6E-4	2.63E-1	1.8E-2
1 5 0	8.07E-3	8.1E-4	8.48E-3	5.9E-4	2.95E-1	2.1E-2
1 6 0	6.84E-3	6.8E-4	5.38E-3	6.5E-4	2.84E-1	2.0E-2
$\sigma_{total}$ (barn)	1.33E+0	1.3E+0	2.01E-1	1.4E-2	3.50E+0	2.5E-1

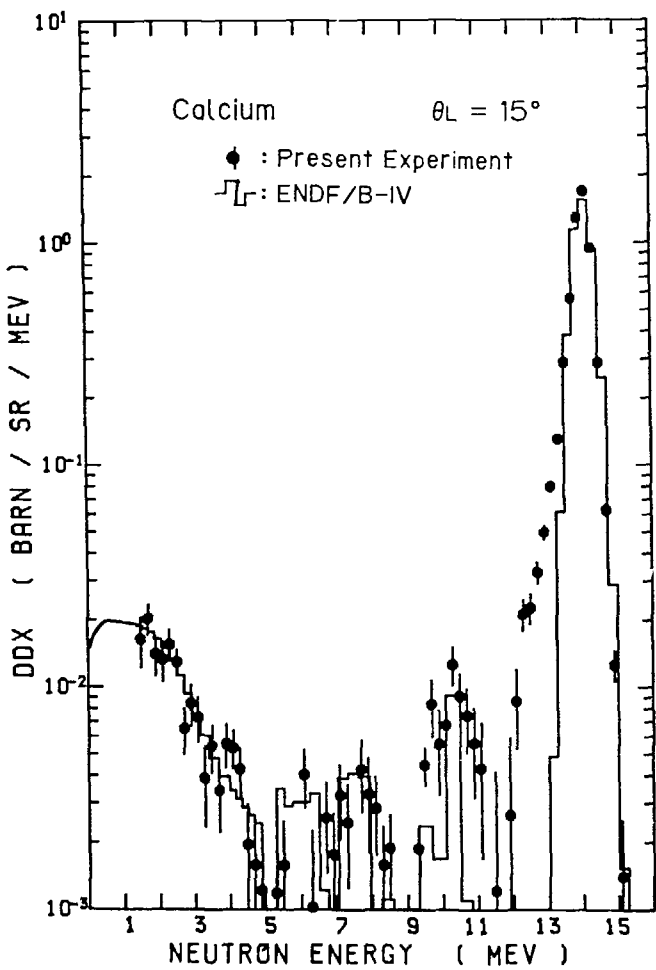


Fig. 1 Double differential neutron emission cross section at 15 deg with  $E_n = 14.1$  MeV, for Ca

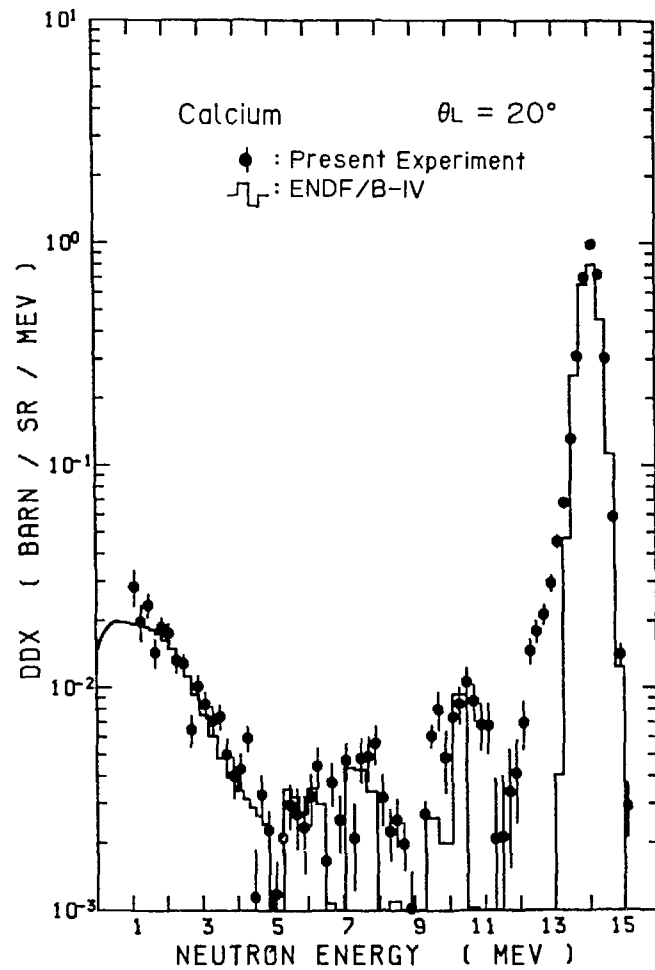


Fig. 2 Double differential neutron emission cross section at 20 deg with  $E_n = 14.1$  MeV, for Ca

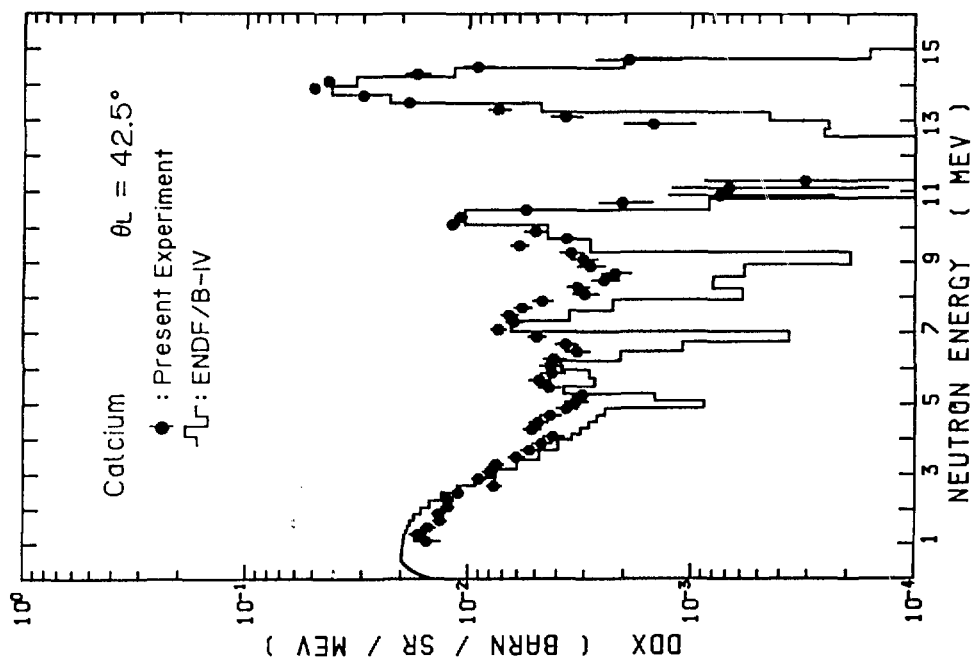


Fig. 4 Double differential neutron emission cross section at 42.5 deg with  $E_n = 14.1$  MeV, for Ca

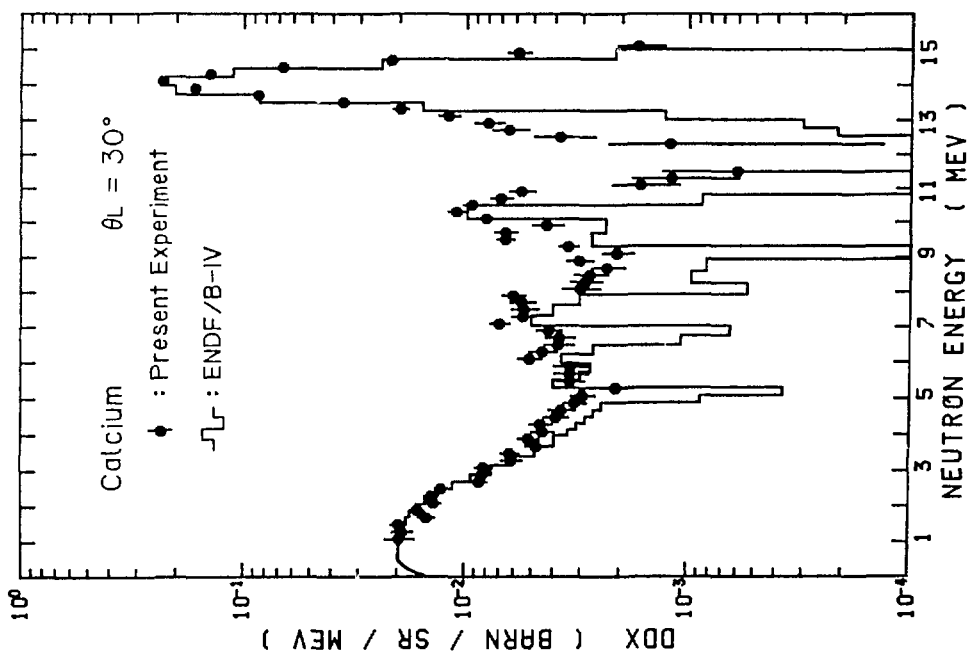


Fig. 3 Double differential neutron emission cross section at 30 deg with  $E_n = 14.1$  MeV, for Ca

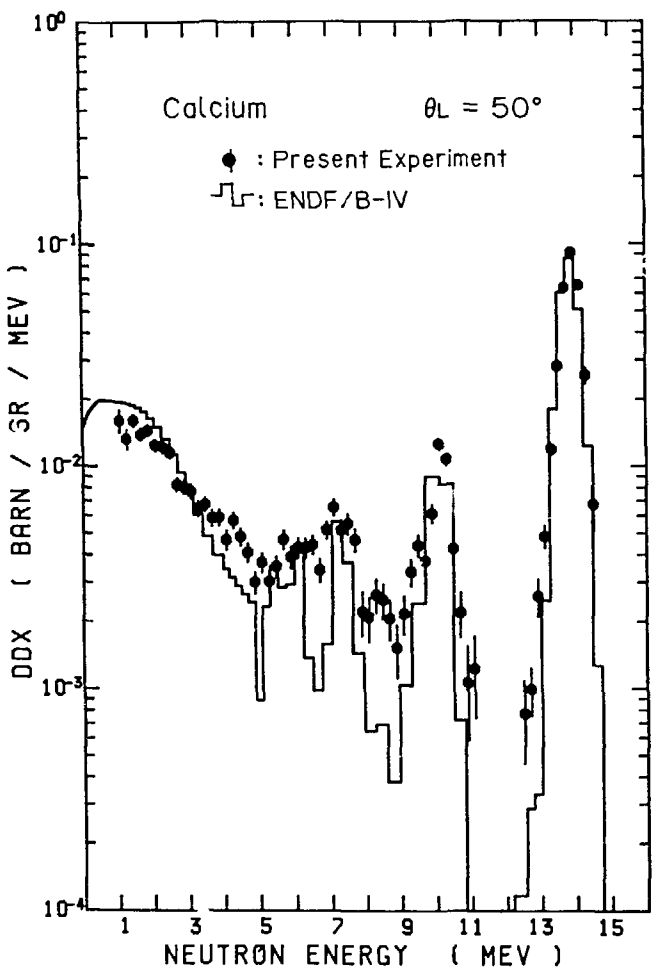


Fig. 5 Double differential neutron emission cross section at 50 deg with  $E_n = 14.1$  MeV, for Ca

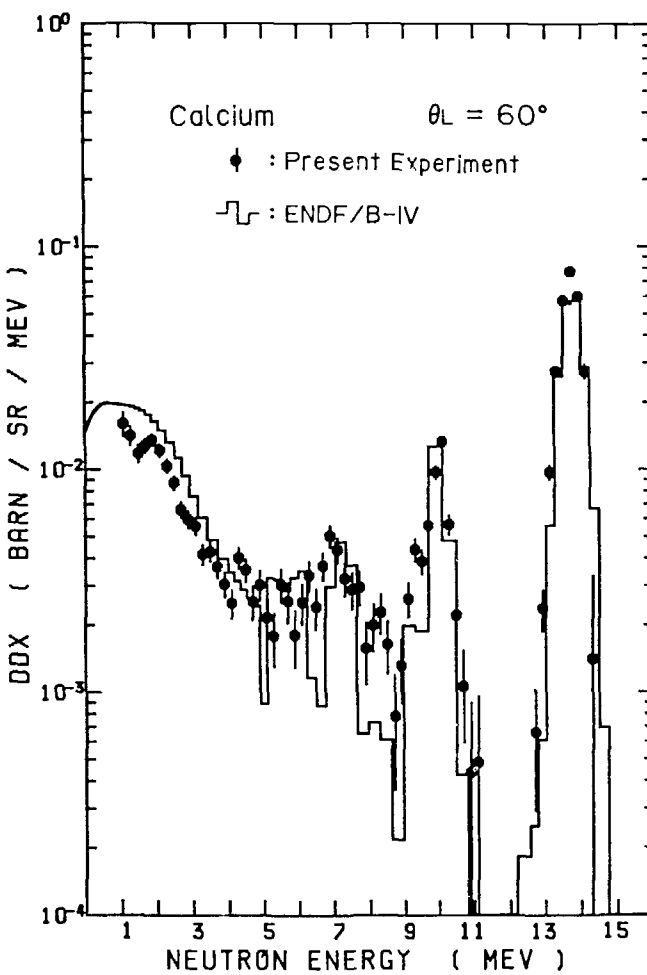


Fig. 6 Double differential neutron emission cross section at 60 deg with  $E_n = 14.1$  MeV, for Ca

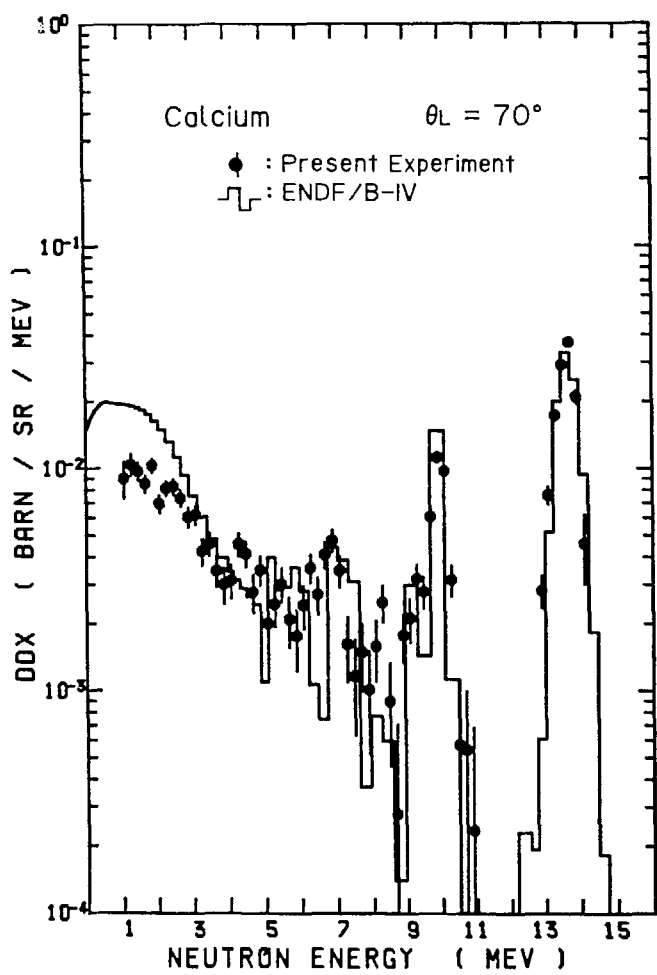


Fig. 7 Double differential neutron emission cross section at 70 deg with  $E_n = 14.1$  MeV, for Ca

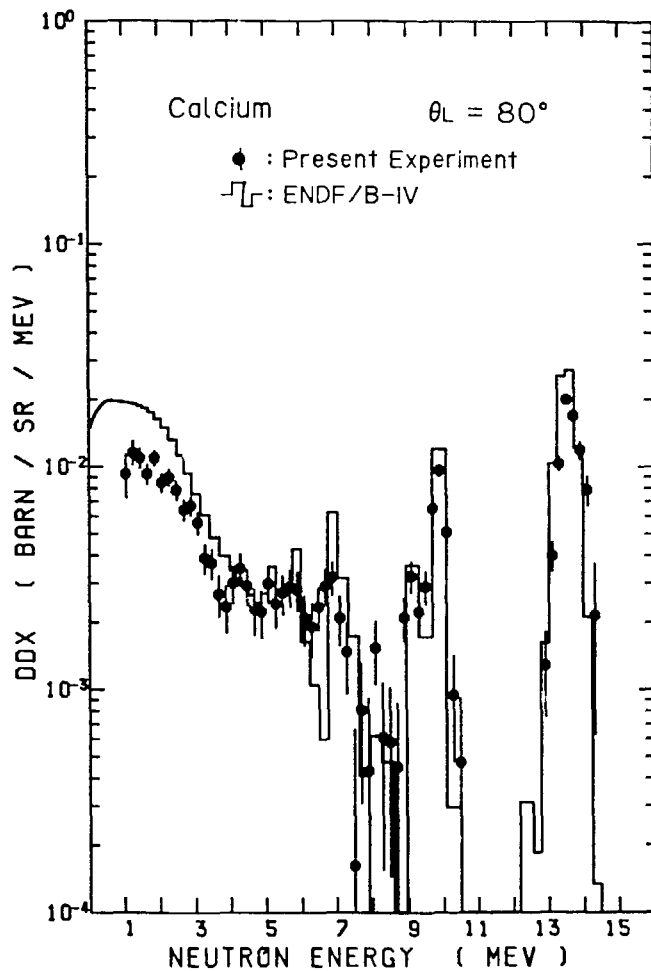


Fig. 8 Double differential neutron emission cross section at 80 deg with  $E_n = 14.1$  MeV, for Ca

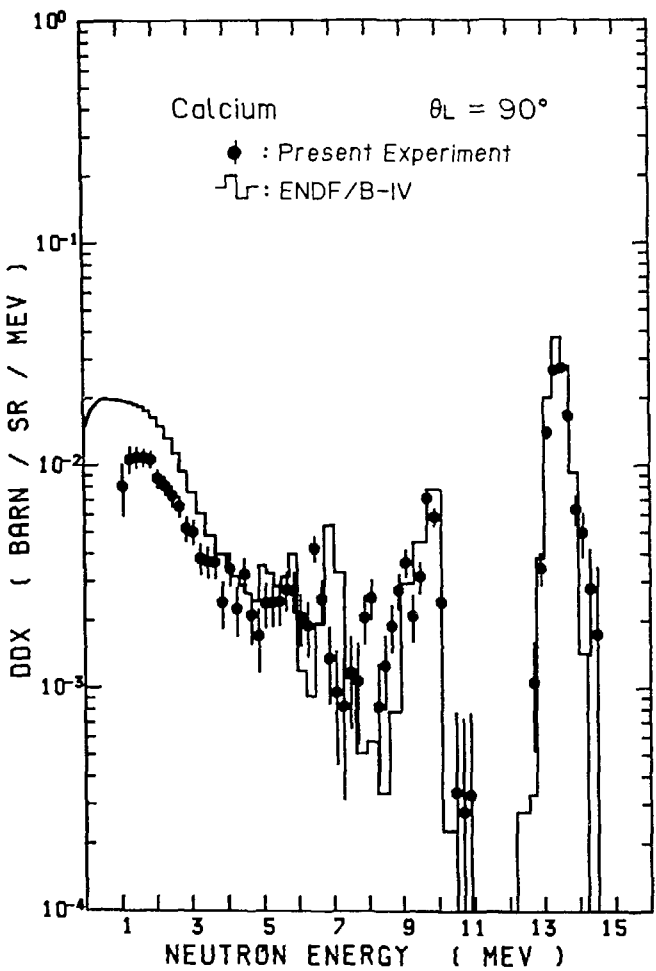


Fig. 9 Double differential neutron emission cross section at 90 deg with  $E_n = 14.1$  MeV, for Ca

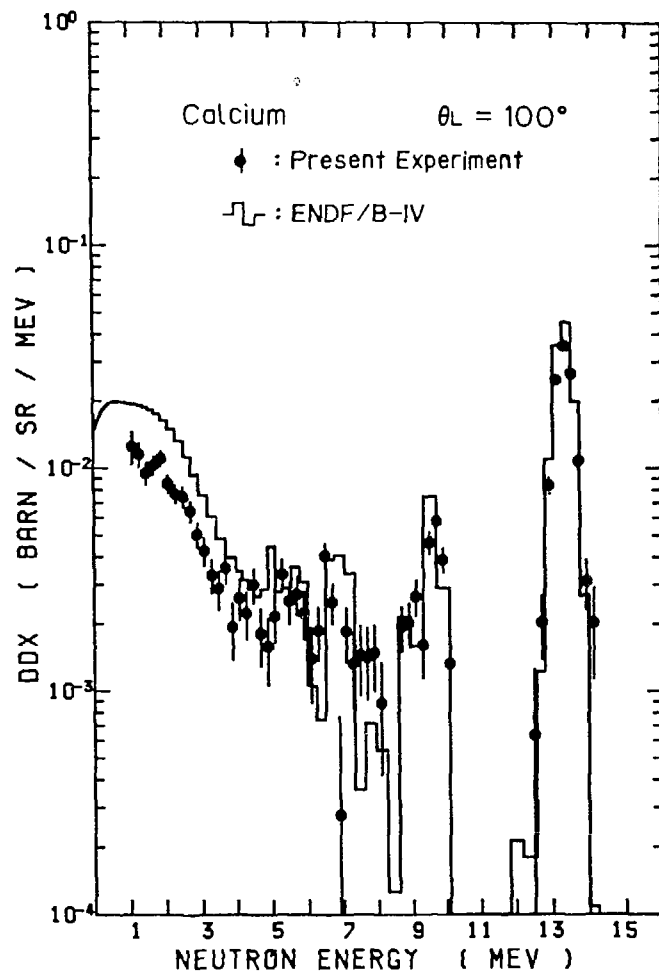


Fig. 10 Double differential neutron emission cross section at 100 deg with  $E_n = 14.1$  MeV, for Ca

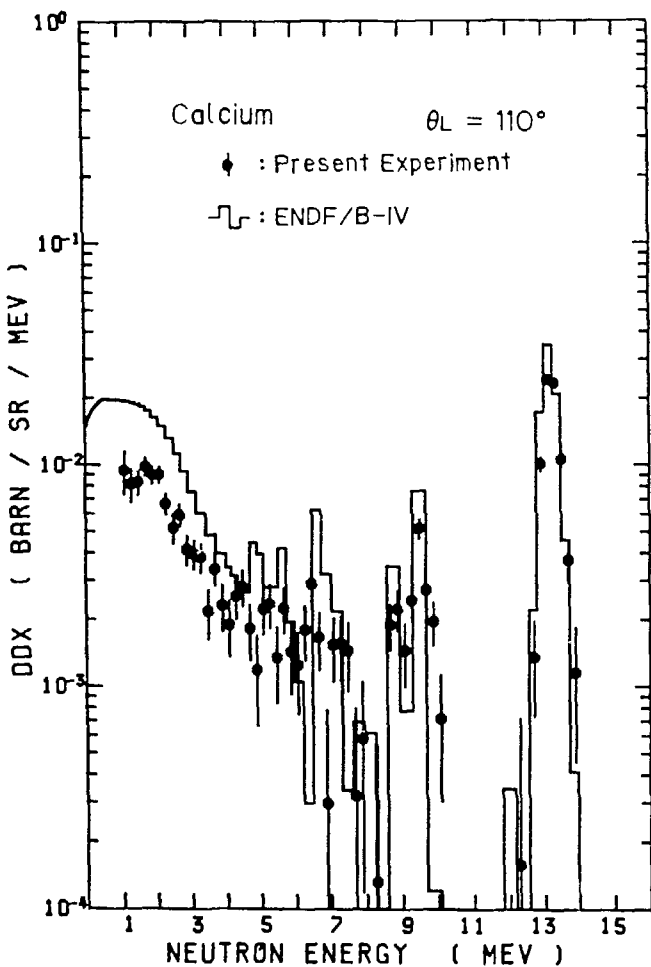


Fig. 11 Double differential neutron emission cross section at 110 deg with  $E_n = 14.1$  MeV, for Ca

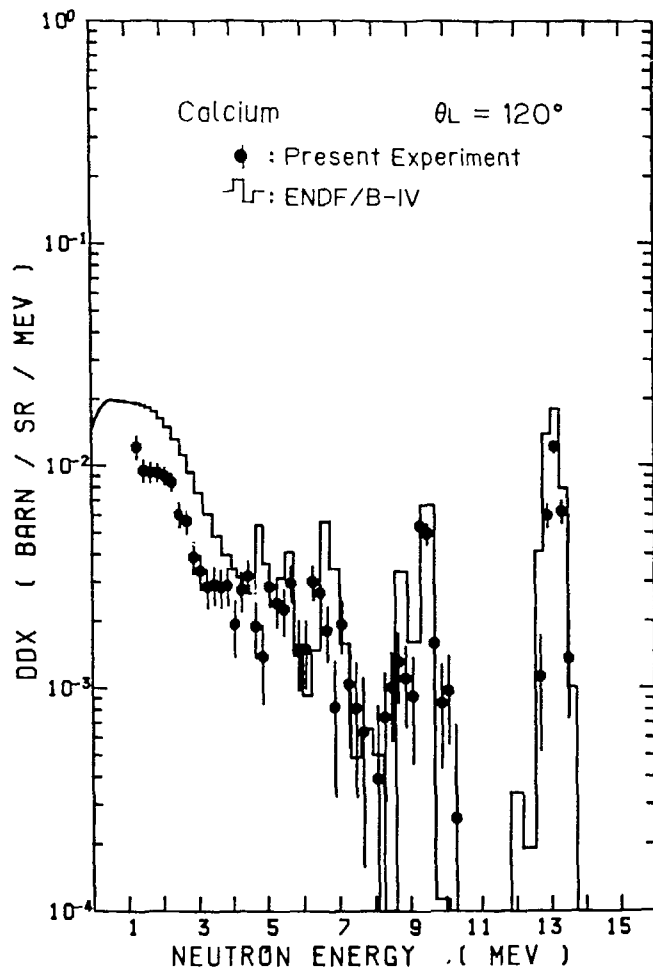


Fig. 12 Double differential neutron emission cross section at 120 deg with  $E_n = 14.1$  MeV, for Ca

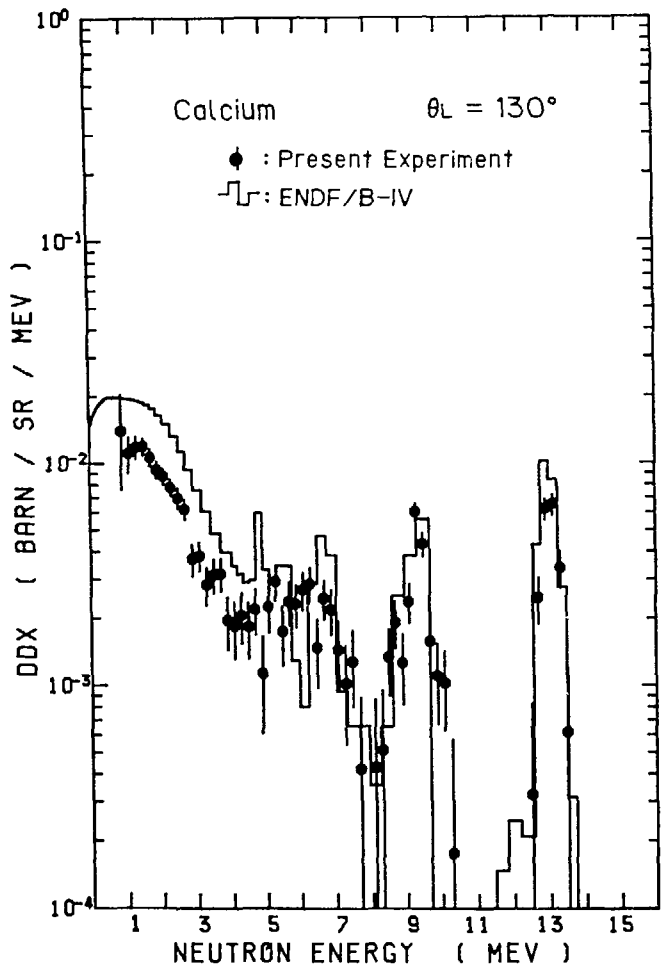


Fig. 13 Double differential neutron emission cross section at 130 deg with  $E_n = 14.1$  MeV, for Ca

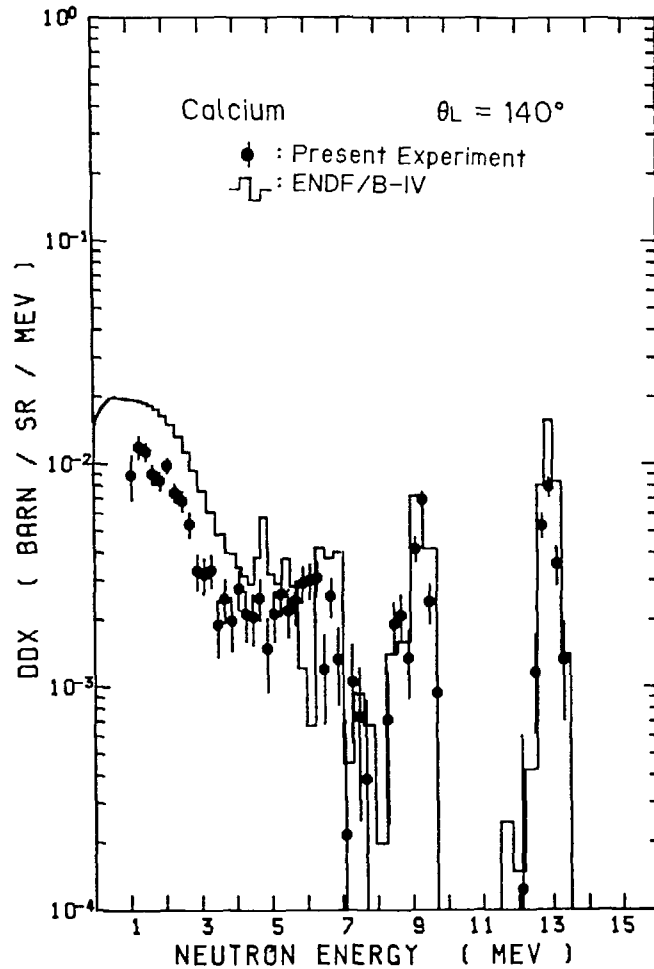


Fig. 14 Double differential neutron emission cross section at 140 deg with  $E_n = 14.1$  MeV, for Ca

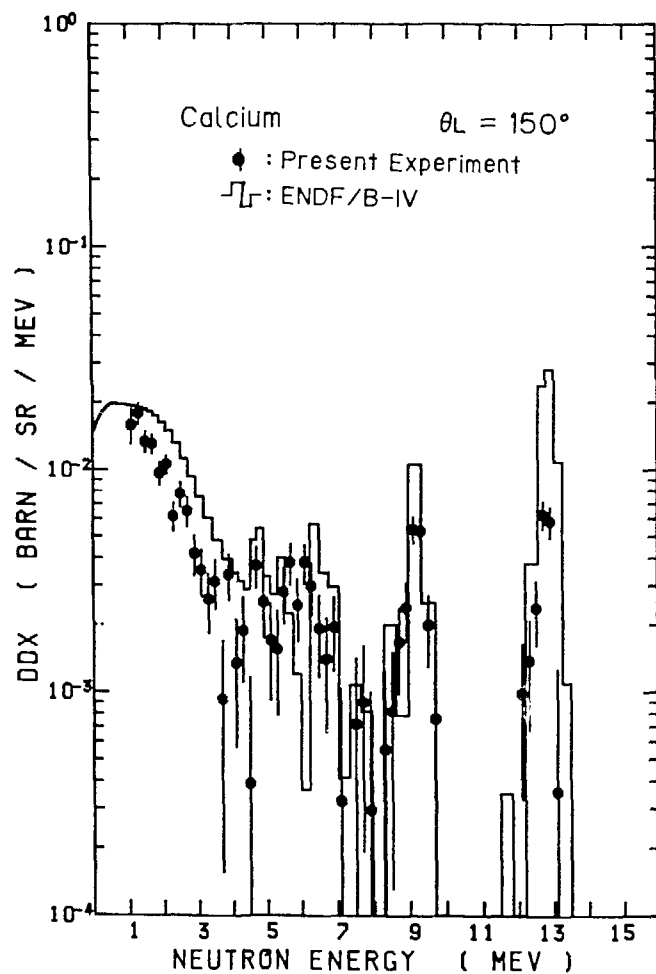


Fig. 15 Double differential neutron emission cross section at 150 deg with  $E_n = 14.1$  MeV, for Ca

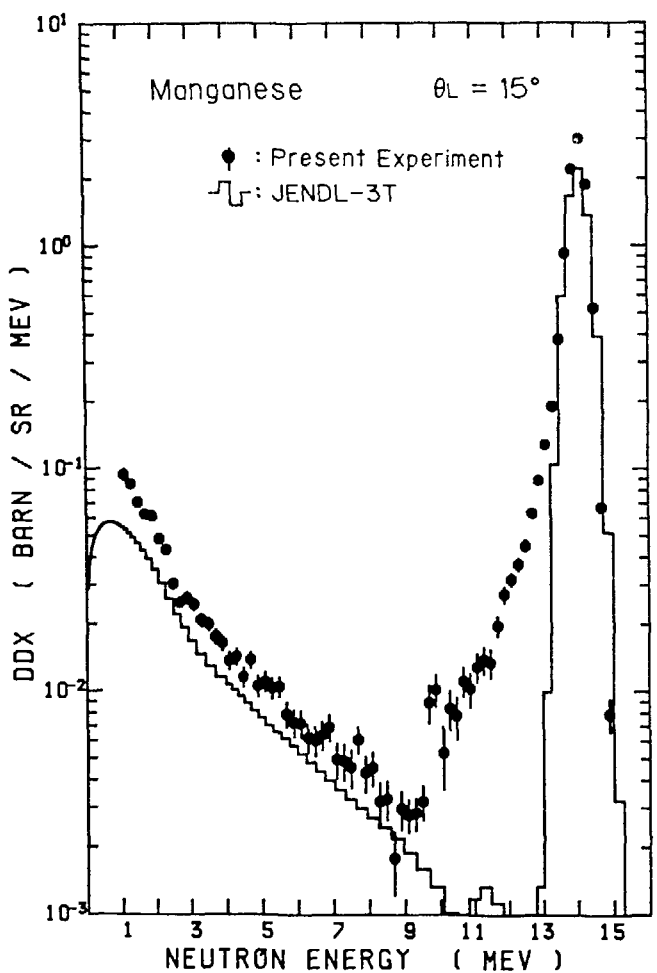


Fig. 16 Double differential neutron emission cross section at 15 deg with  $E_n = 14.1$  MeV, for Mn

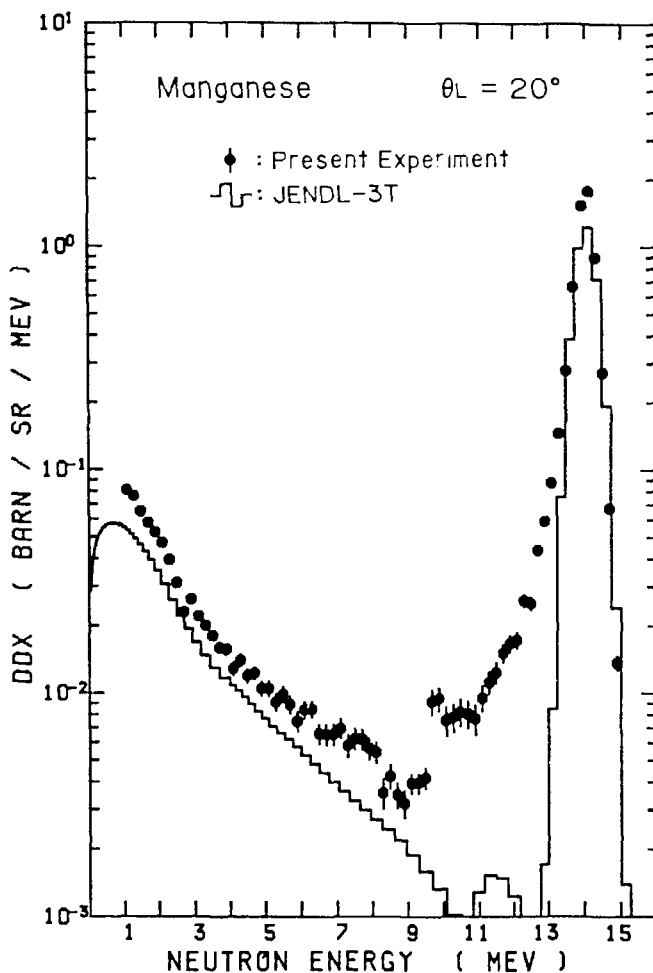


Fig. 17 Double differential neutron emission cross section at 20 deg with  $E_n = 14.1$  MeV, for Mn

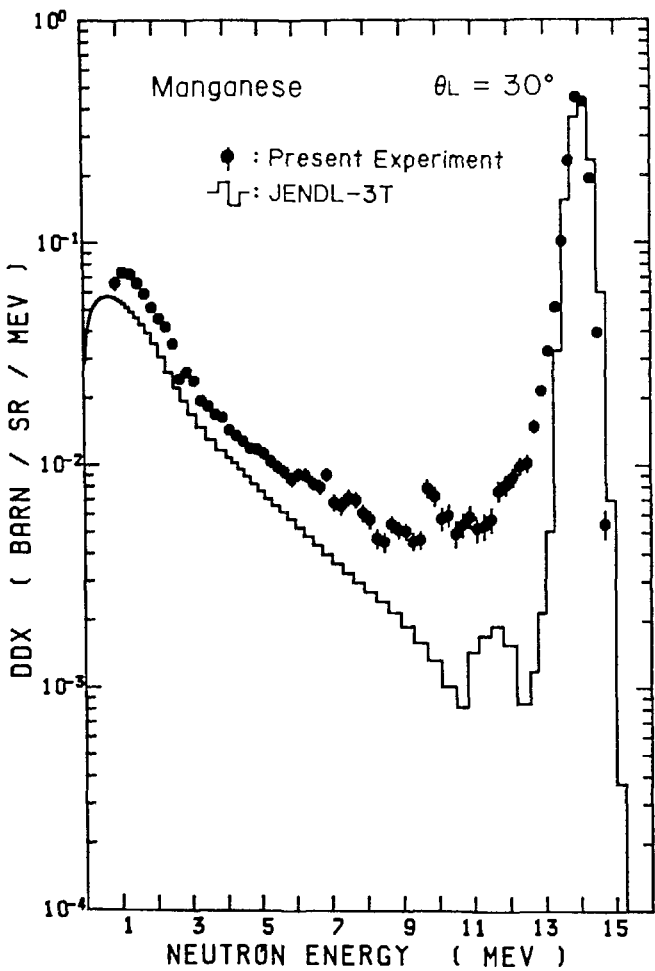


Fig. 18 Double differential neutron emission cross section at 30 deg with  $E_n = 14.1$  MeV, for Mn

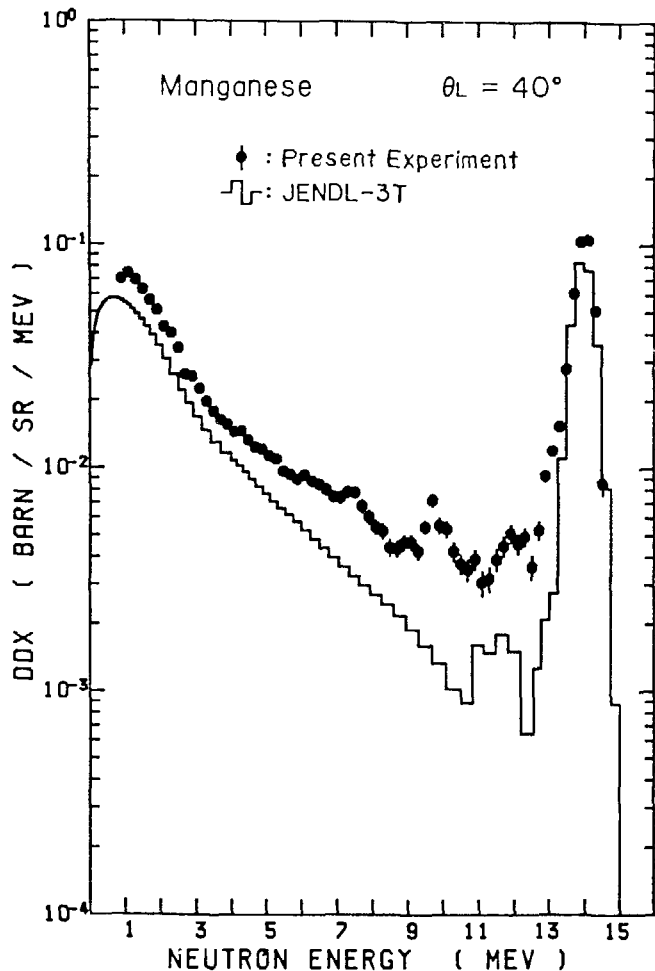


Fig. 19 Double differential neutron emission cross section at 40 deg with  $E_n = 14.1$  MeV, for Mn

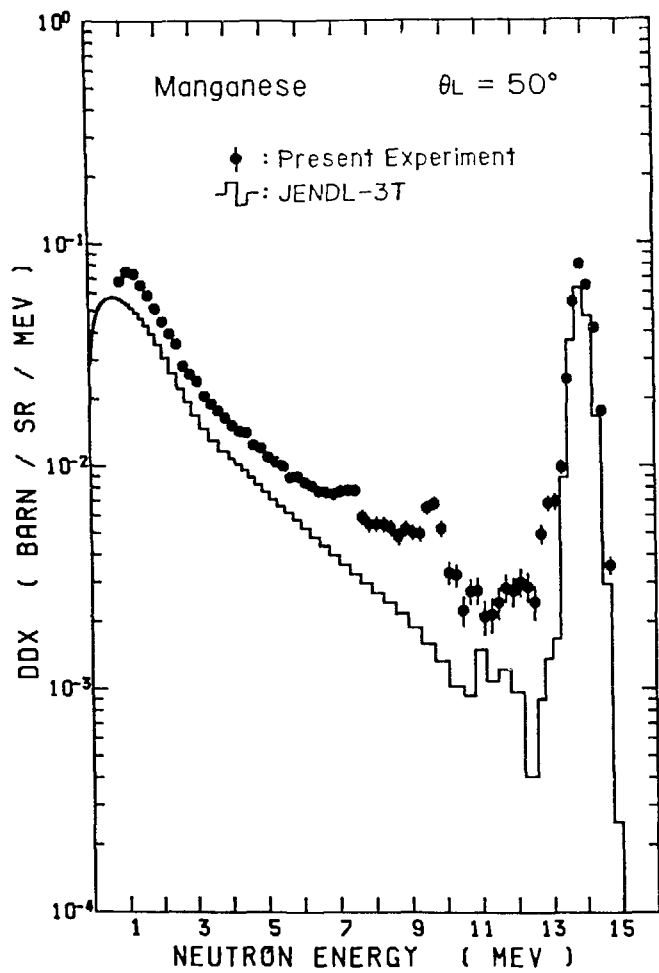


Fig. 20 Double differential neutron emission cross section at 50 deg with  $E_n = 14.1$  MeV, for Mn

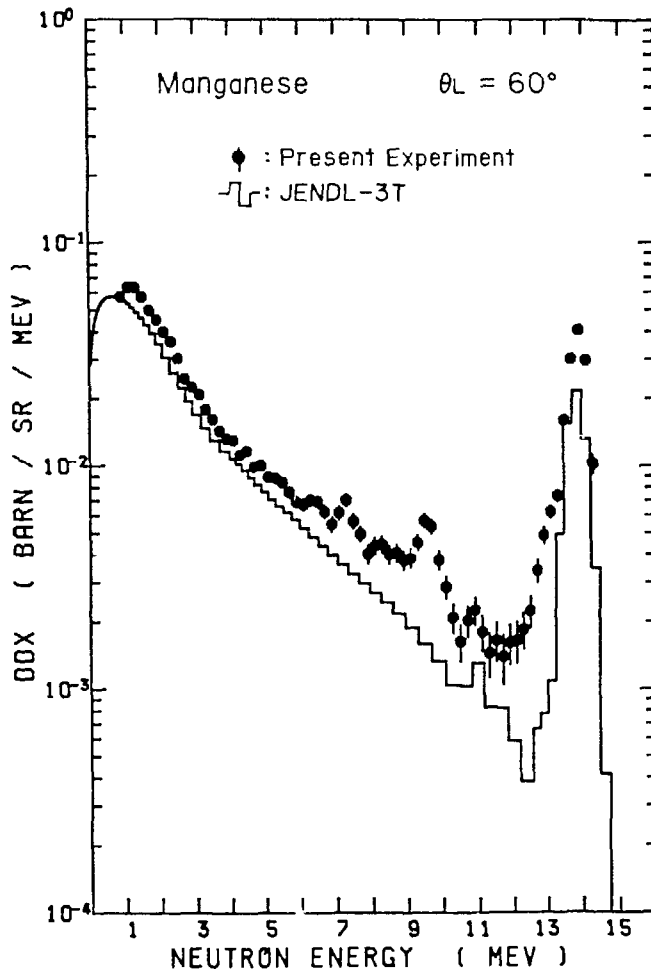


Fig. 21 Double differential neutron emission cross section at 60 deg with  $E_n = 14.1$  MeV, for Mn

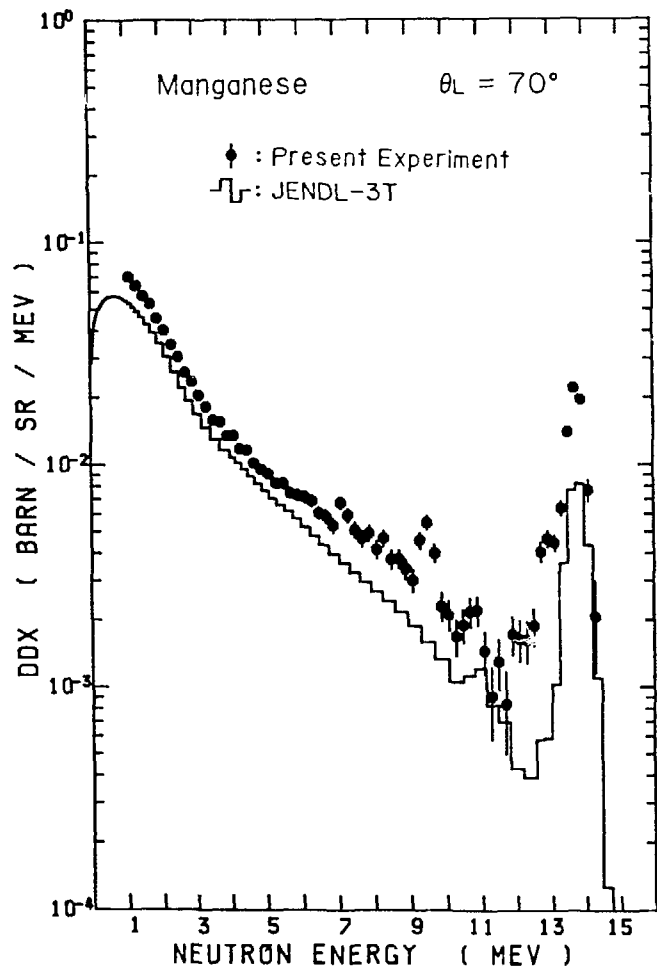


Fig. 22 Double differential neutron emission cross section at 70 deg with  $E_n = 14.1$  MeV, for Mn

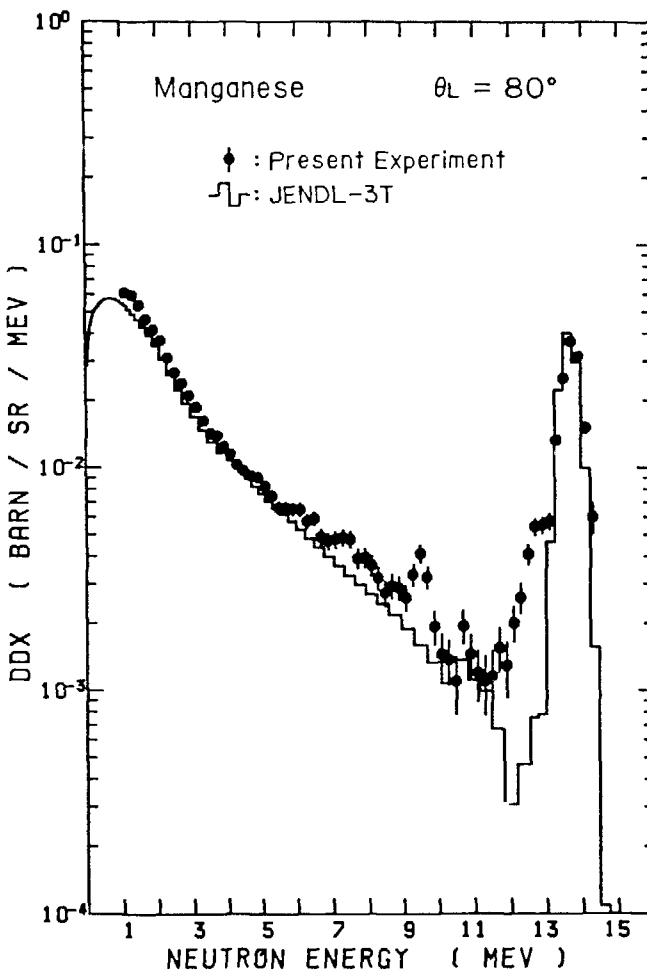


Fig. 23 Double differential neutron emission cross section at 80 deg with  $E_n = 14.1$  MeV, for Mn

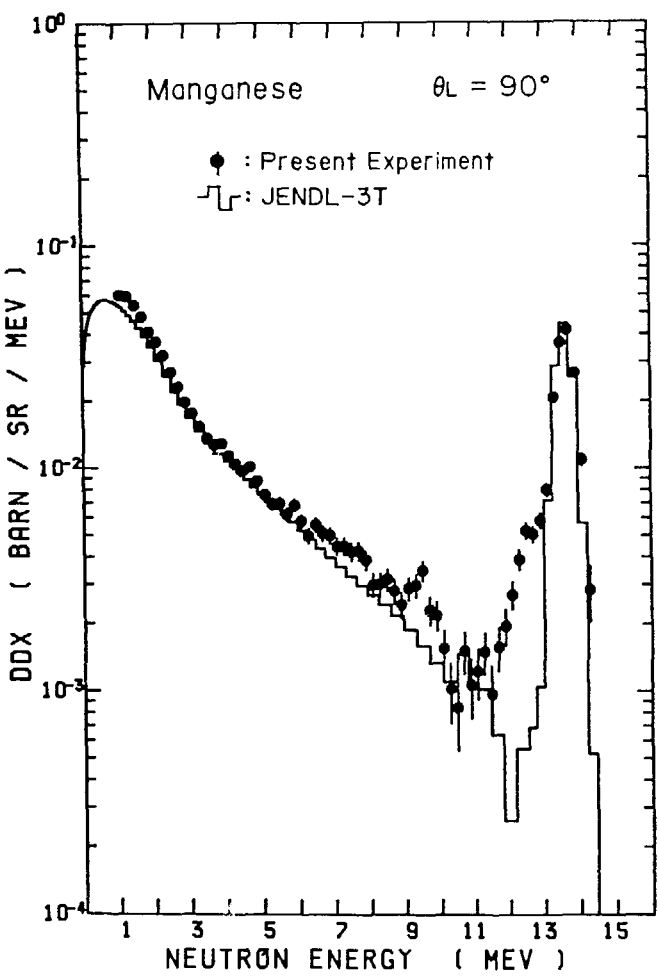


Fig. 24 Double differential neutron emission cross section at 90 deg with  $E_n = 14.1$  MeV, for Mn

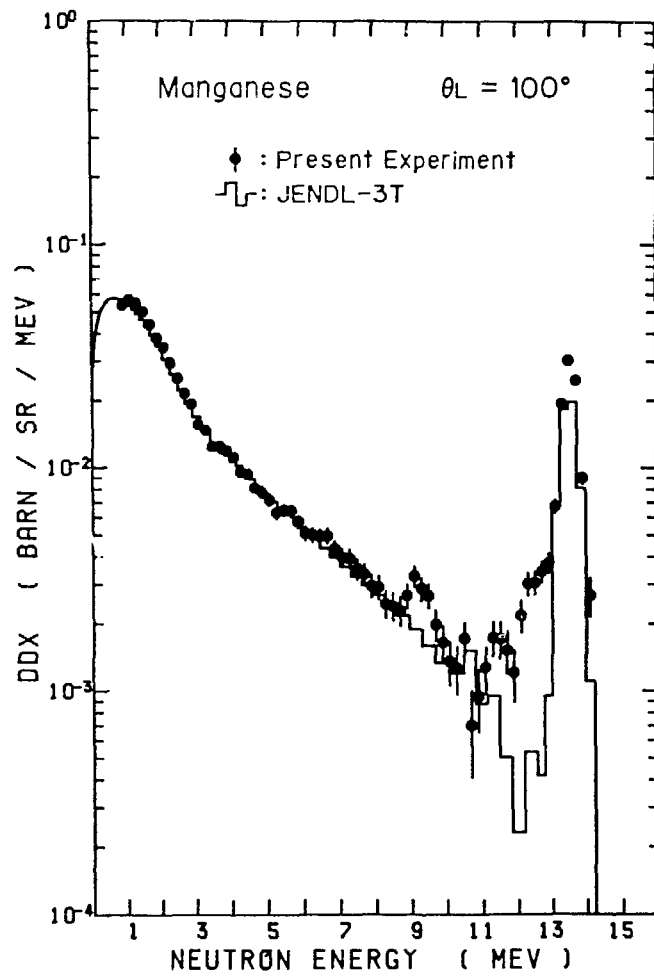


Fig. 25 Double differential neutron emission cross section at 100 deg with  $E_n = 14.1$  MeV, for Mn

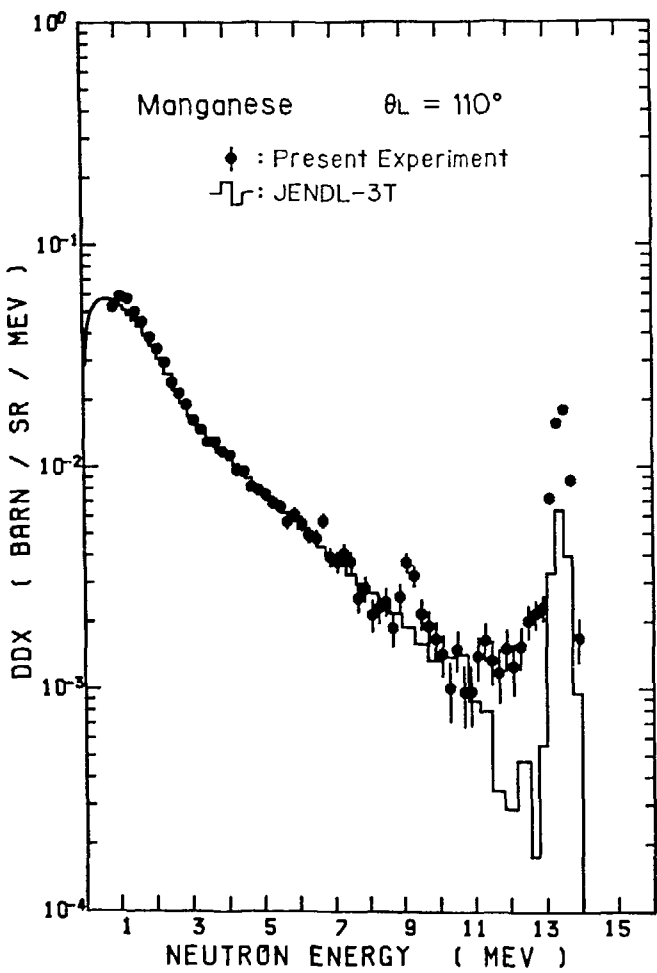


Fig. 26 Double differential neutron emission cross section at 110 deg with  $E_n = 14.1$  MeV, for Mn

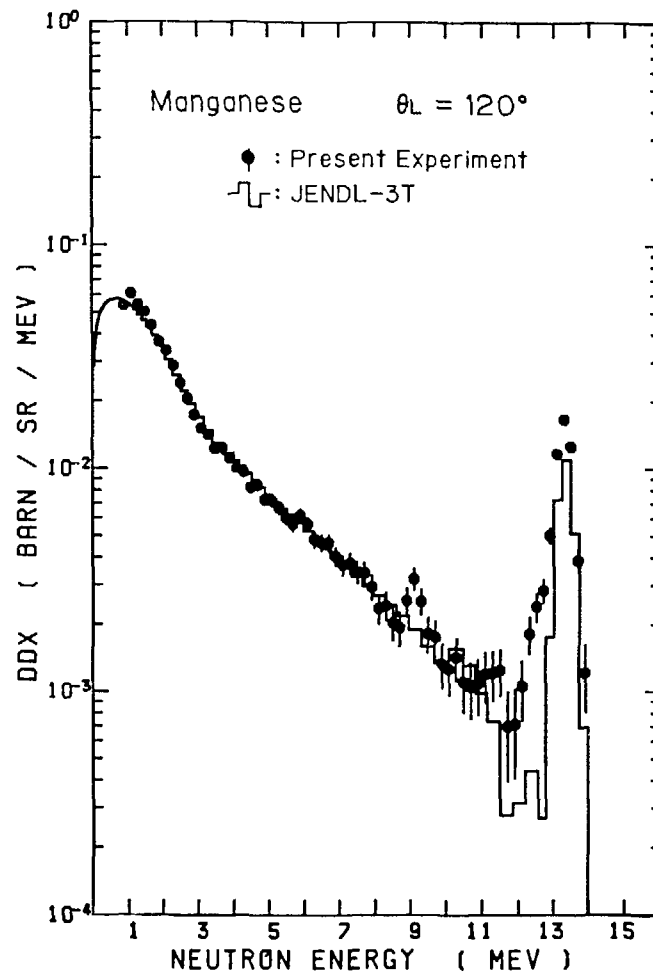


Fig. 27 Double differential neutron emission cross section at 120 deg with  $E_n = 14.1$  MeV, for Mn

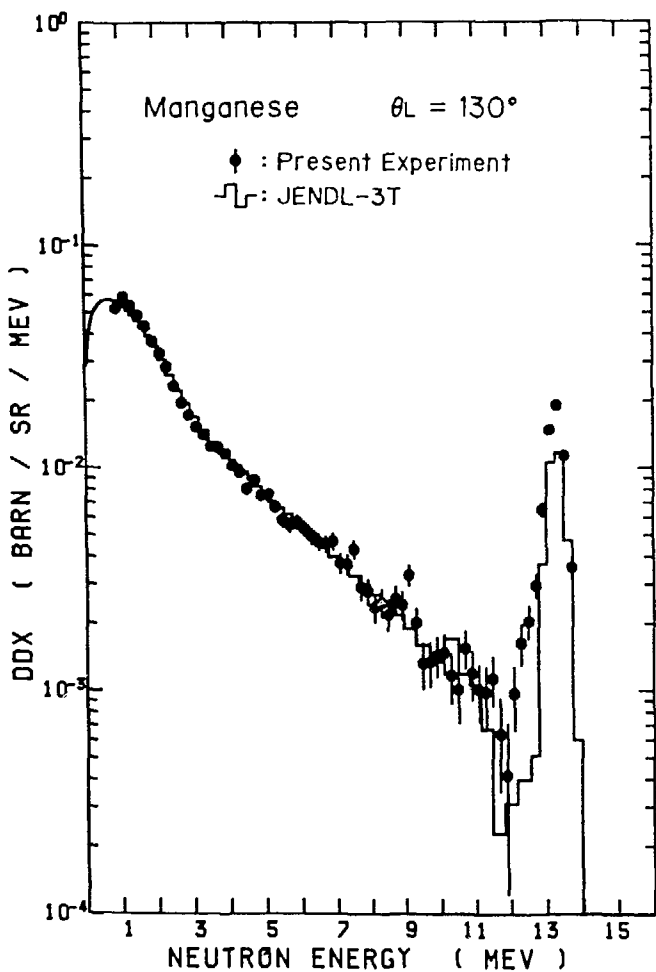


Fig. 28 Double differential neutron emission cross section at 130 deg with  $E_n = 14.1$  MeV, for Mn

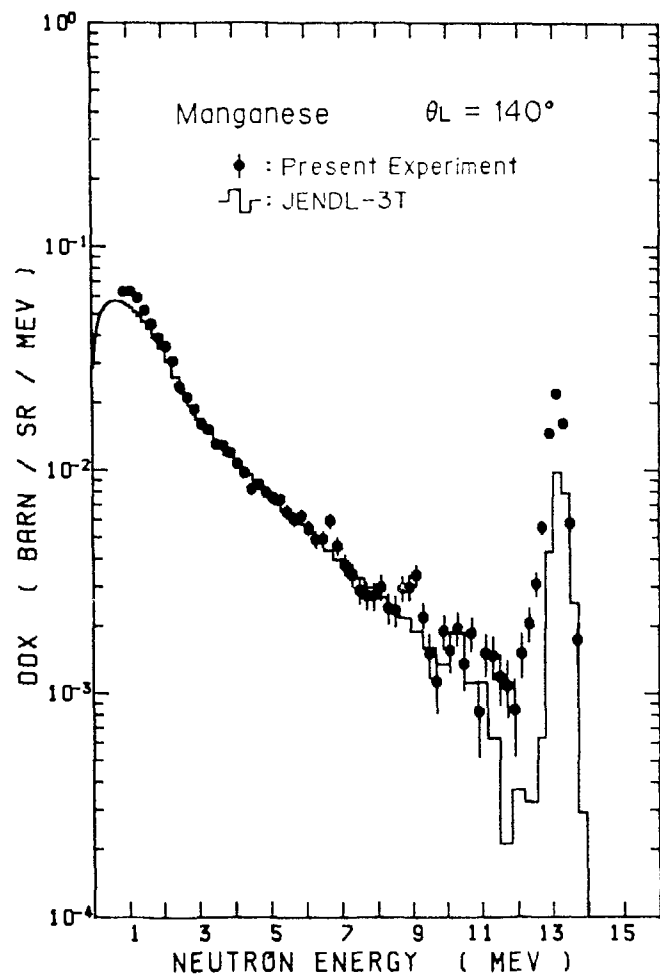


Fig. 29 Double differential neutron emission cross section at 140 deg with  $E_n = 14.1$  MeV, for Mn

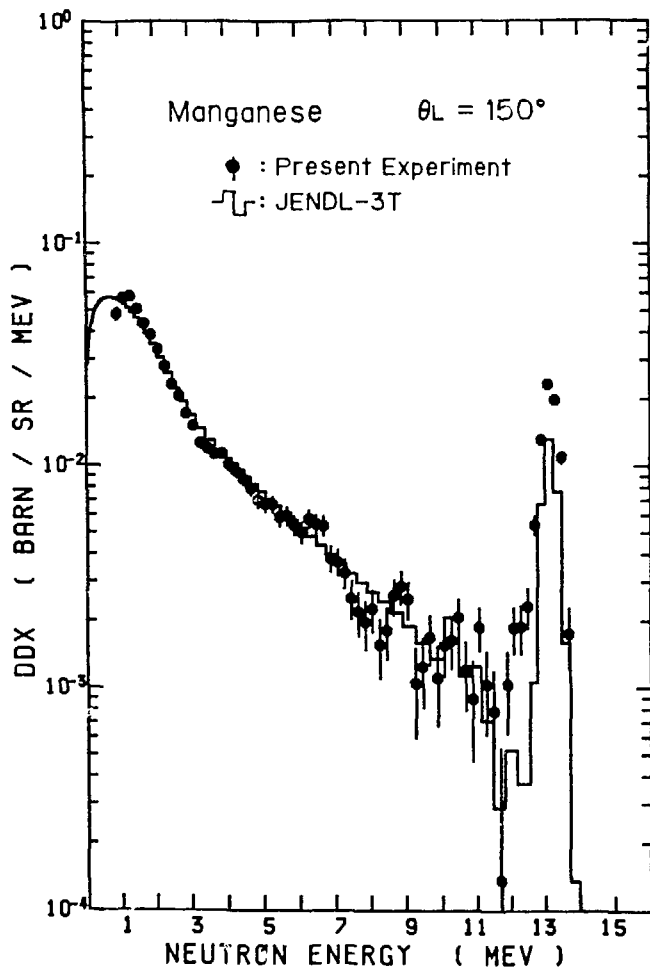


Fig. 30 Double differential neutron emission cross section at 150 deg with  $E_n = 14.1$  MeV, for Mn

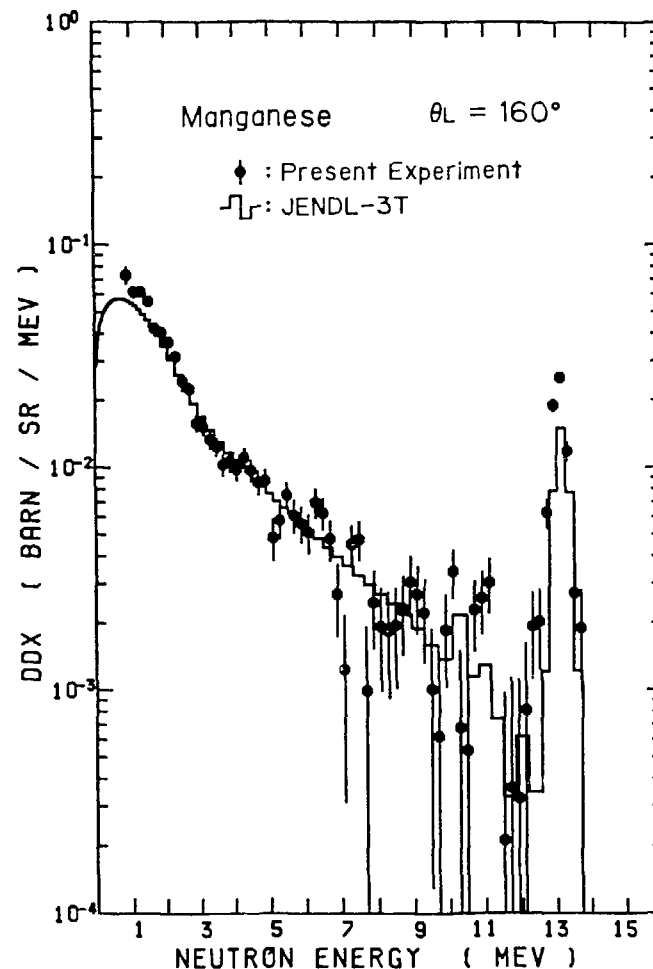


Fig. 31 Double differential neutron emission cross section at 160 deg with  $E_n = 14.1$  MeV, for Mn

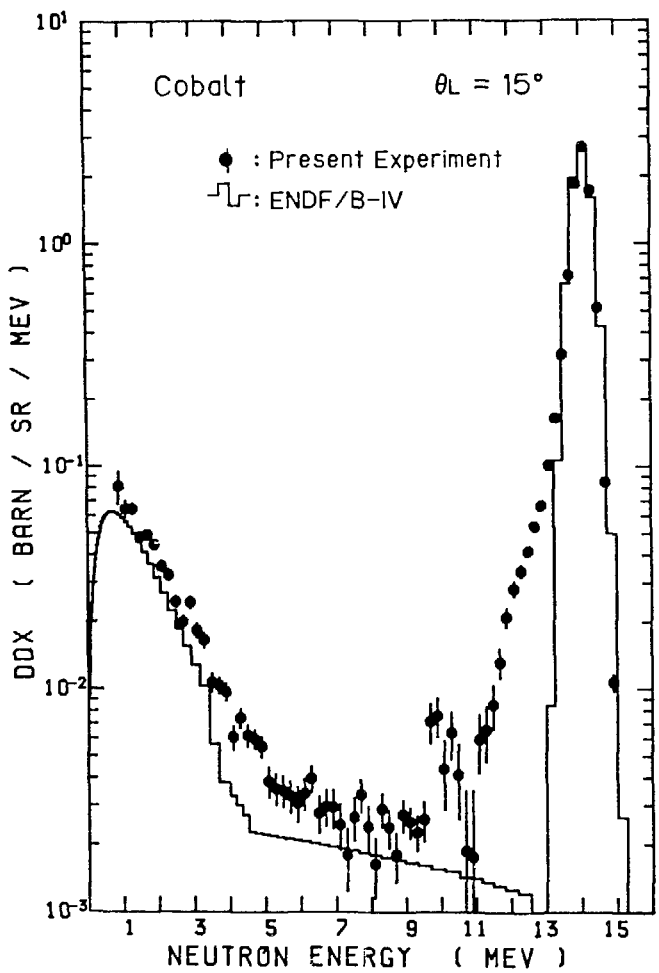


Fig. 32 Double differential neutron emission cross section at 15 deg with  $E_n = 14.1$  MeV, for Co

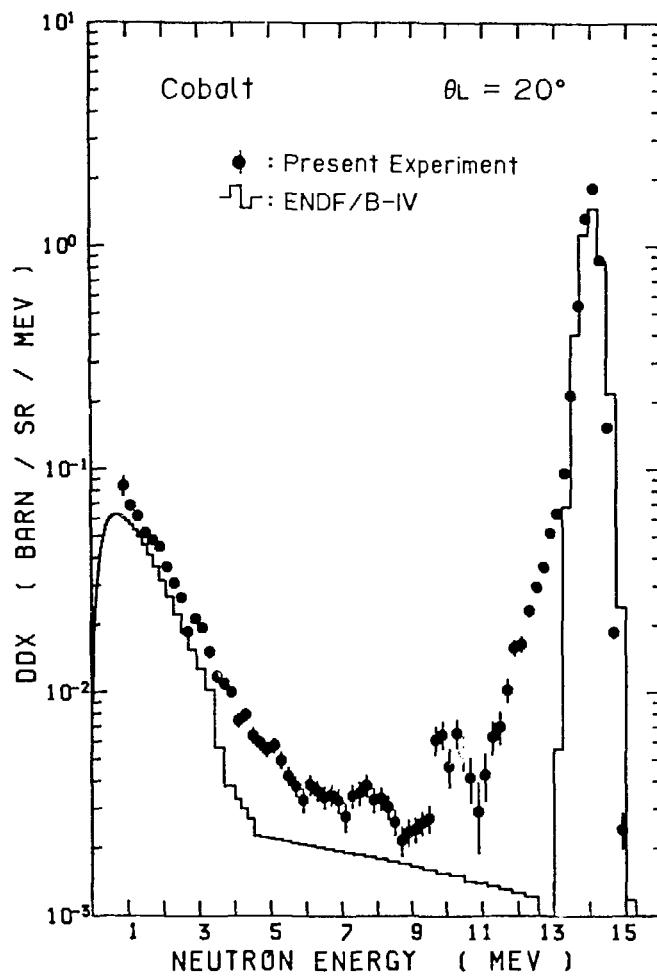


Fig. 33 Double differential neutron emission cross section at 20 deg with  $E_n = 14.1$  MeV, for Co

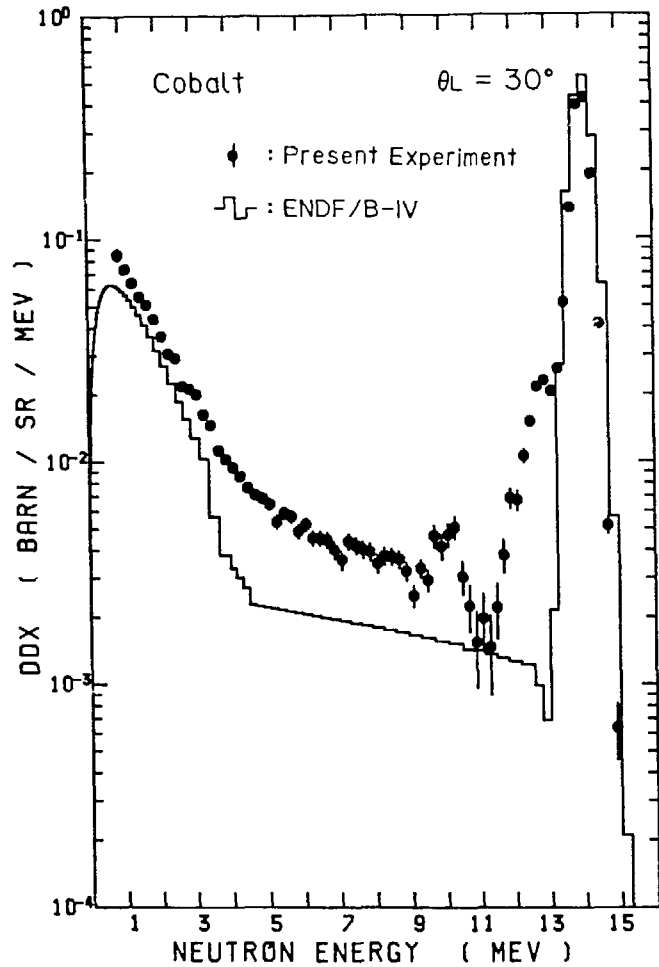


Fig. 34 Double differential neutron emission cross section at 30 deg with  $E_n = 14.1$  MeV, for Co

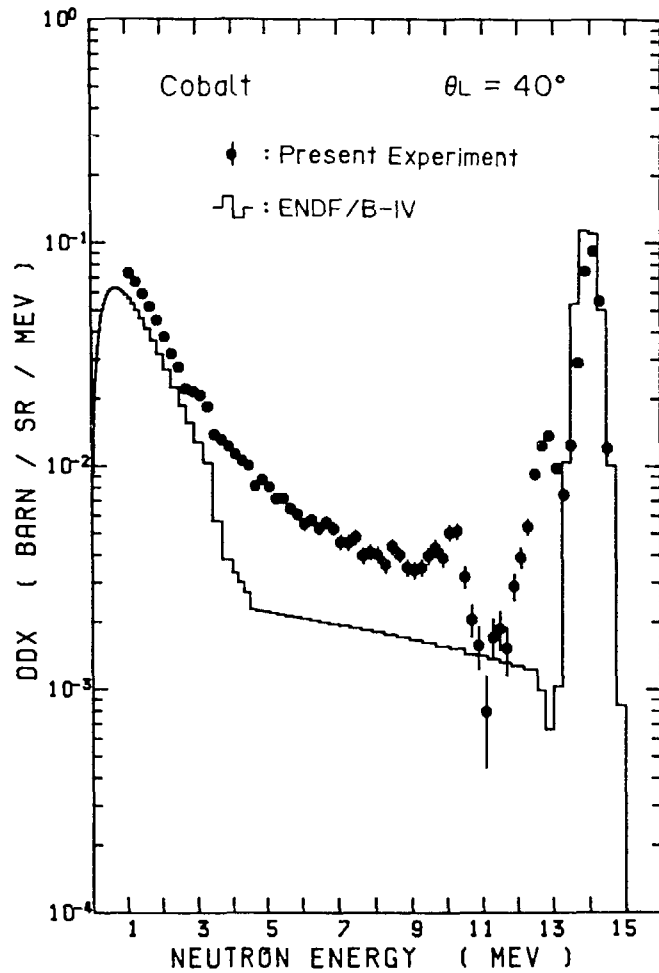


Fig. 35 Double differential neutron emission cross section at 40 deg with  $E_n = 14.1$  MeV, for Co

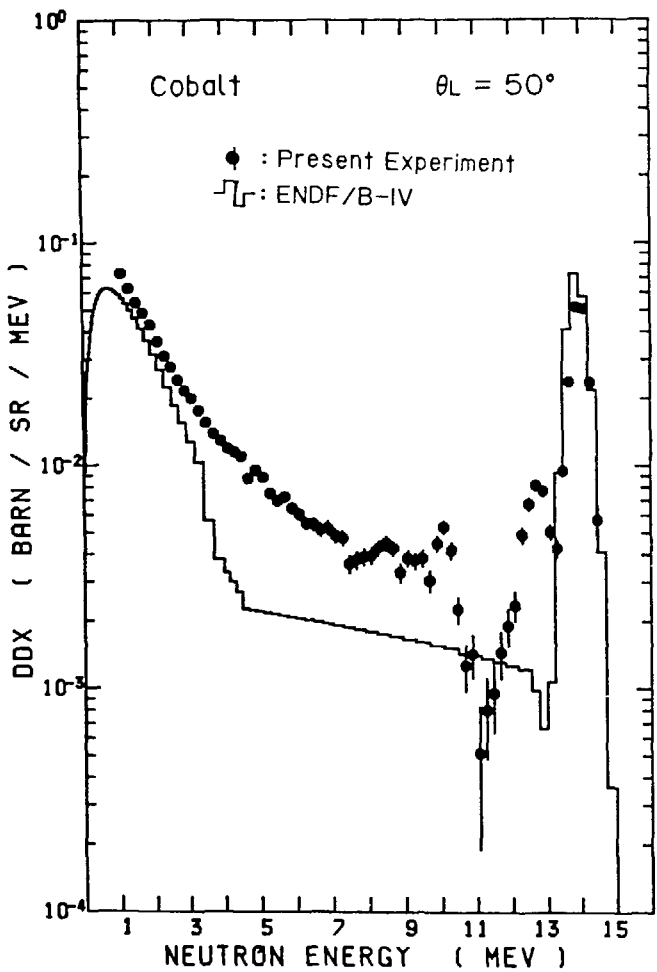


Fig. 36 Double differential neutron emission cross section at 50 deg with  $E_n = 14.1$  MeV, for Co

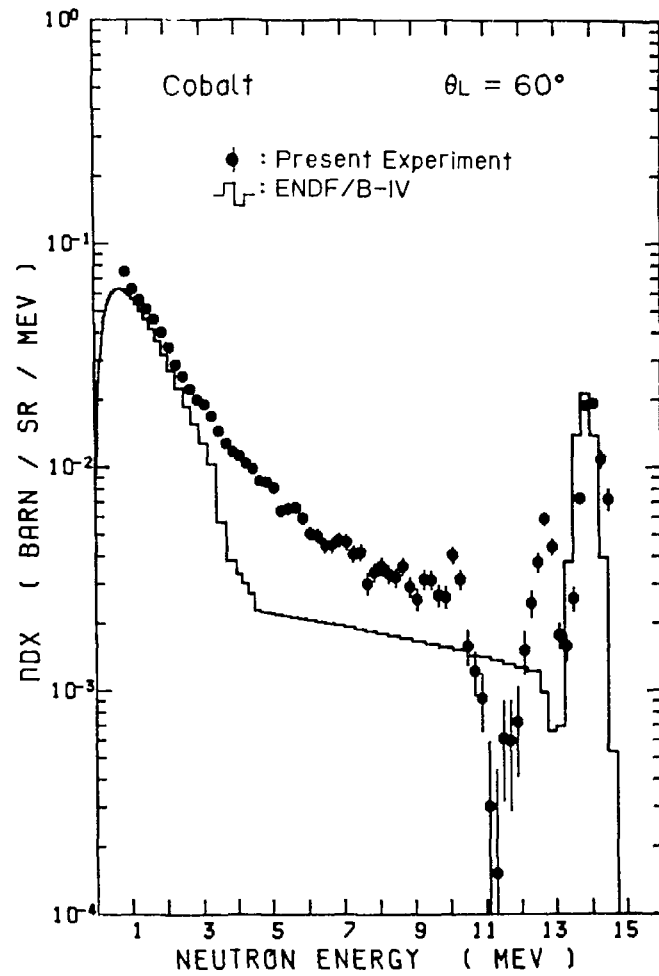


Fig. 37 Double differential neutron emission cross section at 60 deg with  $E_n = 14.1$  MeV, for Co

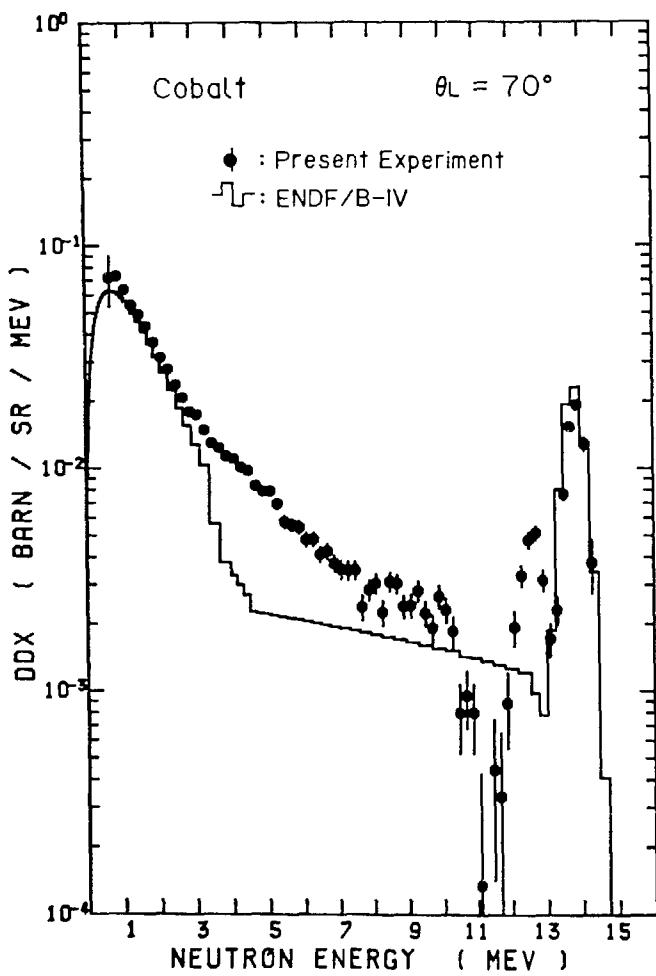


Fig. 38 Double differential neutron emission cross section at 70 deg with  $E_n = 14.1$  MeV, for Co

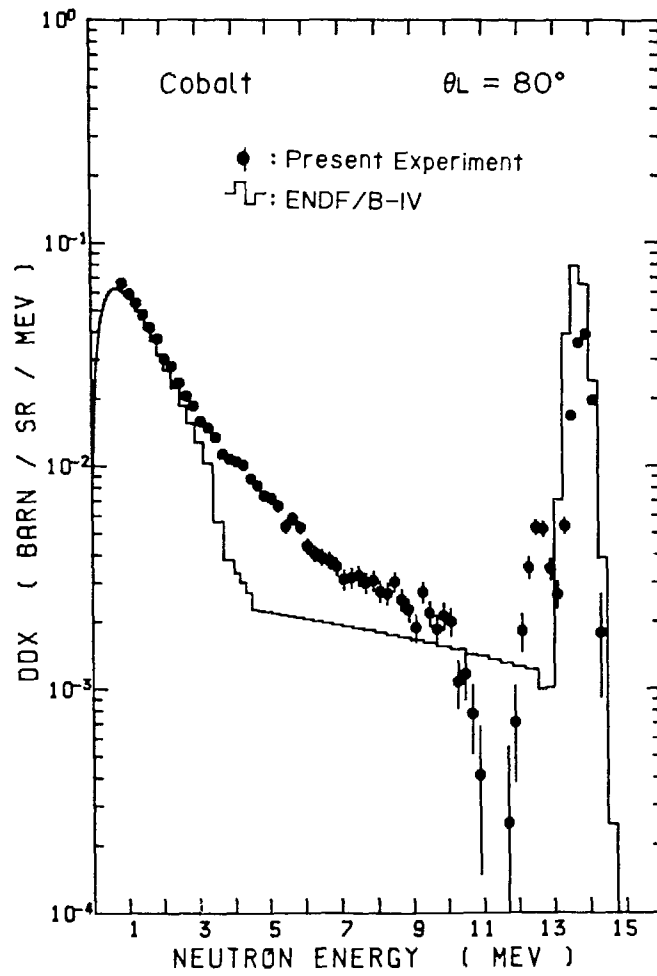


Fig. 39 Double differential neutron emission cross section at 80 deg with  $E_n = 14.1$  MeV, for Co

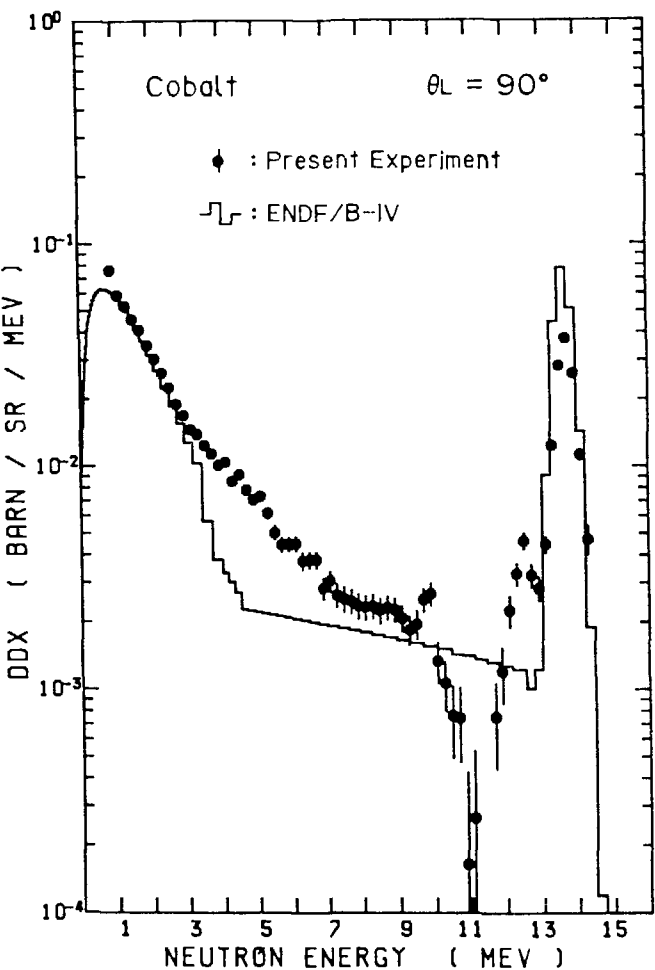


Fig. 40 Double differential neutron emission cross section at 90 deg with  $E_n = 14.1$  MeV, for Co

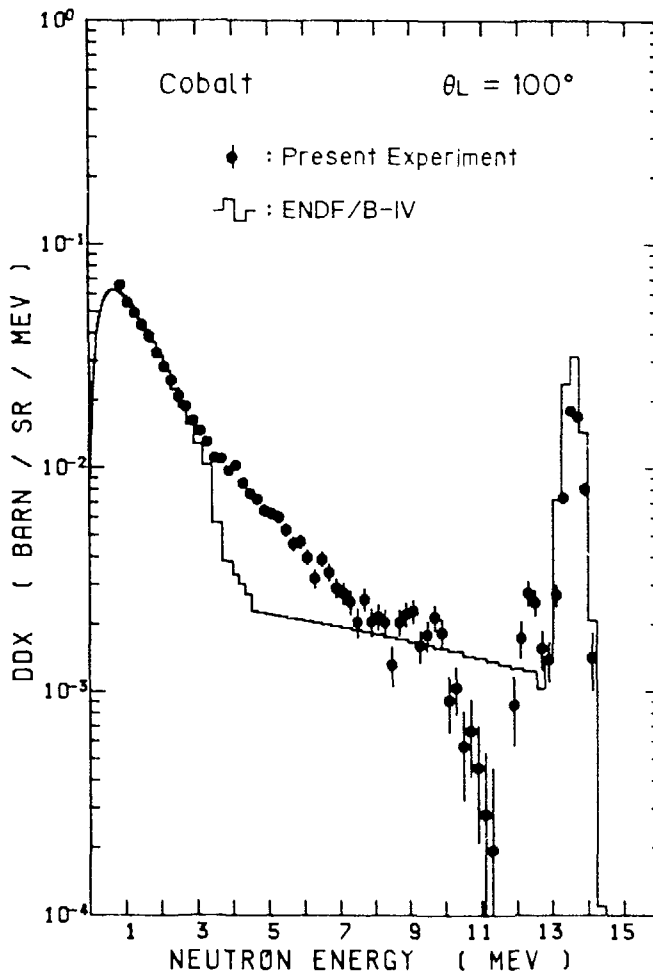


Fig. 41 Double differential neutron emission cross section at 100 deg with  $E_n = 14.1$  MeV, for Co

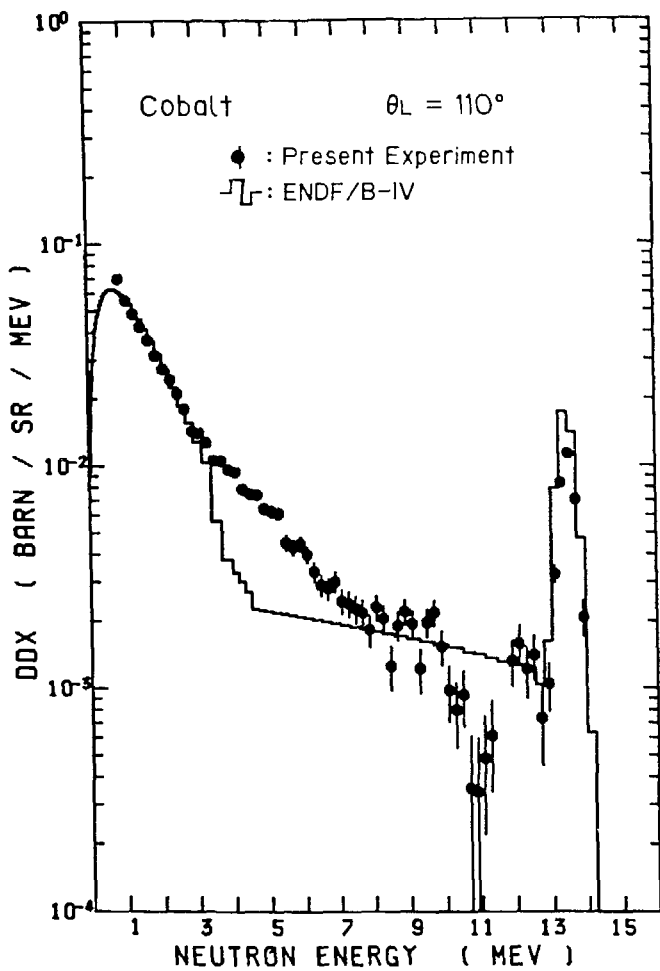


Fig. 42 Double differential neutron emission cross section at 110 deg with  $E_n = 14.1$  MeV, for Co

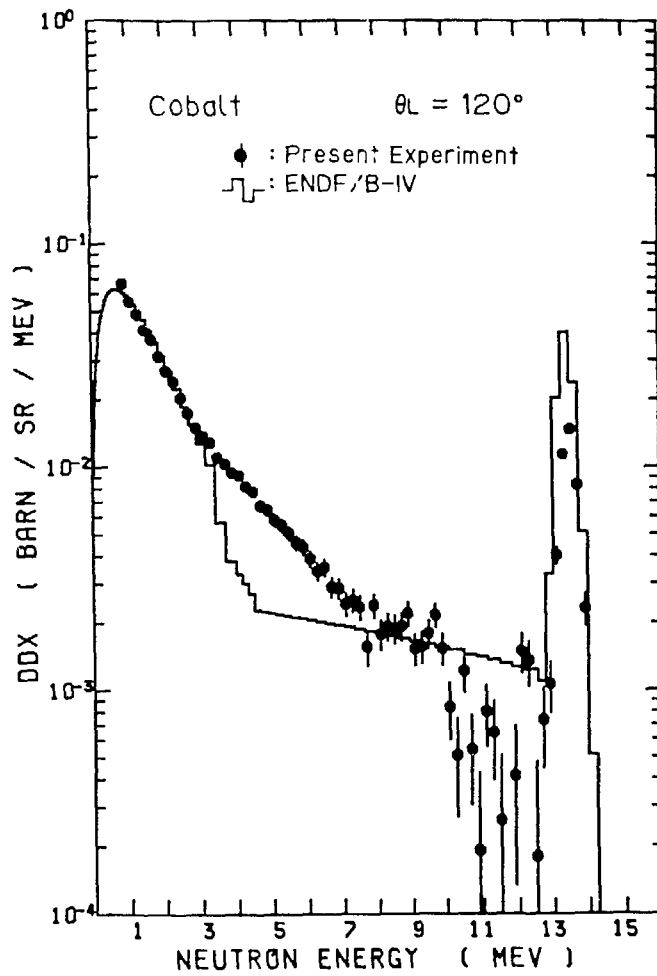


Fig. 43 Double differential neutron emission cross section at 120 deg with  $E_n = 14.1$  MeV, for Co

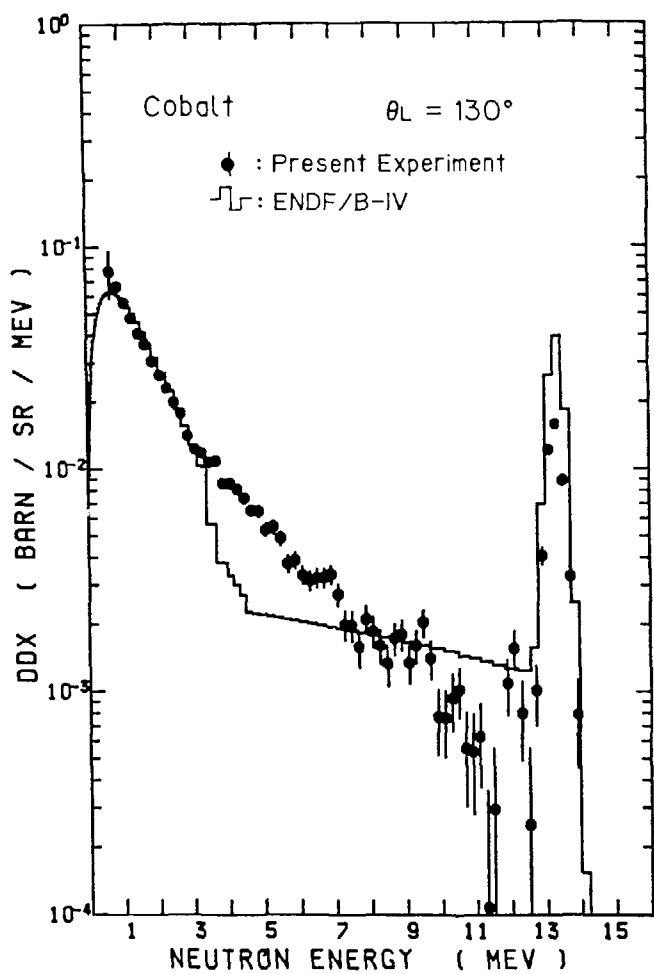


Fig. 44 Double differential neutron emission cross section at 130 deg with  $E_n = 14.1$  MeV, for Co

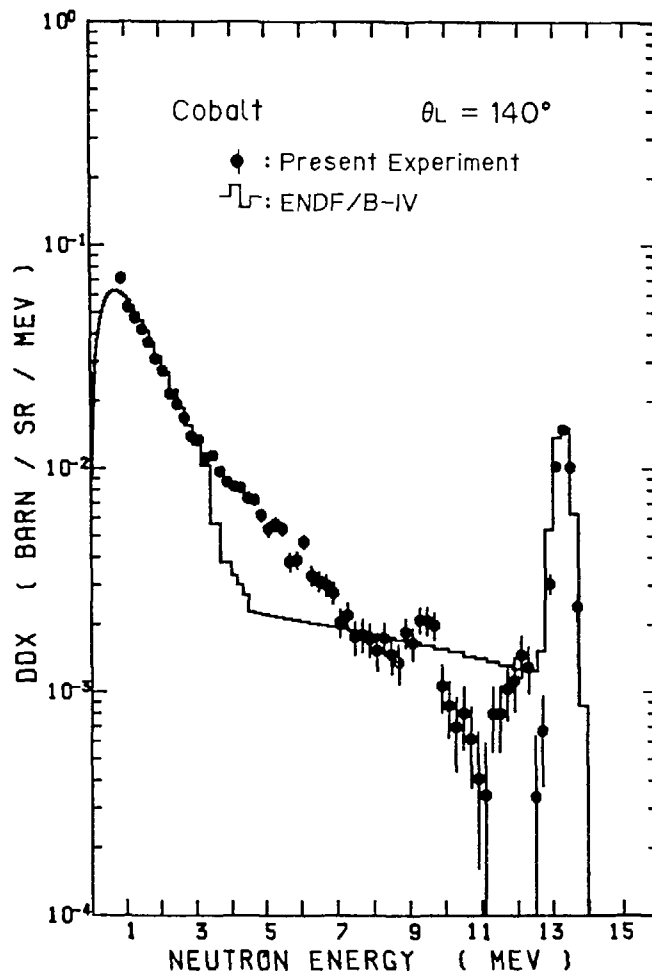


Fig. 45 Double differential neutron emission cross section at 140 deg with  $E_n = 14.1$  MeV, for Co

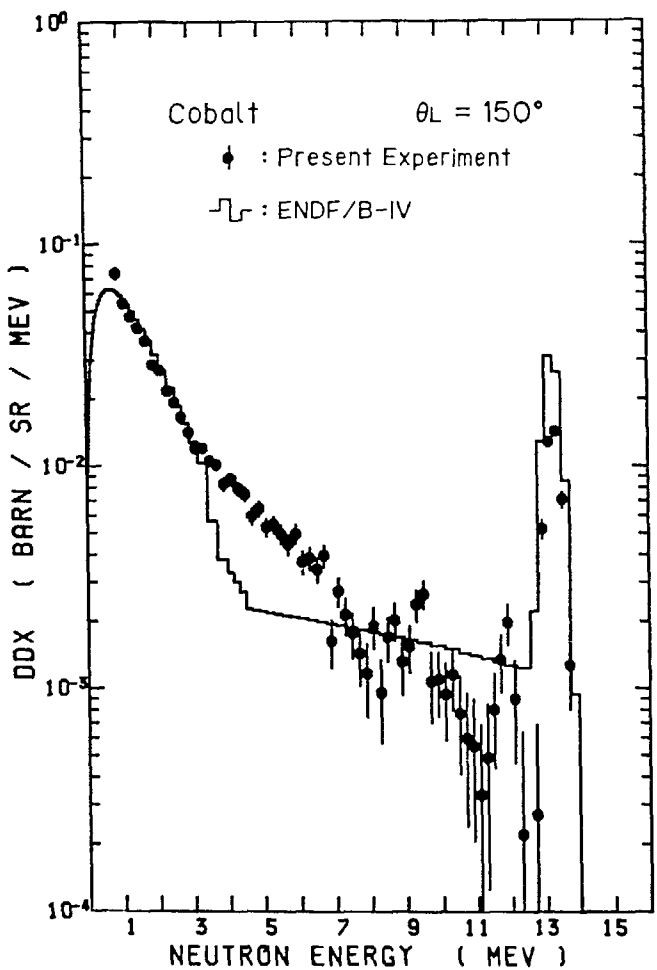


Fig. 46 Double differential neutron emission cross section at 150 deg with  $E_n = 14.1$  MeV, for Co

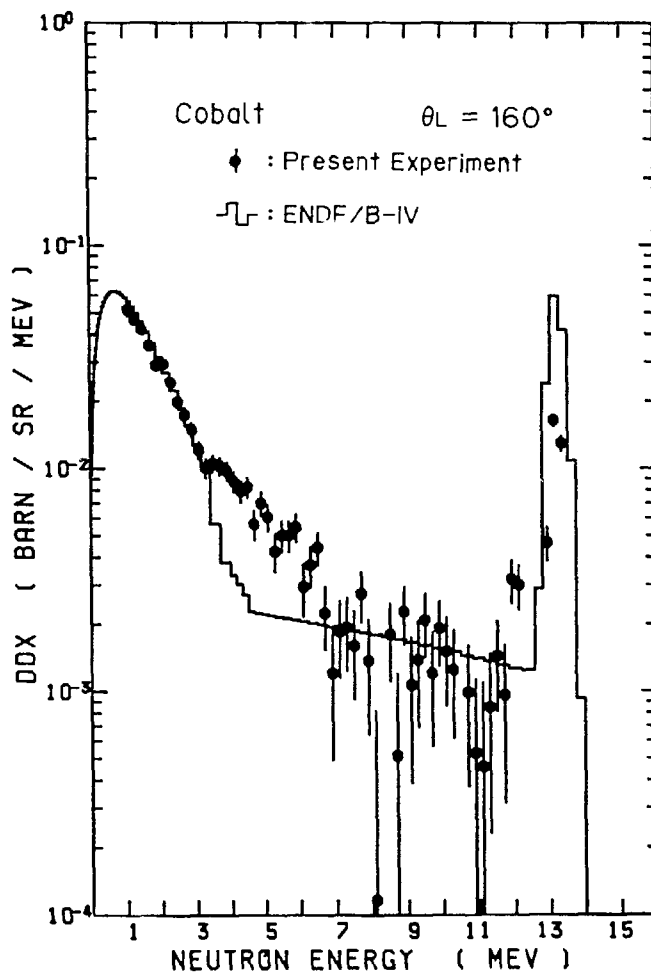


Fig. 47 Double differential neutron emission cross section at 160 deg with  $E_n = 14.1$  MeV, for Co

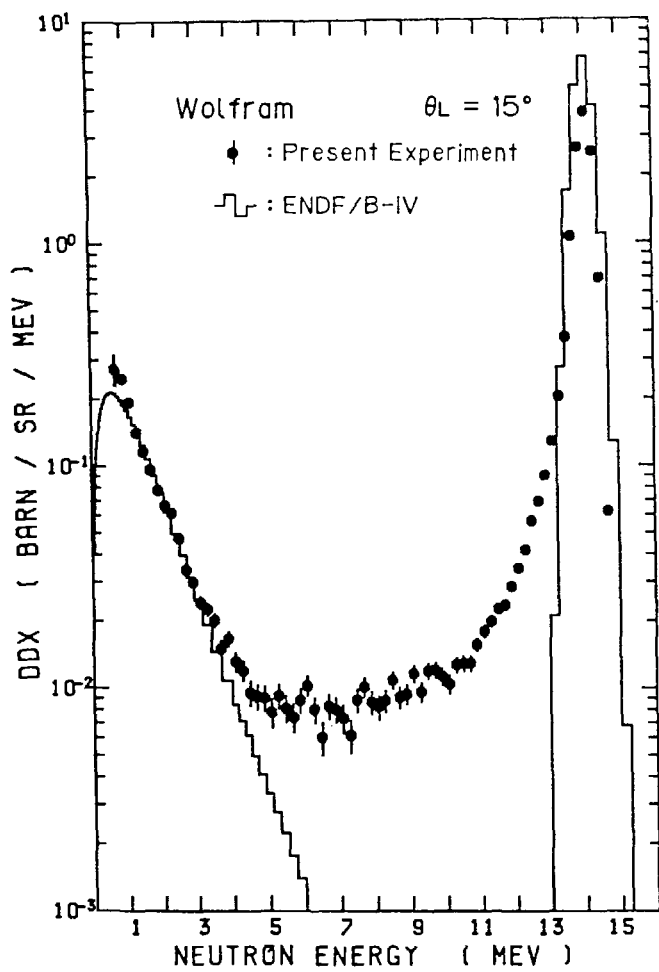


Fig. 48 Double differential neutron emission cross section at 15 deg with  $E_n = 14.1$  MeV, for W

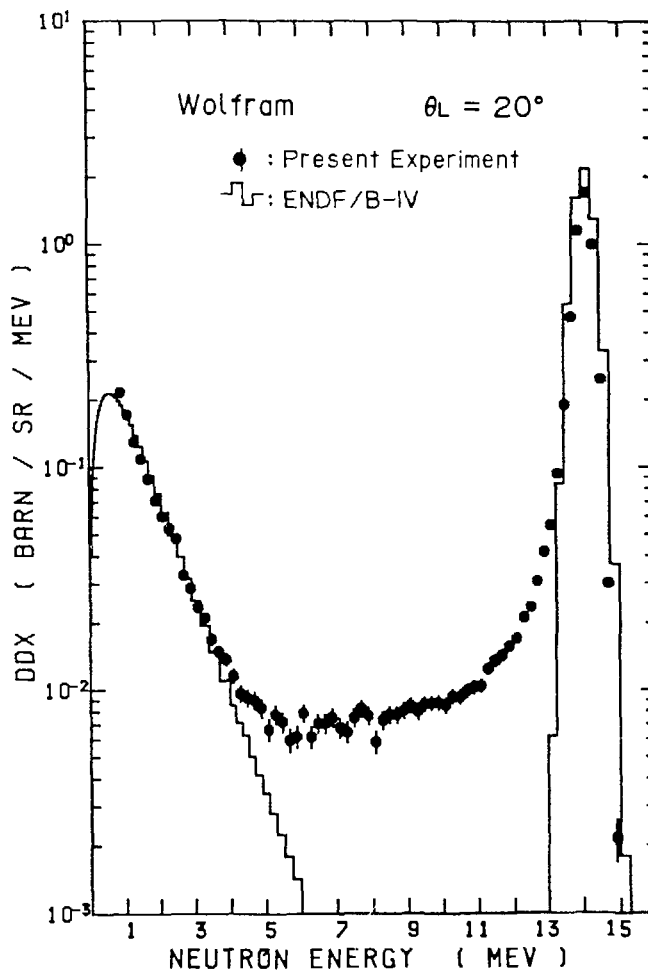


Fig. 49 Double differential neutron emission cross section at 20 deg with  $E_n = 14.1$  MeV, for W

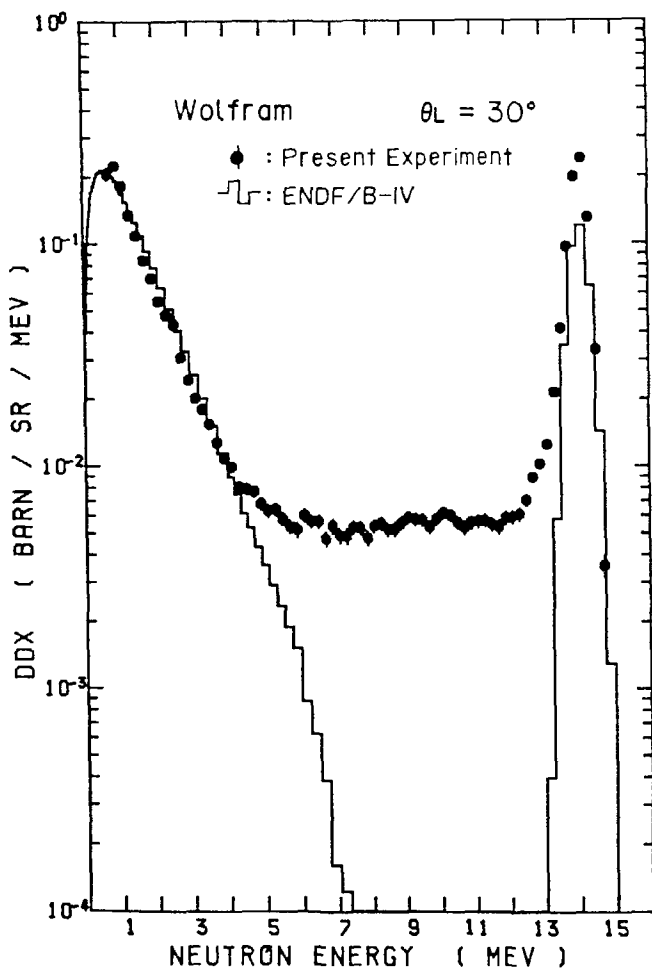


Fig. 50 Double differential neutron emission cross section at 30 deg with  $E_n = 14.1$  MeV, for W

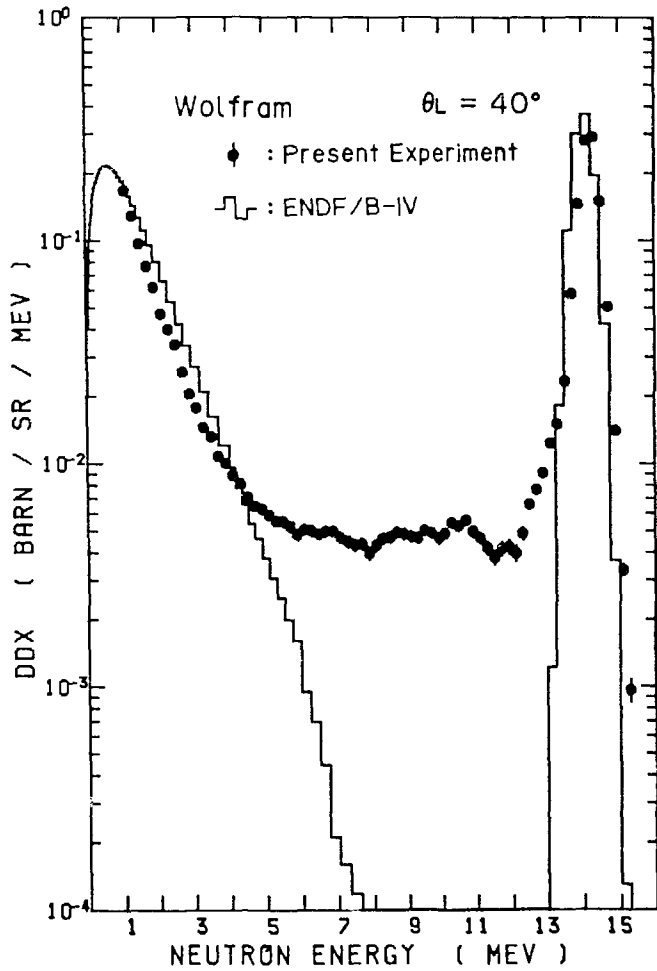


Fig. 51 Double differential neutron emission cross section at 40 deg with  $E_n = 14.1$  MeV, for W

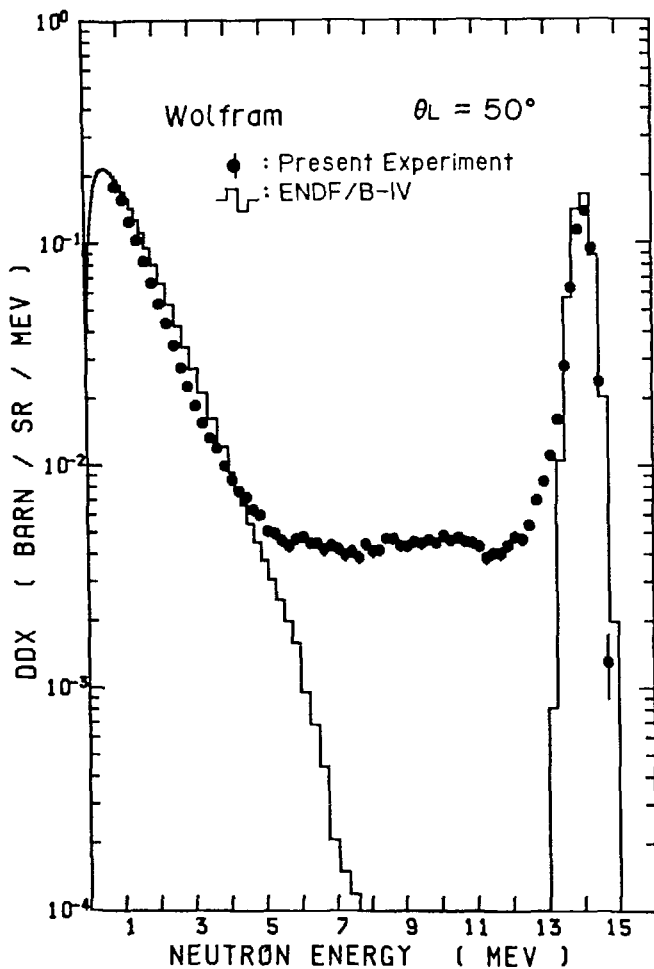


Fig. 52 Double differential neutron emission cross section at 50 deg with  $E_n = 14.1$  MeV, for W

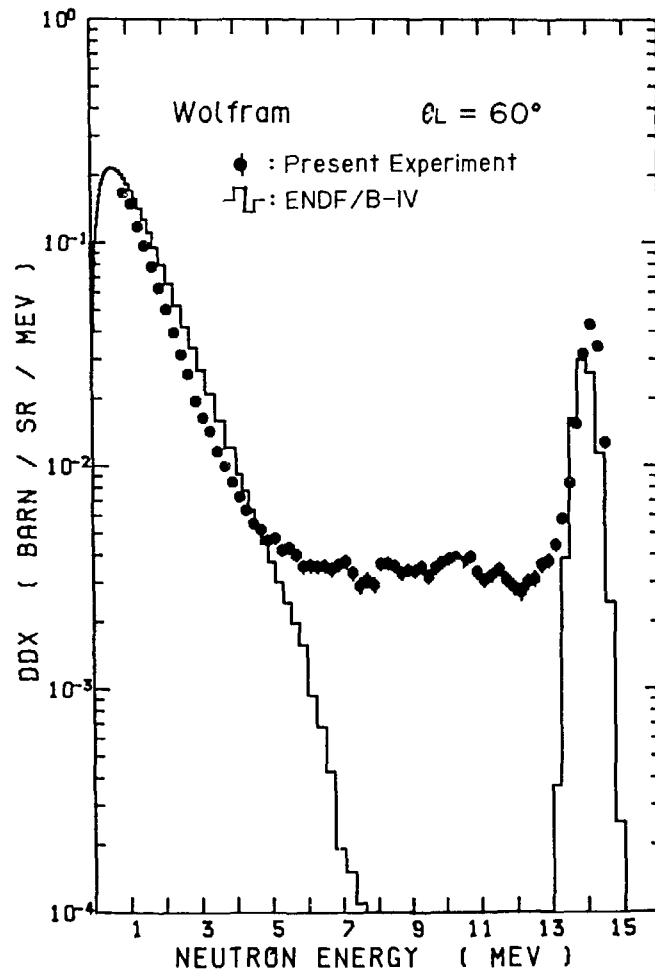


Fig. 53 Double differential neutron emission cross section at 60 deg with  $E_n = 14.1$  MeV, for W

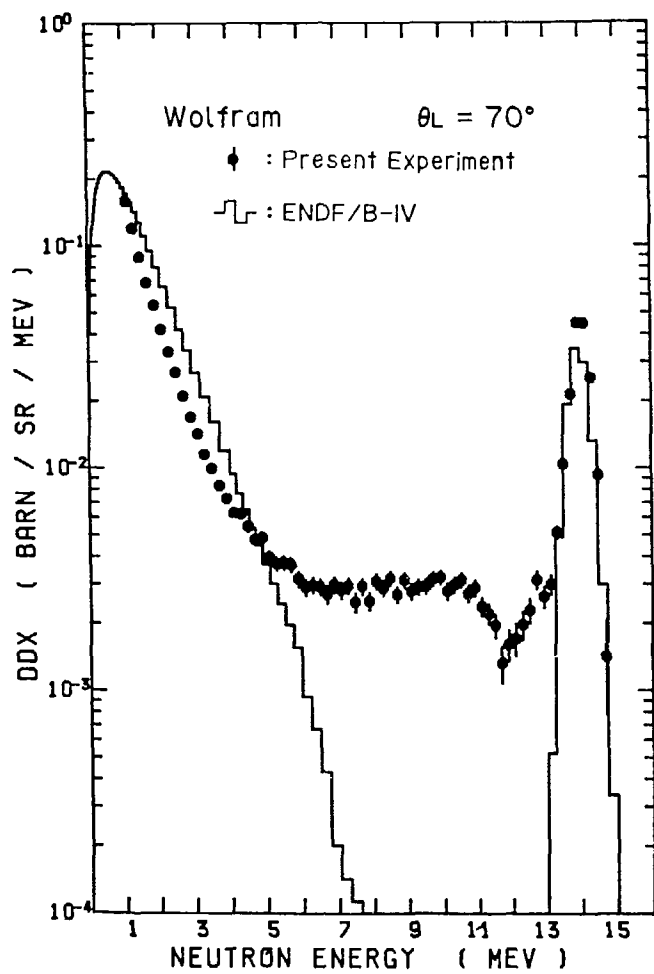


Fig. 54 Double differential neutron emission cross section at 70 deg with  $E_n = 14.1$  MeV, for W

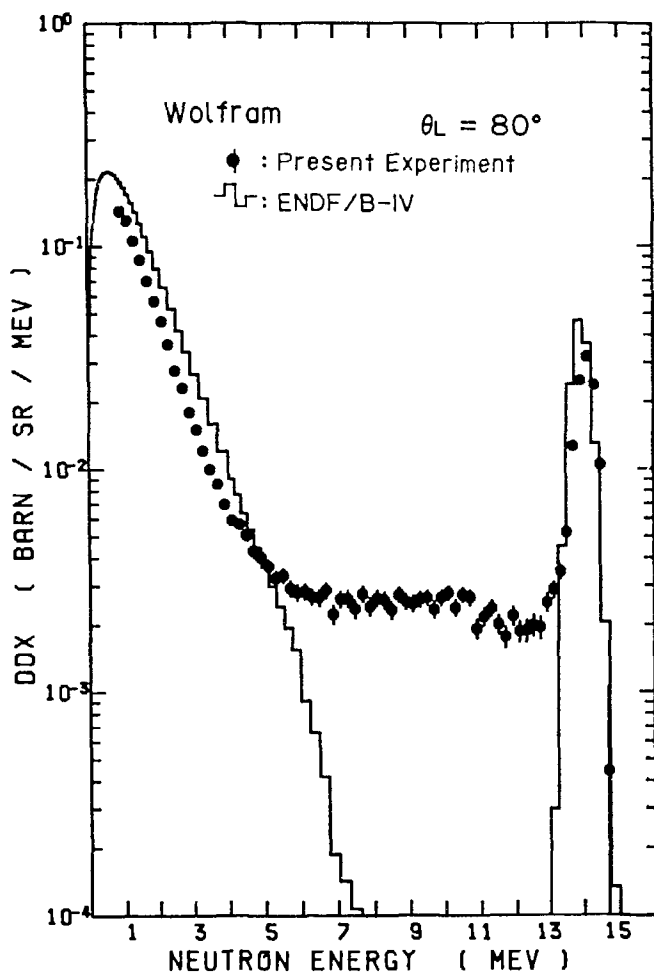


Fig. 55 Double differential neutron emission cross section at 80 deg with  $E_n = 14.1$  MeV, for W

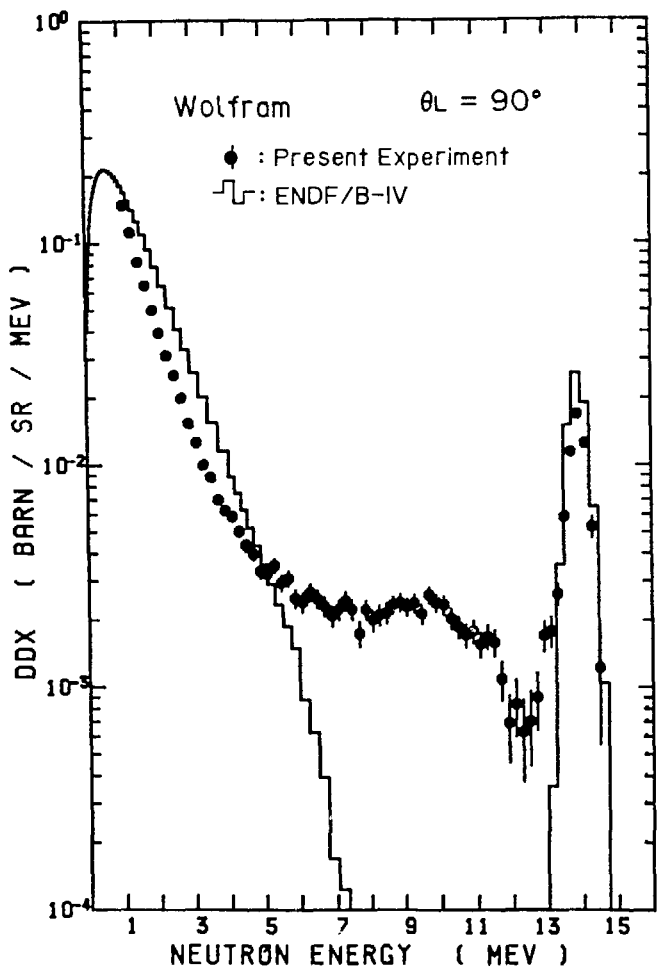


Fig. 56 Double differential neutron emission cross section at 90 deg with  $E_n = 14.1$  MeV, for W

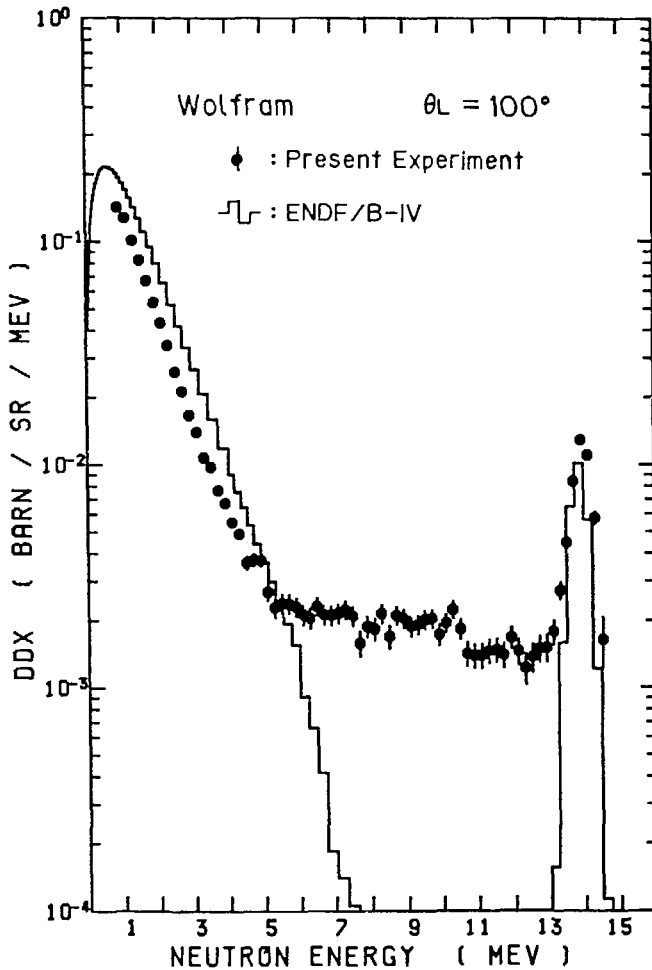


Fig. 57 Double differential neutron emission cross section at 100 deg with  $E_n = 14.1$  MeV, for W

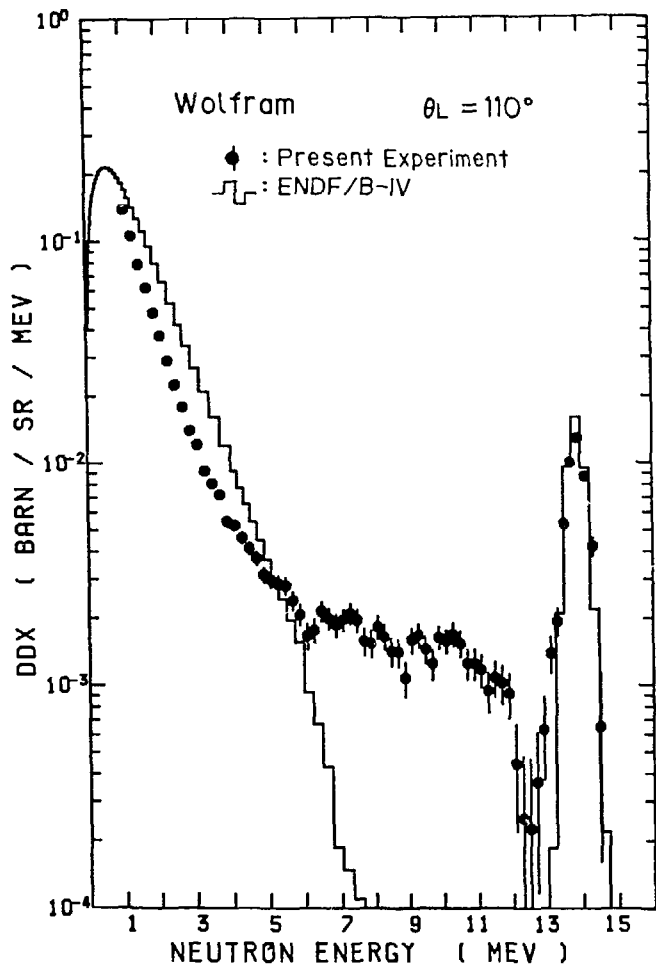


Fig. 58 Double differential neutron emission cross section at 110 deg with  $E_n = 14.1$  MeV, for W

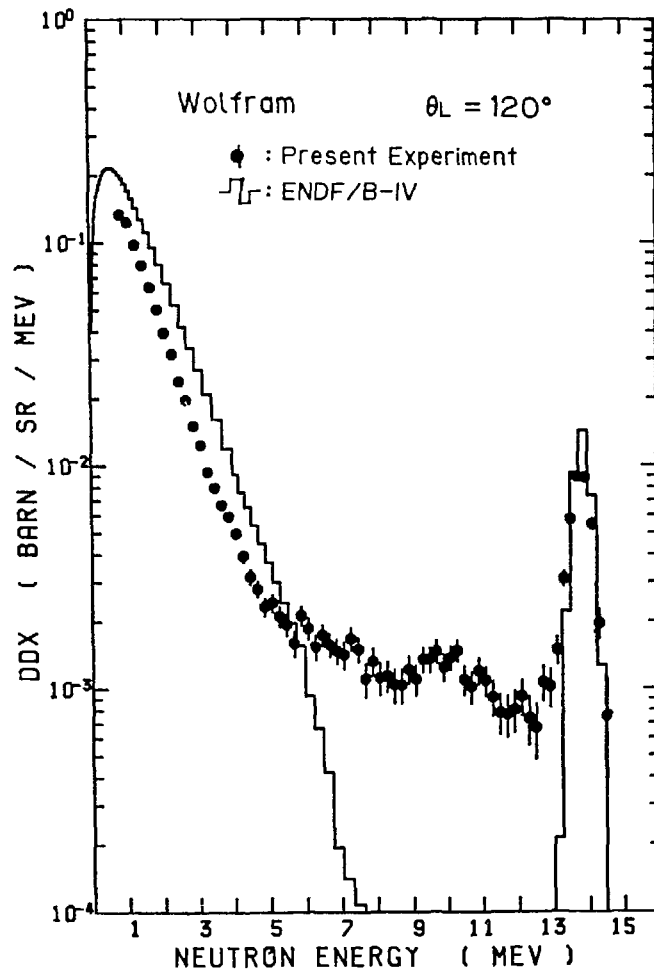


Fig. 59 Double differential neutron emission cross section at 120 deg with  $E_n = 14.1$  MeV, for W

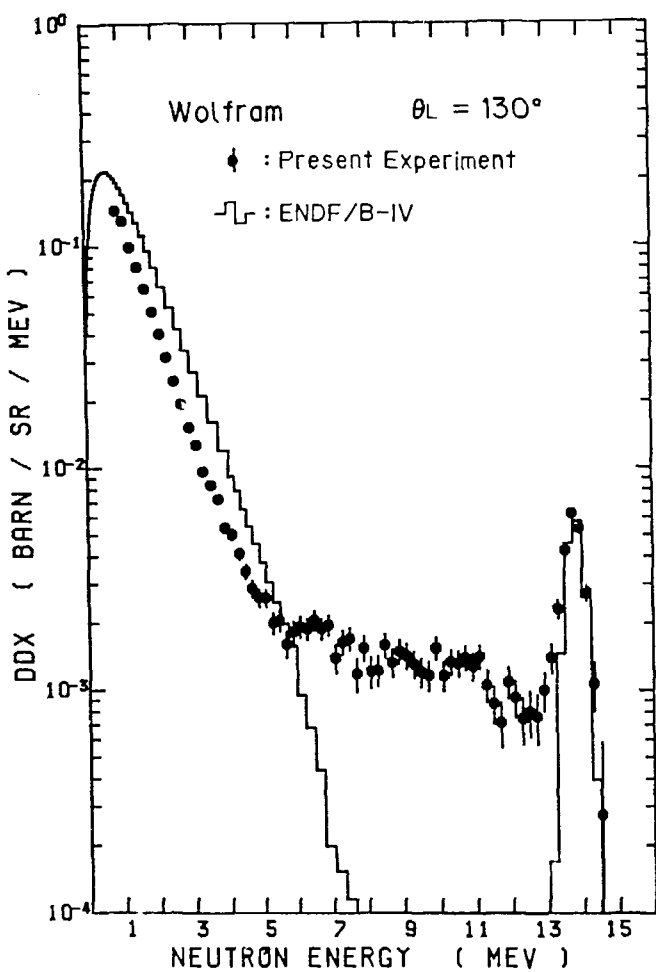


Fig. 60 Double differential neutron emission cross section at 130 deg with  $E_n = 14.1$  MeV, for W

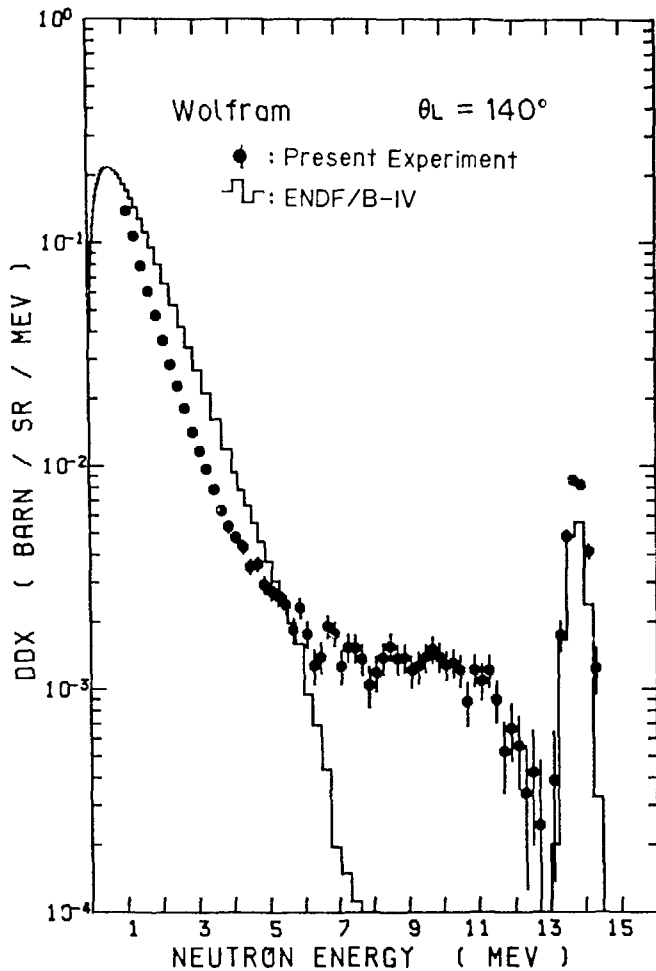


Fig. 61 Double differential neutron emission cross section at 140 deg with  $E_n = 14.1$  MeV, for W

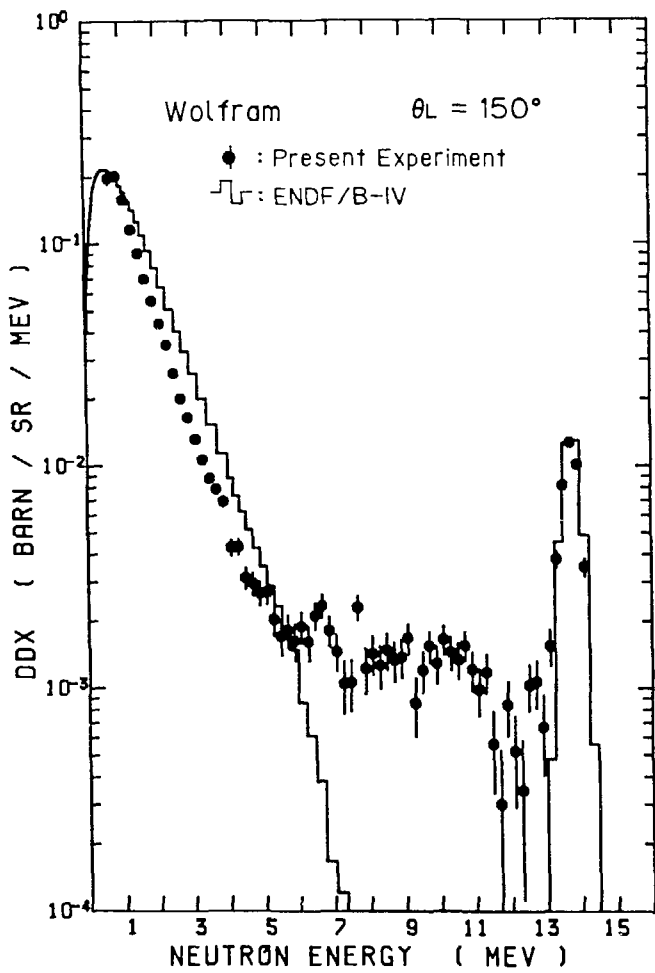


Fig. 62 Double differential neutron emission cross section at 150 deg with  $E_n = 14.1$  MeV, for W

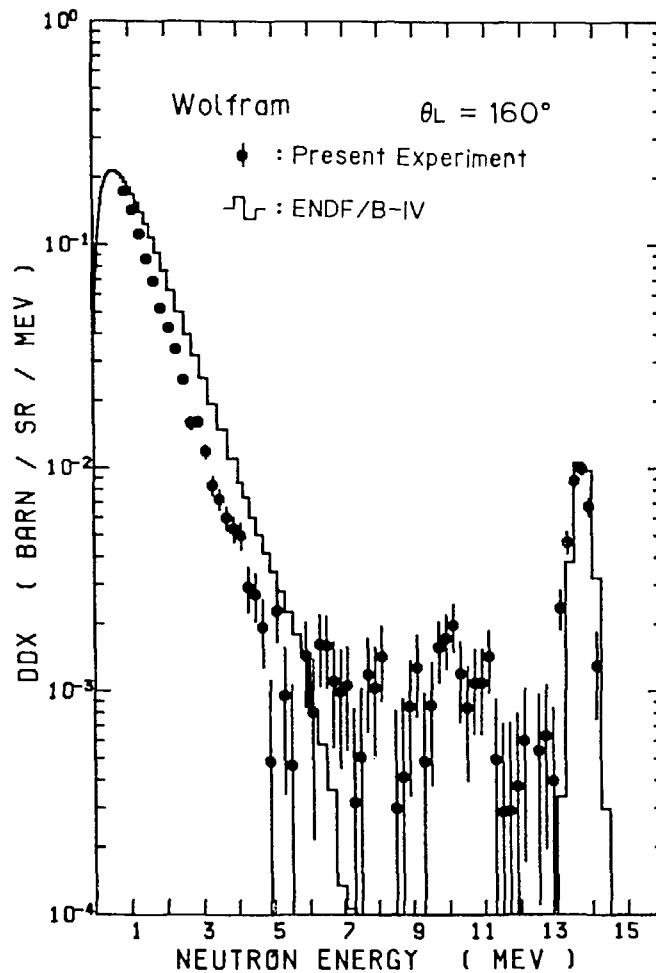


Fig. 63 Double differential neutron emission cross section at 160 deg with  $E_n = 14.1$  MeV, for W

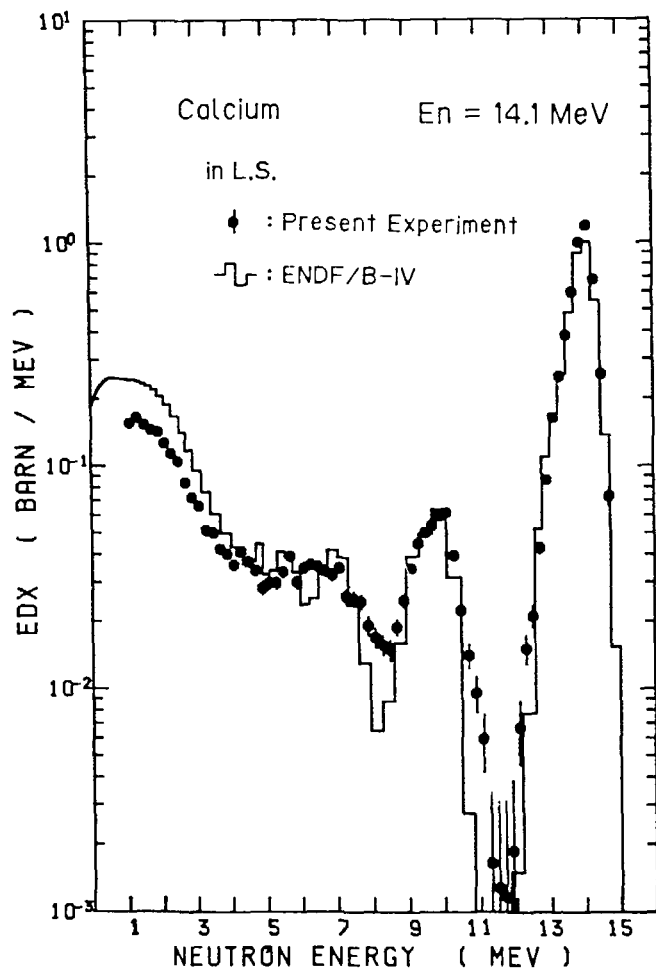


Fig. 64 Angle-integrated neutron emission spectrum in the LAB system with  $E_n = 14.1 \text{ MeV}$ , for Ca

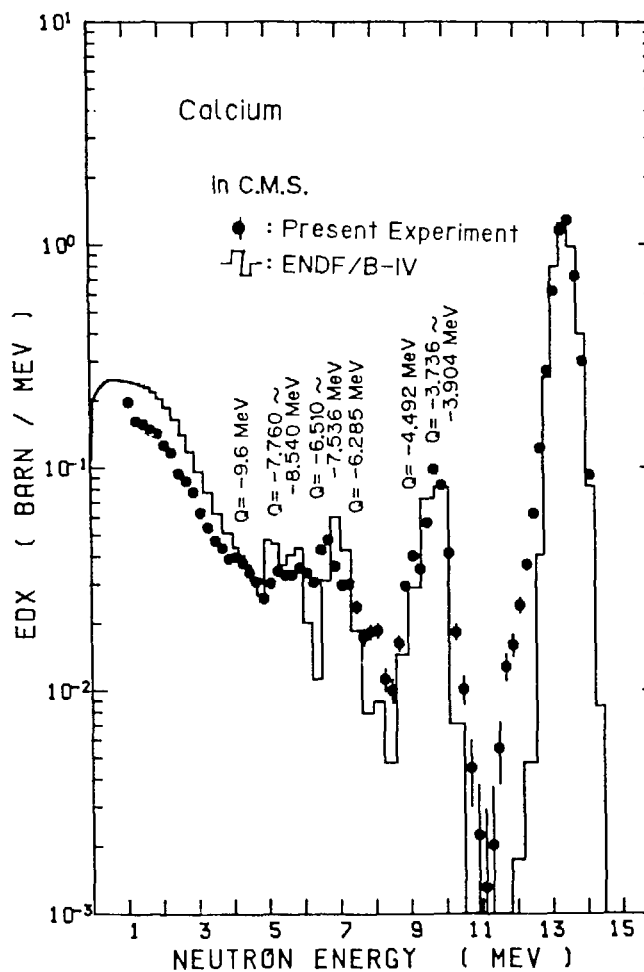


Fig. 65 Angle-integrated neutron emission spectrum in the CM system with  $E_n = 14.1 \text{ MeV}$ , for Ca

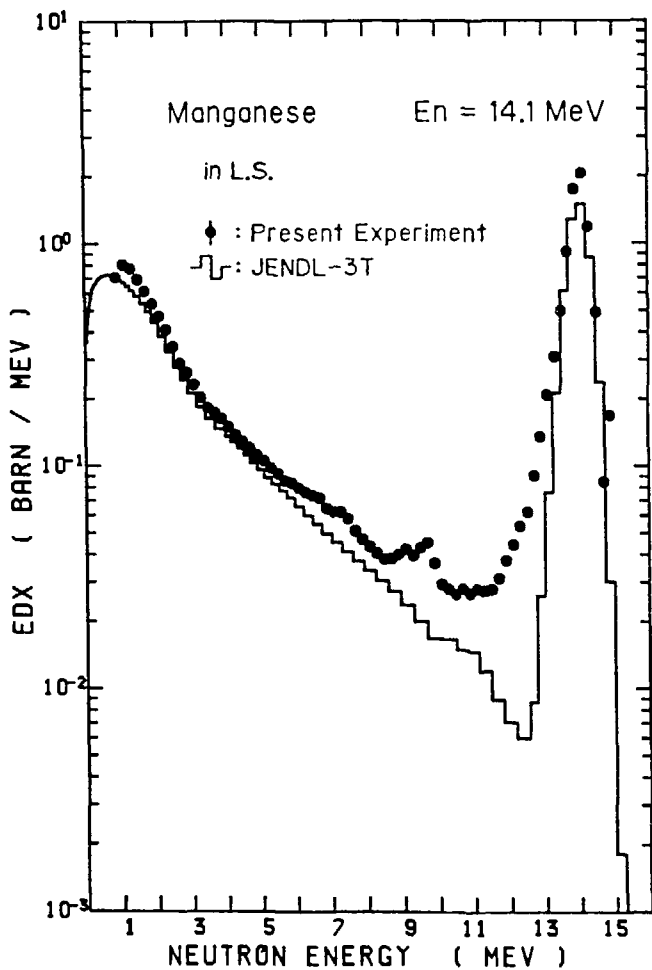


Fig. 66 Angle-integrated neutron emission spectrum in the LAB system with  $E_n = 14.1 \text{ MeV}$ , for Mn

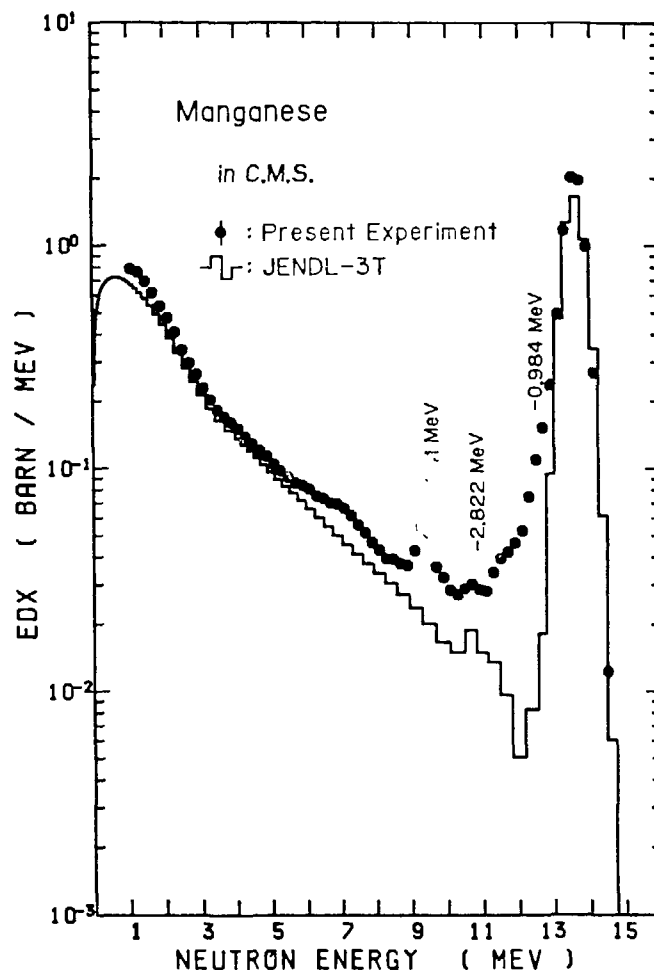


Fig. 67 Angle-integrated neutron emission spectrum in the CM system with  $E_n = 14.1 \text{ MeV}$ , for Mn

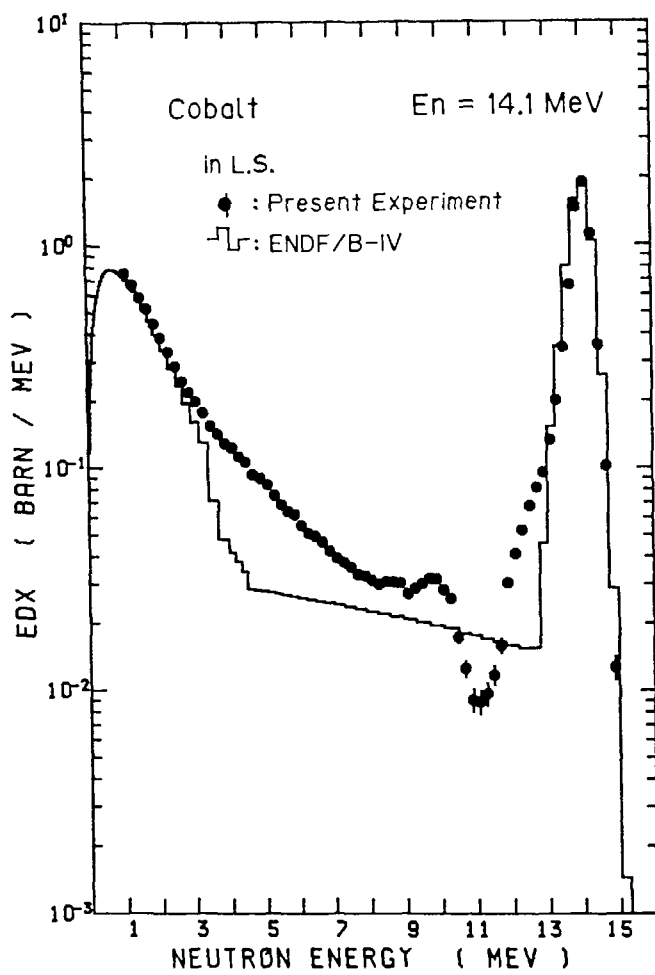


Fig. 68 Angle-integrated neutron emission spectrum in the LAB system with  $E_n = 14.1$  MeV, for Co

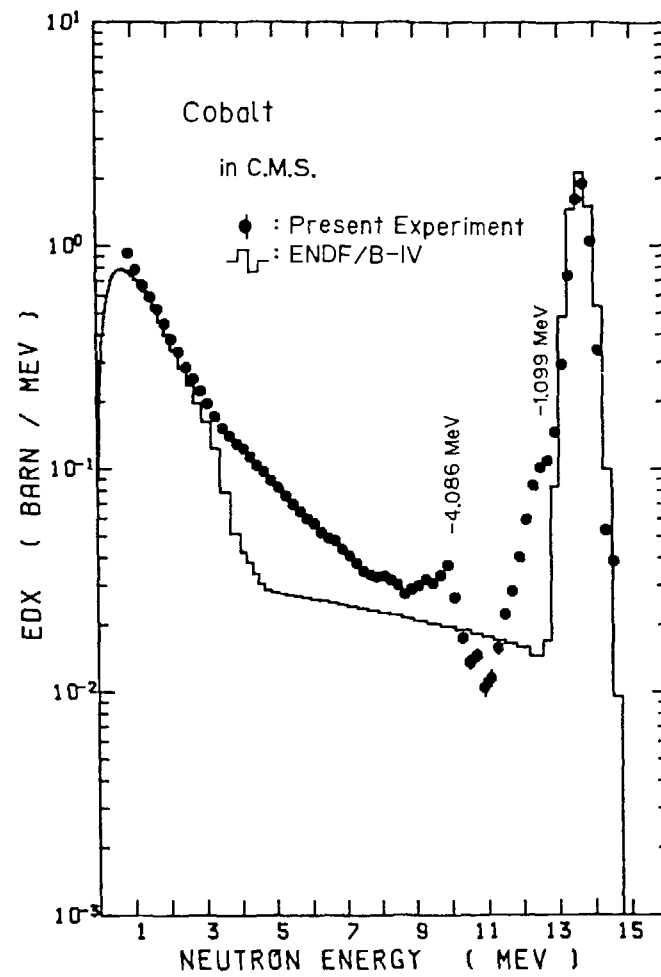


Fig. 69 Angle-integrated neutron emission spectrum in the CM system with  $E_n = 14.1$  MeV, for Co

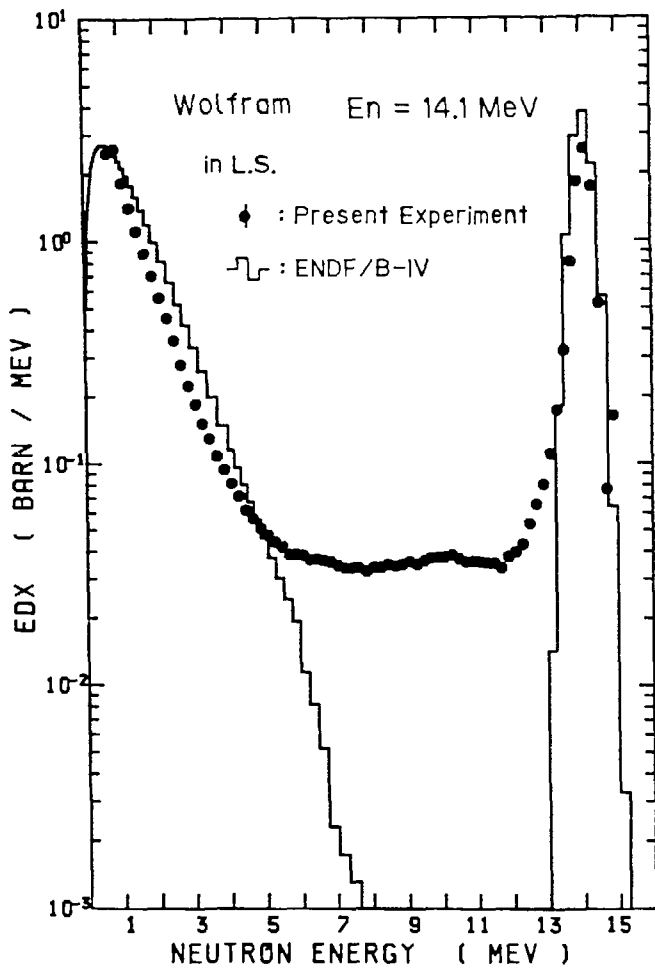


Fig. 70 Angle-integrated neutron emission spectrum in the LAB system with  $E_n = 14.1 \text{ MeV}$ , for W

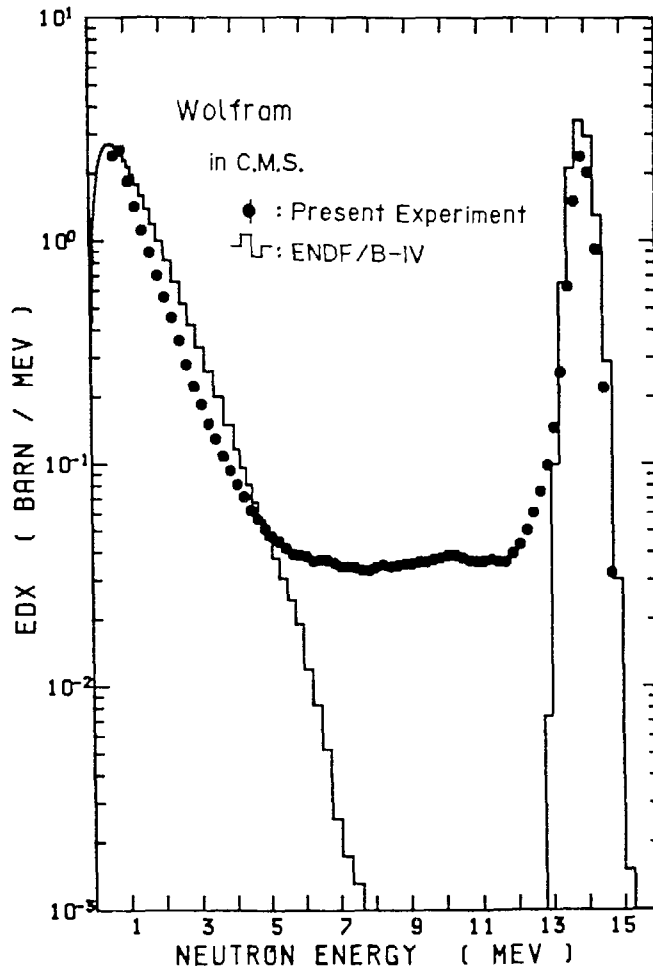


Fig. 71 Angle-integrated neutron emission spectrum in the CM system with  $E_n = 14.1 \text{ MeV}$ , for W

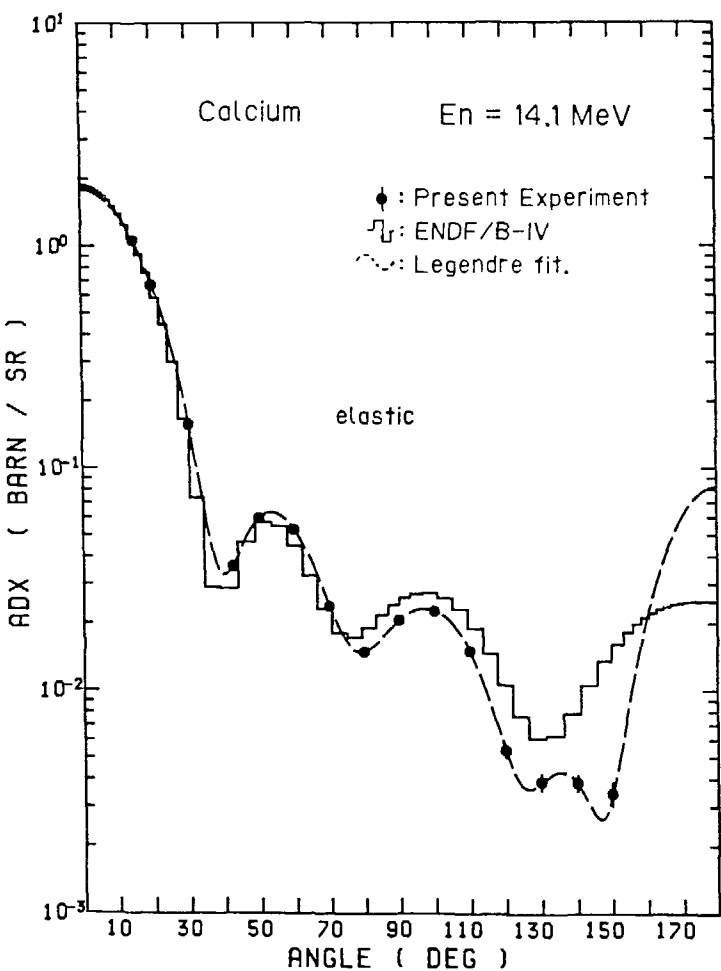


Fig. 72 Differential elastic scattering cross sections at  $E_n = 14.1 \text{ MeV}$ , for Ca

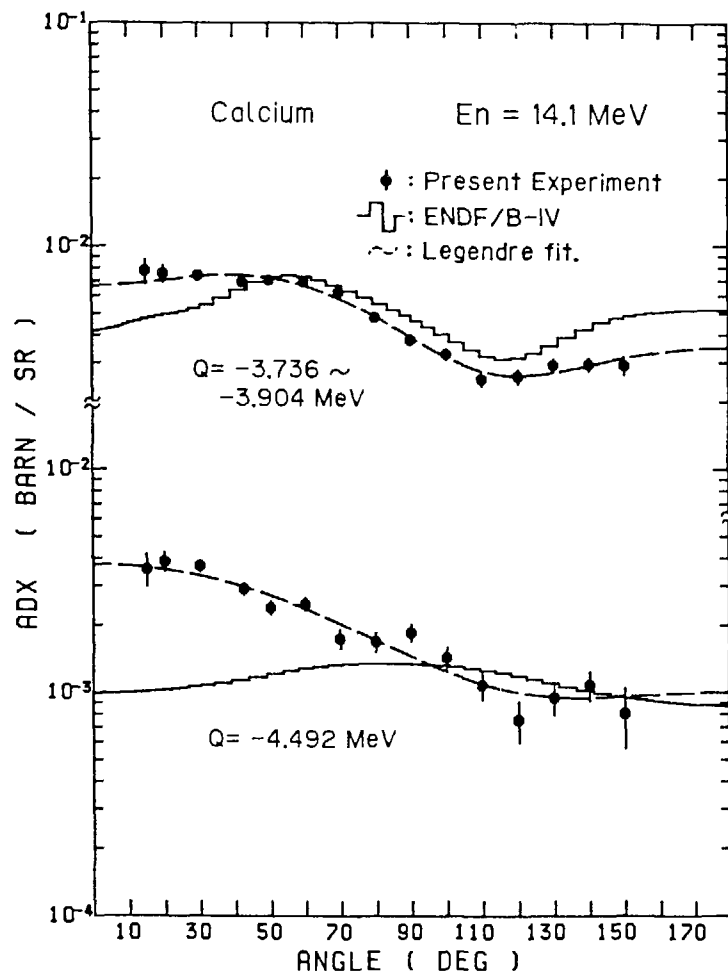


Fig. 73 Differential cross sections of discrete inelastic scattering at  $E_n = 14.1 \text{ MeV}$ , for Ca

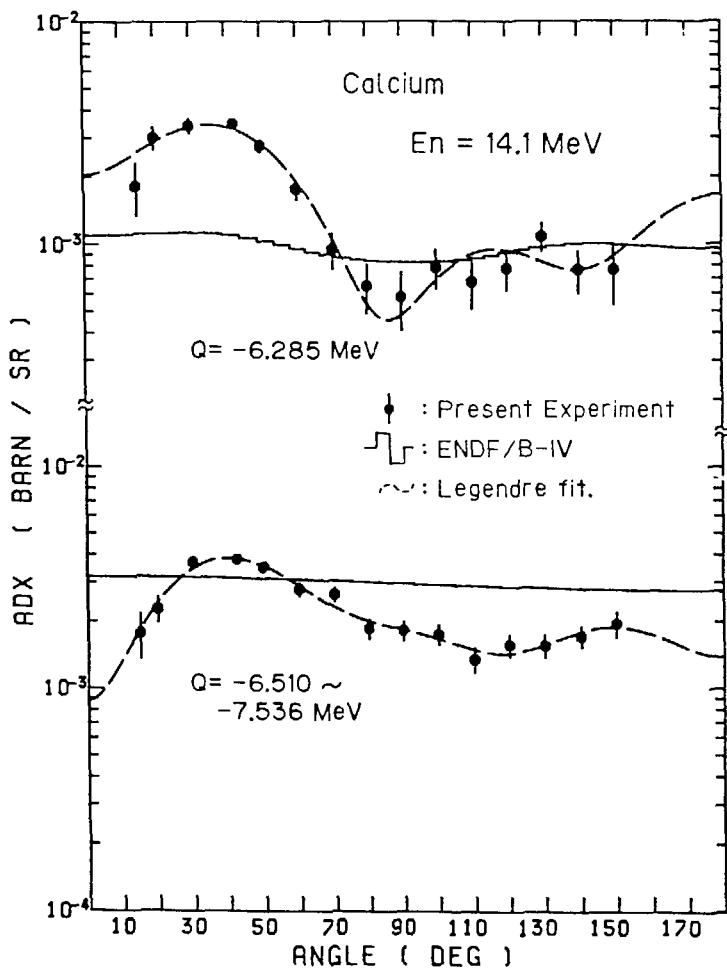


Fig. 74 Differential cross sections of discrete inelastic scattering at  $E_n = 14.1 \text{ MeV}$ , for Ca

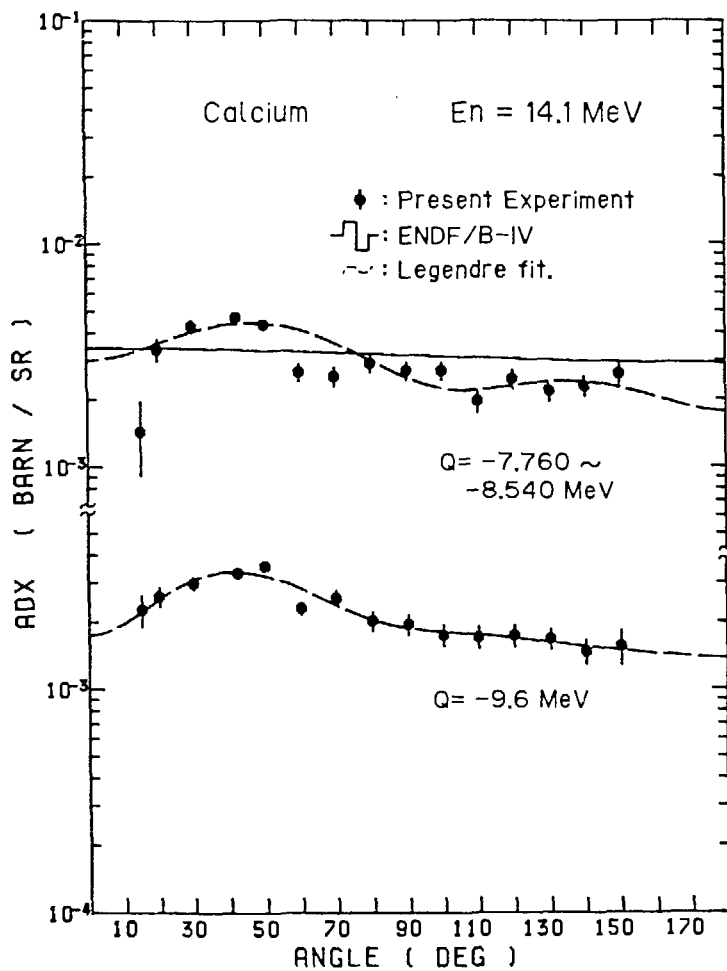


Fig. 75 Differential cross sections of discrete inelastic scattering at  $E_n = 14.1 \text{ MeV}$ , for Ca

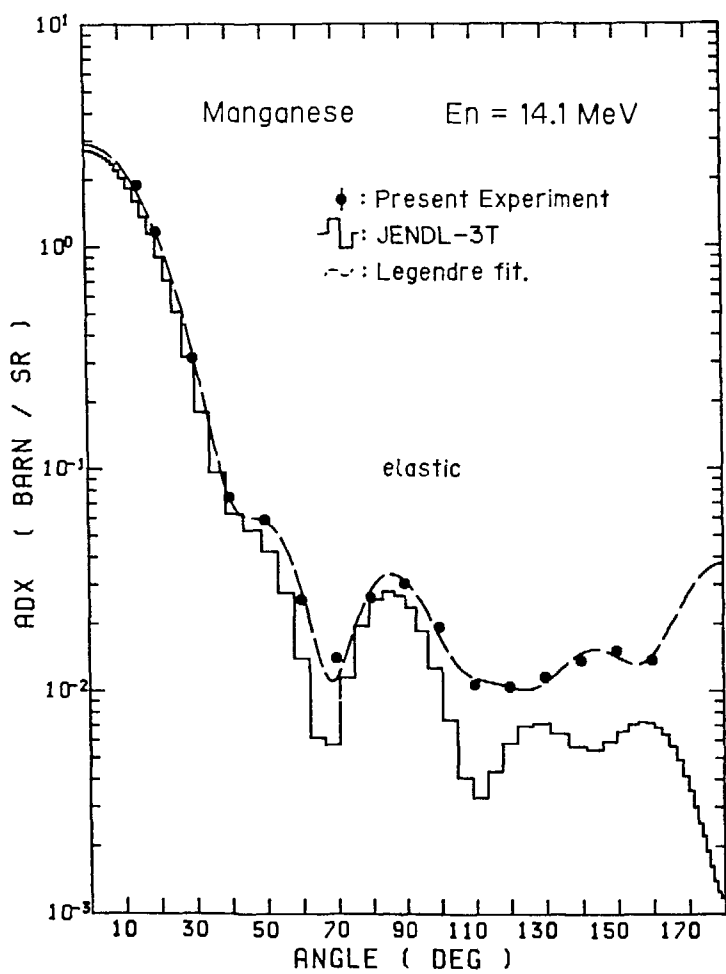


Fig. 76 Differential elastic scattering cross sections at  $E_n = 14.1 \text{ MeV}$ , for Mn

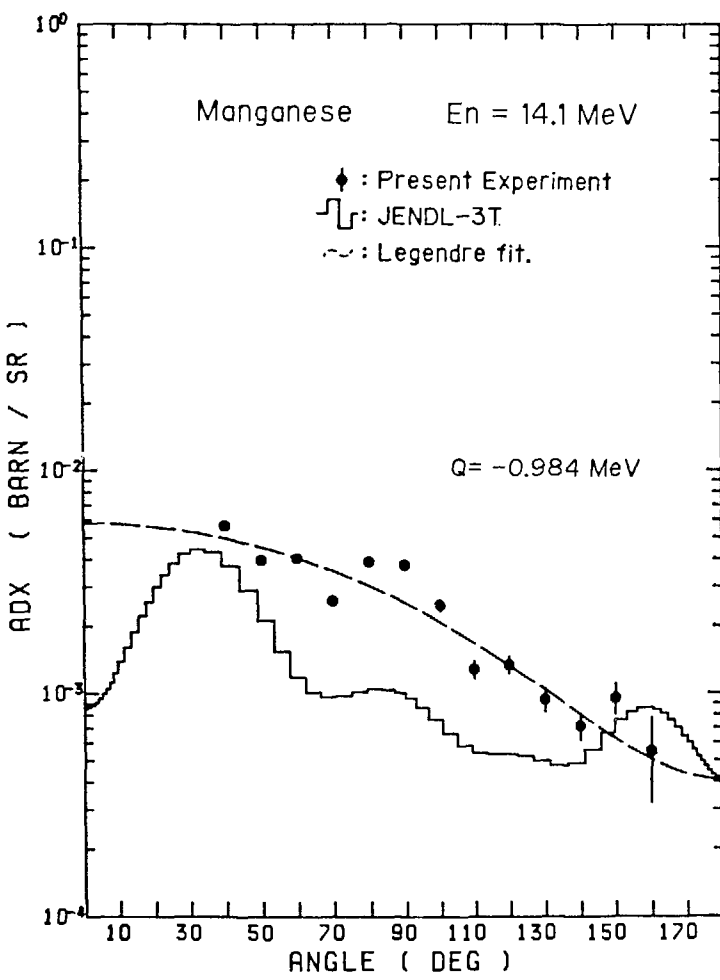


Fig. 77 Differential cross sections of discrete inelastic scattering ( $0.984 \text{ MeV}$  level) at  $E_n = 14.1 \text{ MeV}$ , for Mn

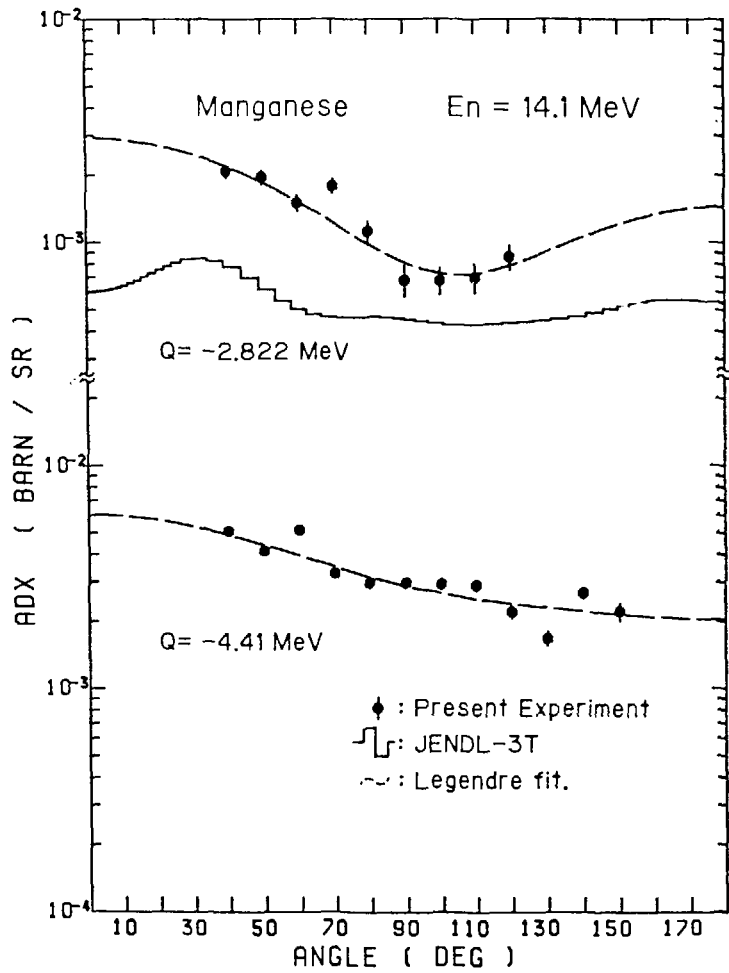


Fig. 78 Differential cross sections of discrete inelastic scattering at  $E_n = 14.1 \text{ MeV}$ , for Mn

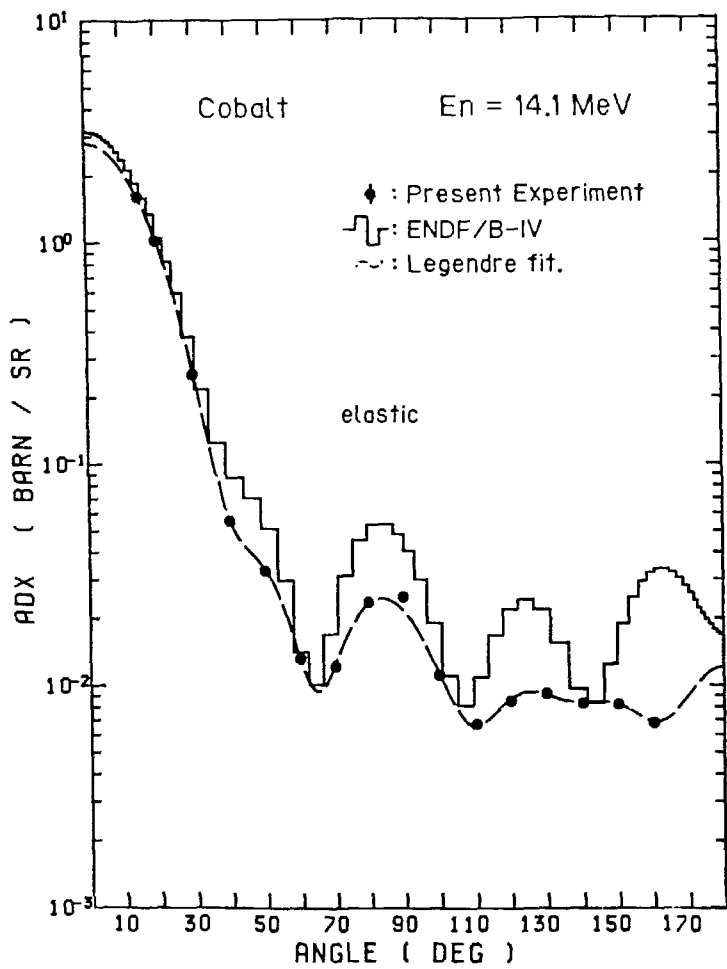


Fig. 79 Differential elastic scattering cross sections at  $E_n = 14.1 \text{ MeV}$ , for Co

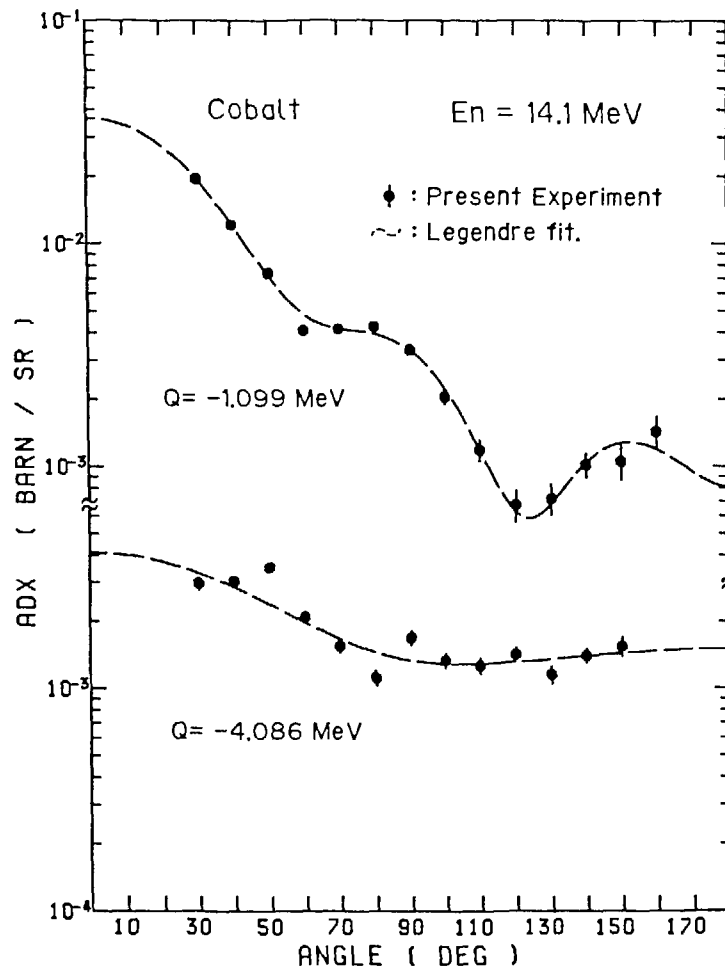


Fig. 80 Differential cross sections of discrete inelastic scattering at  $E_n = 14.1 \text{ MeV}$ , for Co

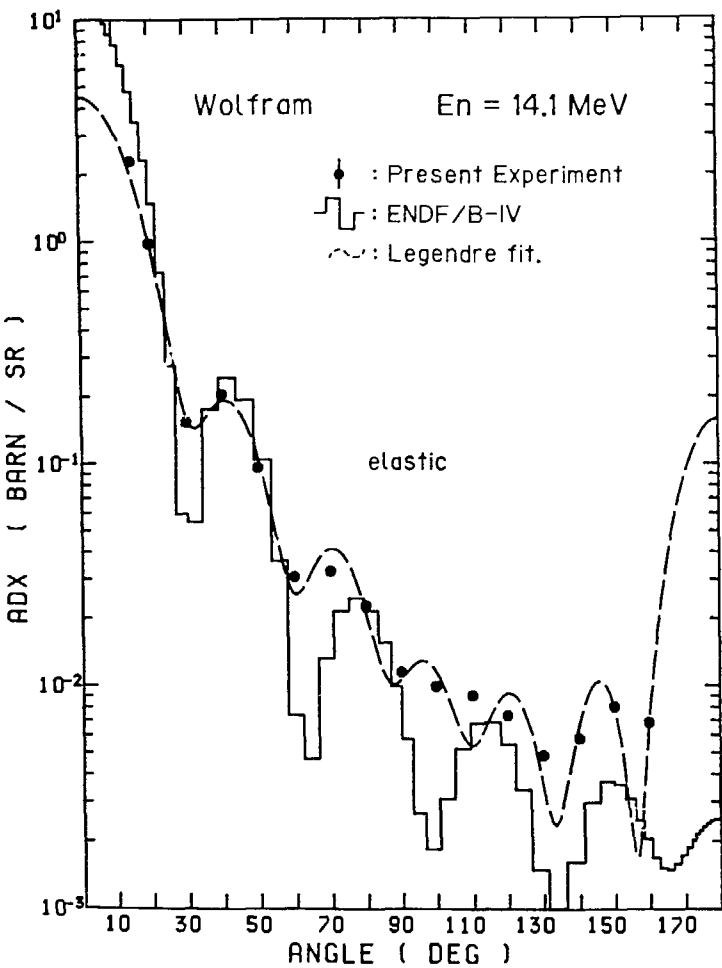


Fig. 81 Differential elastic scattering cross sections at  $E_n = 14.1 \text{ MeV}$ , for W

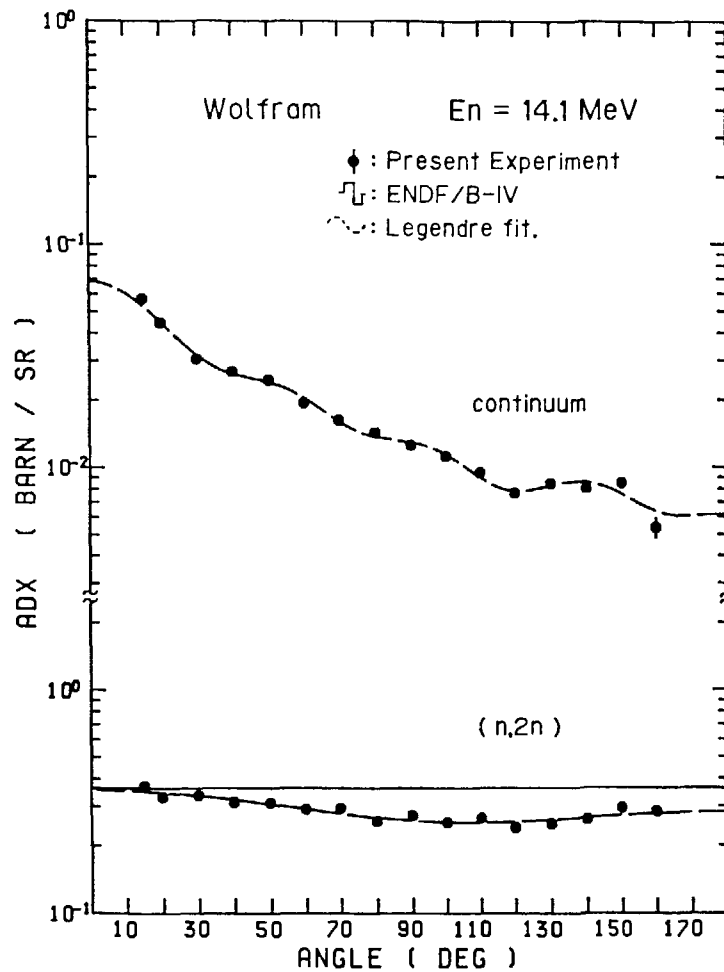


Fig. 82 Angular distributions of continuum-inelastic and  $(n, 2n)$  channels with  $E_n = 14.1 \text{ MeV}$ , for W